



LUND UNIVERSITY

Anti-Reset Windup for PID Controllers

Rundqvist, Lars

1991

Document Version:

Publisher's PDF, also known as Version of record

[Link to publication](#)

Citation for published version (APA):

Rundqvist, L. (1991). *Anti-Reset Windup for PID Controllers*. Department of Automatic Control, Lund Institute of Technology (LTH).

General rights

Unless other specific re-use rights are stated the following general rights apply:

Copyright and moral rights for the publications made accessible in the public portal are retained by the authors and/or other copyright owners and it is a condition of accessing publications that users recognise and abide by the legal requirements associated with these rights.

- Users may download and print one copy of any publication from the public portal for the purpose of private study or research.
- You may not further distribute the material or use it for any profit-making activity or commercial gain
- You may freely distribute the URL identifying the publication in the public portal

Read more about Creative commons licenses: <https://creativecommons.org/licenses/>

Take down policy

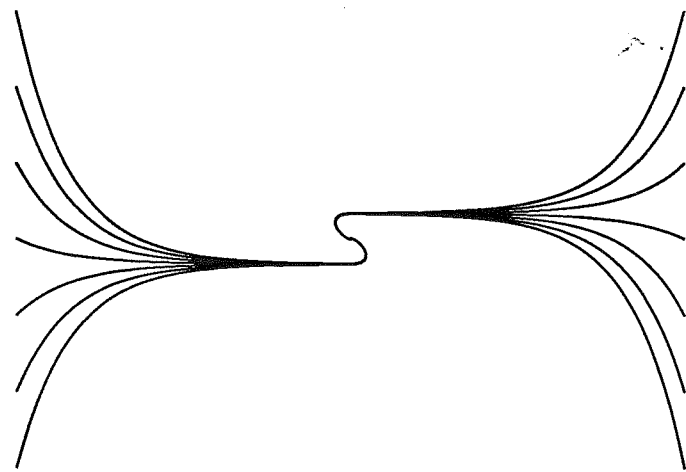
If you believe that this document breaches copyright please contact us providing details, and we will remove access to the work immediately and investigate your claim.

LUND UNIVERSITY

PO Box 117
221 00 Lund
+46 46-222 00 00

Anti-Reset Windup for PID Controllers

Lars Rundqvist



Lund 1991

To Ann-Christin, Anna and Mattias

Department of Automatic Control
Lund Institute of Technology
Box 118
S-221 00 LUND
Sweden

© 1991 by Lars Rundqvist
Published 1991
Printed in Sweden by Studentlitteratur AB

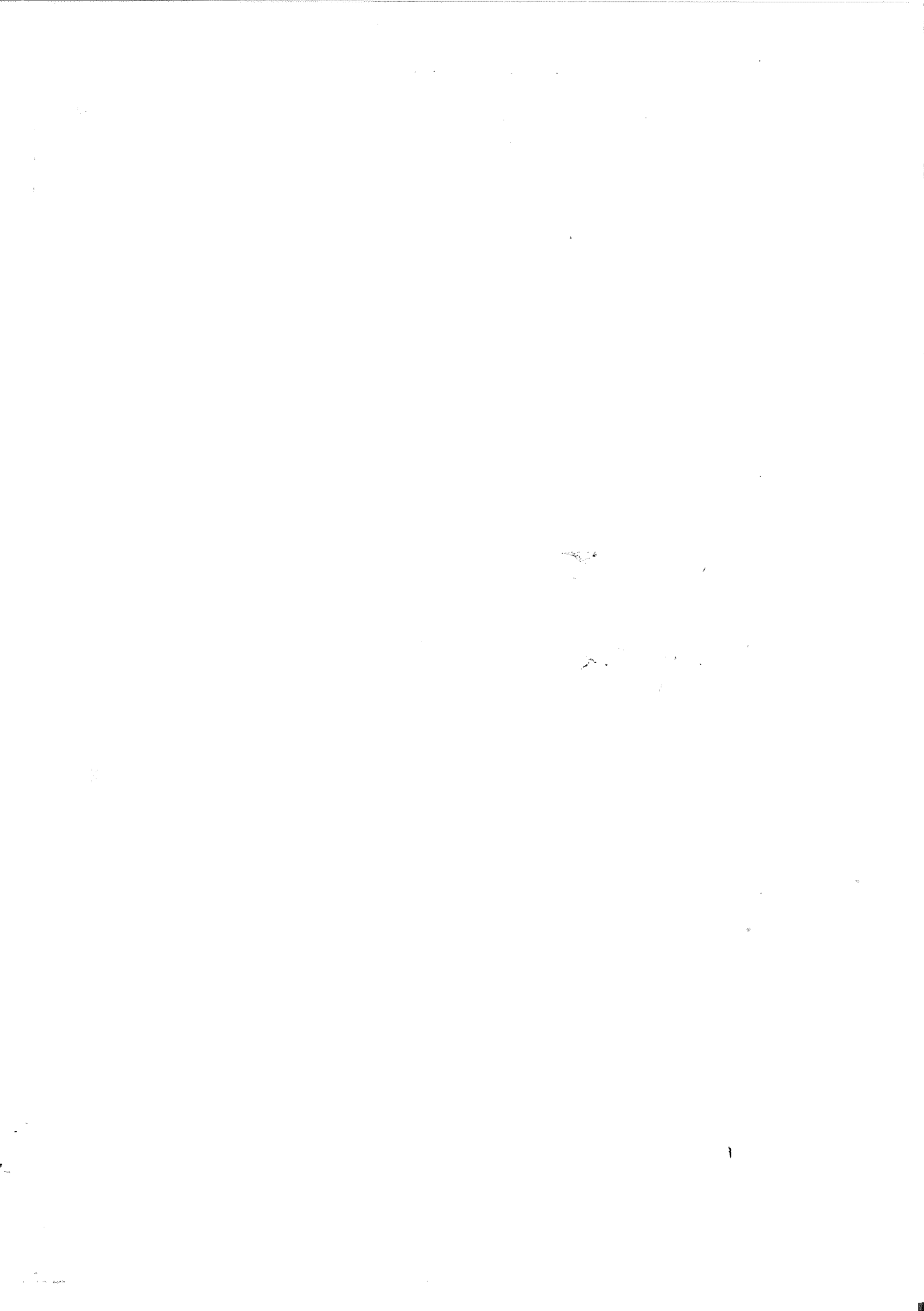
Department of Automatic Control Lund Institute of Technology P.O. Box 118 S-221 00 Lund Sweden		<i>Document name</i> DOCTORAL DISSERTATION <i>Date of issue</i> March 1991 <i>Document Number</i> CODEN: LUTFD2/(TFRT-1033)/1-143/(1991)
Author(s) Lars Rundqvist		<i>Supervisor</i> Karl Johan Åström and Björn Wittenmark <i>Sponsoring organisation</i>
Title and subtitle Anti-Reset Windup for PID Controllers		
Abstract <p>This thesis deals with proportional-integral-derivative (PID) controllers and their anti-reset windup. Much of the earlier work in this area treats anti-reset windup in the context of set point changes, while this thesis instead analyzes the performance for disturbances. The analysis leads to design rules for anti-reset windup in PID controllers. The design rules are evaluated on different processes and are found to give good performance.</p> <p>The thesis also surveys the area of methods for handling control systems with saturations. The survey includes a classification and unification of many published methods.</p>		
Key words PID control, actuators, saturation, anti-reset windup, survey.		
Classification system and/or index terms (if any)		
Supplementary bibliographical information		
ISSN and key title		ISBN
Language English	Number of pages 143	Recipient's notes
Security classification		

The report may be ordered from the Department of Automatic Control or borrowed through the University Library 2, Box 1010, S-221 03 Lund, Sweden, Telex: 33248 lubbis lund.



Contents

Preface	7
Acknowledgements	7
1. Introduction	9
2. Anti-Windup Methods — A Survey	11
2.1 Classification of Anti-Windup Methods	11
2.2 Modified Controller Realizations	13
2.3 Conditional Integration Methods	14
2.4 Observer Methods	22
2.5 Input Limitation Methods	31
2.6 Nonlinear Control Design	32
2.7 Theory	35
2.8 Summary	39
3. PID Control with Anti-Windup	40
3.1 PID Controllers	40
3.2 Anti-Windup Methods for PID Controllers	43
3.3 Stability Improvements when using Anti-Windup	46
3.4 Disturbances	54
3.5 Impulse Disturbances and Anti-Windup Design	56
3.6 Sinusoidal Measurement Disturbances	73
3.7 Summary	80
4. Evaluation of Anti-Windup for PID Controllers	82
4.1 The Double-Tank Process	82
4.2 A DC Motor	96
4.3 Inverse-Response Processes	105
4.4 An Unstable Process	111
4.5 Time-Delay and High-Order Processes	114
4.6 Poorly Damped Processes	121
4.7 Summary	123
5. Conclusions	127
6. References	130
A. Derivations for Section 4.2	137
B. PID Parameter Optimization	140



Preface

Most industrial processes have saturations and other nonlinearities and constraints which make control more difficult. When the controllers have integrators the nonlinearities may give a severe deterioration of the performance. Some of the constraints are almost unique for certain processes and require special solutions. However, saturations are always present and then general solutions can be applied.

My interest for these nonlinearities and the methods for protecting controllers and processes from their negative effects grew substantially during the work with my licentiate thesis. As one part of that work a full-scale control system was implemented at the Käppala Sewage Works, Lidingö, Sweden. A large part of the work at Käppala dealt with process nonlinearities and constraints. Then my research gradually specialized on anti-reset windup (or anti-windup for short) in control systems with saturations. One reason was that the saturation is a common nonlinearity while many of the constraints at Käppala are more special.

A great deal of papers and reports have been written on anti-windup. They mostly consider anti-windup in the context of set point changes. In some cases disturbances give highly undesirable responses in cases where the responses for set point changes are satisfactory. One such case was discovered during laboratory experiments for undergraduates at the department. Using disturbances it is possible to derive design rules for anti-windup. In the thesis this has been done for two anti-windup methods for PID controllers. For one of the methods, which is in common use, the design rule gives good performance both for set point changes and disturbances.

One usual comment about anti-windup in PID controllers is that it is an already solved problem. This thesis, however, shows that some of the well-known solutions may give deteriorated performance in experiments with disturbances. The reason is simply that the closed-loop system is nonlinear. Any input signal or initial condition that has not been considered may give poor performance. This also holds for the design rules in this thesis, but they are of more general nature than design rules which are based only on set point changes. The analysis has also added more insight into the anti-windup problem.

Acknowledgements

First of all I would like to thank my two supervisors, Professors Karl Johan Åström and Björn Wittenmark. Karl Johan Åström suggested the analysis of a disturbance causing poor performance, which in the end led to design rules for anti-windup. Björn Wittenmark took over the supervision during

Karl Johan Åström's sabbatical in 1989–90, and during the last year they have both shared the work. Björn Wittenmark's criticism on early versions of the manuscript led to substantial improvements of the theoretical results. Björn Wittenmark is also greatly acknowledged for arranging my financial support during the last year.

I would also like to thank all my colleagues at the department. I have had interesting discussions with Per Hagander and Tore Hägglund. Ola Dahl's SIM2DDC program provided an easy way of testing anti-windup methods in laboratory experiments. Kjell Gustafsson, Michael Lundh and Mats Lilja has supplied a good set of Matlab routines. Many functions in the latest versions of Simnon, implemented by Tomas Schöntal, has been used extensively. The excellent computer facilities at the department have been invaluable. *TEX*, PostScript, and type-setting support has been provided by Eva Dagnegård, Leif Andersson and Anders Blomdell. Agneta Tuszynski has patiently typed several versions of the manuscript and Britt-Marie Mårtensson has skillfully prepared the figures.

Finally, I would like to thank my family for their patience, love, and support.

1

Introduction

This thesis is devoted to some of the problems arising in control systems when actuator nonlinearities interfere with the linear control. Saturations, i.e., constraints in magnitude and rate of the actuator are common actuator nonlinearities. An example is a control valve which ranges from closed to fully opened and also has a limited rate of change. Large command signals and disturbances require large control signals, which then may be outside the allowed range or change too fast for the actuator. Other common actuator nonlinearities are, e.g., backlash and hysteresis.

Consequences of these nonlinearities are controller windup, instability, and limit cycles. In general, windup denotes an undesirable transient in the process output caused by, e.g., saturation when a controller with integrators is used. Open-loop unstable controllers, phase-retarding controllers and other controllers with slow stable modes give similar problems. In case of instability or limit cycles the process output grows towards infinity or some boundary, e.g., a full or empty tank, or it oscillates with a constant nonzero amplitude. Anti-windup (or anti-reset windup) denotes precautions in the controller to protect it from winding up.

This thesis focuses on proportional-integral-derivative (PID) controllers and their anti-windup. The reason for specializing on PID controllers is that they are (still) the most common controllers. E.g., in Japan more than 90% of the installed controllers are PID controllers. Further, all aspects of anti-windup in PID controllers are not yet fully understood. Usually, the anti-windup is tuned or derived to handle set-point changes. In this thesis PID anti-windup will be treated for disturbances, e.g., measurement noise and load disturbances. In general, anti-windup which is well tuned for disturbances

will also give good set-point performance, while disturbance performance may be very bad when anti-windup is tuned for set-point changes. Many of the PID anti-windup methods can be used also for general controllers.

In most plants there are not only single-loop controllers and saturations. Cascaded control loops are frequently used. Feedforward and multiple-input multiple-output controllers are also used. Other constraints than saturations, e.g., maximum or minimum values of states or measurements are common. These issues are not covered in this work. The author has, however, in earlier work, see, e.g., Rundqvist (1986) and Rundqvist (1988), dealt with windup problems in cascaded control loops where the master controller is a self-tuning controller with integral action. In this control loop the saturation limits for the master controller are unknown until some of the actuators (control valves) are saturated. During special conditions (start of a compressor) it is necessary to *deliberately introduce windup* in the controller, otherwise a severe pressure rise would be obtained. Other plant constraints also had to be considered.

This thesis covers the following topics: A survey over different methods of handling control systems with saturations is given in Chapter 2. The survey includes a classification and unification of many published methods. In Chapter 3 some anti-windup methods for PID controllers are examined and design rules are derived. In Chapter 4 the anti-windup methods and design rules for PID anti-windup are examined in simulations and experiments. Conclusions and suggestions for future work are given in Chapter 5. Preliminary results regarding design rules and evaluation of anti-windup have been reported in Rundqvist (1990).

The main results in the thesis are design rules for anti-windup methods for PID controllers. It is clearly demonstrated that the responses to measurement noise and impulse disturbances to the process are sensitive to the choice of anti-windup parameters. Responses to set-point changes and load disturbances are much less sensitive and, most important, they are well behaved when anti-windup is well chosen with respect to measurement noise and impulse disturbances.

2

Anti-Windup Methods — A Survey

This chapter contains a survey and classification of methods and results regarding control systems with saturations, where many published methods are unified. One class of anti-windup methods is evaluated, using a simple example. There is a bias towards PID controllers in this chapter, although the surveyed anti-windup methods are not limited to PID controllers. General controllers, which are designed to handle saturations, are also briefly discussed.

2.1 Classification of Anti-Windup Methods

A common way to design a controller is to neglect actuator nonlinearities and design a controller based on a linear model, typically with specifications on stability, performance and robustness. To ensure a correct stationary output from the process the controller often contains integrators. In other cases unstable controllers result from the design procedure. This is the case when the desired closed-loop bandwidth is significantly higher than the open-loop bandwidth, see Lilja (1989), or significantly lower, Sternby (1990). Another case is a controller where an unstable mode attempts to capture an exponentially increasing demand in the control signal, see Axelsson (1989). In reality nonlinearities are always present and they must be accounted for.

The first class of anti-windup methods presumes a given linear controller. When the actuator saturates the feedback path is broken. Integrators and

unstable modes must then be prevented from growing too large. Slow stable modes, e.g., in lag controllers, also grow large during saturation and thus also need to be limited. This can be done by a modification of the controller which is active only during saturation. These anti-windup methods are classified as *modified realizations* of linear controllers. The term modified realization includes a number of *ad hoc* methods which are added to a linear controller in order to cope with actuator nonlinearities. Anti-windup methods for PID controllers are among these methods. The purposes of these methods are to both *stabilize* the controller and to give the controller states, e.g., an integrator, good values during saturation.

Another approach to controller design is to include the actuator nonlinearity already at the design stage and the result is denoted *nonlinearly designed controllers*. This covers both linear and nonlinear controllers. Controllers based on mathematical programming are also included in this class.

Some of the nonlinear design and modified realization methods are also available for controllers for multiple-input multiple-output systems.

Discussion

The issues of stability, performance, and robustness are equally important for control systems with constraints. In case of a saturation nonlinearity sufficiently small inputs and initial values keep the process and controller in the linear region where the closed-loop system is stable by design. Thus the control system has a stability region. By either a nonlinear design method or a modified realization it may be possible to extend the stability region. Sometimes the region can be extended to the whole state space.

The nonlinear design methods and the modified realizations must result in satisfactory performance. Usually only command signal performance is considered, while performance for disturbances is neglected. Noise disturbances causing controller saturation may result in a poor performance while command signal performance is satisfactory.

The term *saturation* is well-known and widely used to describe that a control signal exceeds actuator limits. In this work the term *desaturation* is used to describe that the control signal has ceased to exceed these limits. The term *resaturation* is used to describe that saturation occurs after desaturation during the same transient.

The following sections in this chapter give a survey of anti-windup methods based on modified realizations (Sections 2.2–2.5), and nonlinearly designed controllers (Section 2.6). Analysis, discussions and examples are given. In Section 2.7 some analysis methods for nonlinear systems, the describing function method and circle criteria, are briefly recapitulated. These methods are later used for analysis of anti-windup problems.

2.2 Modified Controller Realizations

In this section a number of modified controller realizations will be classified. Most of them originate from PID controllers and are often called anti-windup methods. Thus much of the discussion will focus on the integrator in a PID controller. Therefore PID controllers are briefly recapitulated. For a detailed discussion of PID control, see Åström and Hägglund (1988).

A simple textbook PID controller is

$$V(s) = K \left(1 + \frac{1}{sT_i} + \frac{sT_d}{1 + sT_d/N} \right) E(s) \quad (2.1)$$

where K is the controller gain, T_i and T_d are the integral and derivative times respectively, N is a filter factor, V is the control signal and E is the control error. The actuator nonlinearity, e.g., a saturation, is part of the process. Usually a saturation is included also in the controller, such that only a saturated control signal is the input to the actuator. The saturation limits in the controller must then agree well with corresponding limits in the actuator. The saturated control signal is

$$u(t) = \text{sat}(v(t)) \quad (2.2)$$

where the unit gain saturation function is given by

$$\text{sat}(u) = \begin{cases} u_{\max} & \text{if } u > u_{\max} \\ u & \text{if } u_{\min} \leq u \leq u_{\max} \\ u_{\min} & \text{if } u < u_{\min} \end{cases} \quad (2.3)$$

and where u_{\max} and u_{\min} are upper and lower controller limits respectively. Besides limiting the control output with a saturation, it is also common to limit the derivative part or limit the rate of change of the control signal.

Classification of Modified Realization Methods

The modified realization methods intend to prevent controller states from growing large during saturation, and, in some cases, to give the controller states good values. One approach, used in *conditional integration methods*, is to switch off integration at certain conditions. Another approach is to use feedback from the control signal and the saturated control signal, such that the difference between the signals drives the control signal to a good value. This approach has similarities with state observers and is denoted the *observer approach*. In a third approach the *controller input is limited* in order to avoid growing controller states. These three groups of modified realizations will be discussed in more detail in the following sections.

2.3 Conditional Integration Methods

The purpose of an integrator is to remove steady-state errors in the process output. A simple approach to avoid integrator windup is to switch off integration when the controller is far from steady-state. Five basic methods for switching off integration will be discussed.

- C1 Stop integrating when the control error is large, i.e., when $|e(t)| > e_0$.
- C2 Stop integrating when the controller saturates, i.e., when $u \neq v$ in (2.2).
- C3 Stop integrating when the controller saturates (as in C2) and the control error e has the same sign as the control signal v .
- C4 Limit the integrator i such that, e.g., $|i(t)| \leq i_0$.
- C5 Stop integrating and assign a predetermined or computed value to the integrator when a specified condition is true.

Methods C4–C5 are classes of methods while C1–C3 are exact descriptions. The methods are characterized by an `if ... then ... else`-structure in the controller code where the integrator is updated either proportionally to the control error or by an entirely different expression. The update is usually a discontinuous function.

Methods C1–C2 are textbook methods. They are rarely used in practice but are useful in the comparison below. Method C3 is found in, e.g., Fertik and Ross (1967) and Gallun *et al.* (1985), where it is used in position form digital PID controllers, and in Phelan (1977, p. 187), where it is used in analog PI and PID controllers. Method C4 is sometimes called the “Intelligent Integrator”, see Phelan (1977, p. 117), Krikilis (1980) and Krikilis and Barkas (1984). It is also used in commercial controllers, e.g., the TL106 from Fisher Controls. Method C5 is used mainly during start-up.

Evaluation of Conditional Integration Methods

The conditional integration methods will now be compared. Their behaviors are illustrated using a simple example.

EXAMPLE 2.1

Let the process be an integrator, $1/s$, with PI control where $K = T_i = 1.5$, i.e., the closed-loop system has natural frequency $\omega = 1$ rad/s and relative damping $\zeta = 0.75$. The controller output is limited to the interval $[-1, 1]$. The performance for different initial values will be presented in a phase plane, where the integral part, i , of the controller is plotted versus control error e . Set-point changes correspond to initial values $e \neq 0$, $i = 0$ and load disturbances correspond to $e = 0$, $i \neq 0$. \square

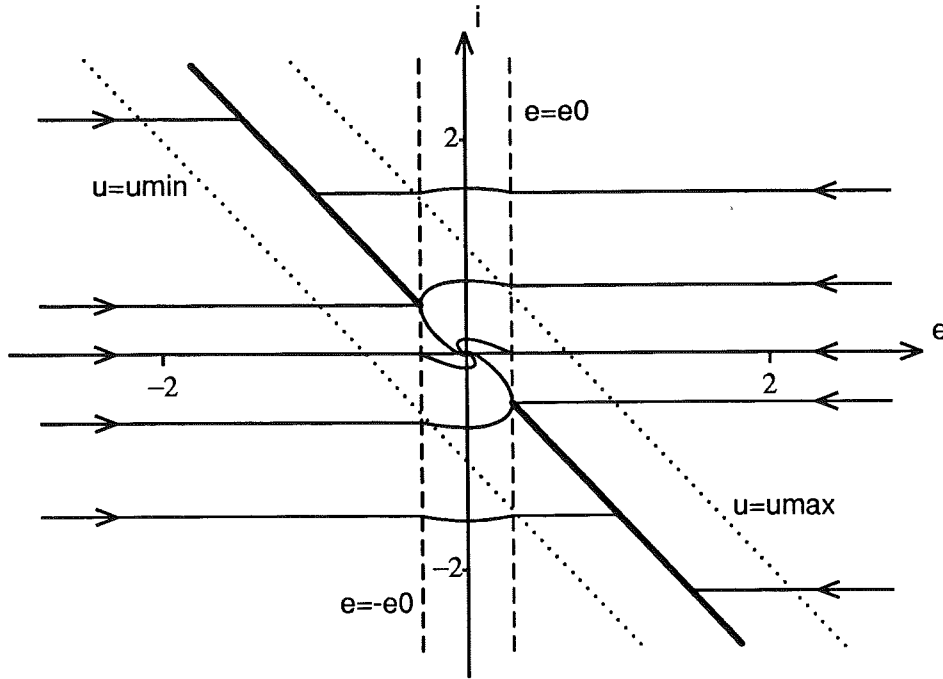


Figure 2.1 Evaluation of method C1, which suspends integration when $|e| > e_0$, using Example 2.1. The integrator state i is plotted versus control error e . The stationary points are the origin and the thick solid lines, at which $u = 0$ when integration is suspended.

Method C1

In Figure 2.1 method C1, which suspends integration when $|e| > e_0$, is simulated using Example 2.1. The stationary points are in the origin and at $u = 0$ when $|e| > e_0$. Thus all set-point changes without load disturbances (which in this example has $i = 0$ initially) are handled well, but trajectories with large initial values of i get stuck at $e \neq 0$. Note that this may happen for i such that $u_{\min} \leq i \leq u_{\max}$, see Figure 2.1. The main drawback in method C1 is that integration may be stopped even if u is far from saturation, i.e., in the “linear strip” around $u = 0$, and integration may not be resumed. Thus it is not advisable to use this method.

Method C2

Method C2 is a natural modification of method C1: integration is suspended during saturation but continues in a “linear strip” around $u = 0$. In Figure 2.2 method C2 is simulated using Example 2.1. The origin is the only stationary point. However, large initial values for the integrator, give large overshoots since integration is stopped until desaturation. It would be advantageous to resume integration as soon as the control error has changed sign. Feedforward signals added to the control signal, causing saturation, may also give large

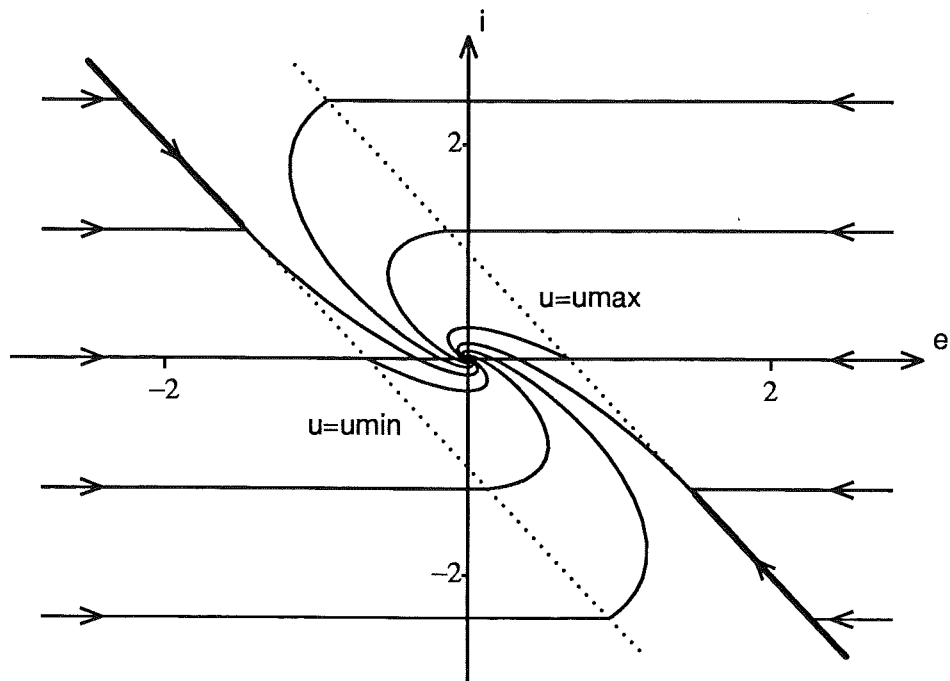


Figure 2.2 Evaluation of method C2, which suspends integration during controller saturation, using Example 2.1. The origin is the only stationary point. The method gives chattering at the thick solid lines.

overshoots. If the process has finite gain there are stationary points $e = -G_p(0)u_{\max}$ for large positive i and $e = -G_p(0)u_{\min}$ for large negative i outside the “linear strip”. Using method C2 the process is then stuck at one of the output limits.

Method C3

Method C3 is a modification of method C2 where the integral is updated if the saturation and the control error have opposite signs, even if the controller is saturated. In Figure 2.3 method C3 is simulated using Example 2.1. The overshoot for trajectories with large integrator initial values are smaller than for method C2. Feedforward signals causing saturation do not give large overshoots either. There are no stationary points outside the “linear strip” for processes with finite static gain.

Comparison of Methods C1, C2 and C3

Methods C1–C3 have an almost identical performance for set-point changes, when $i = 0$ initially. There are, however, differences between the methods when the integrator i has large initial values. Method C3 is best for Example 2.1, since it has only one stationary point and in general smaller overshoots.

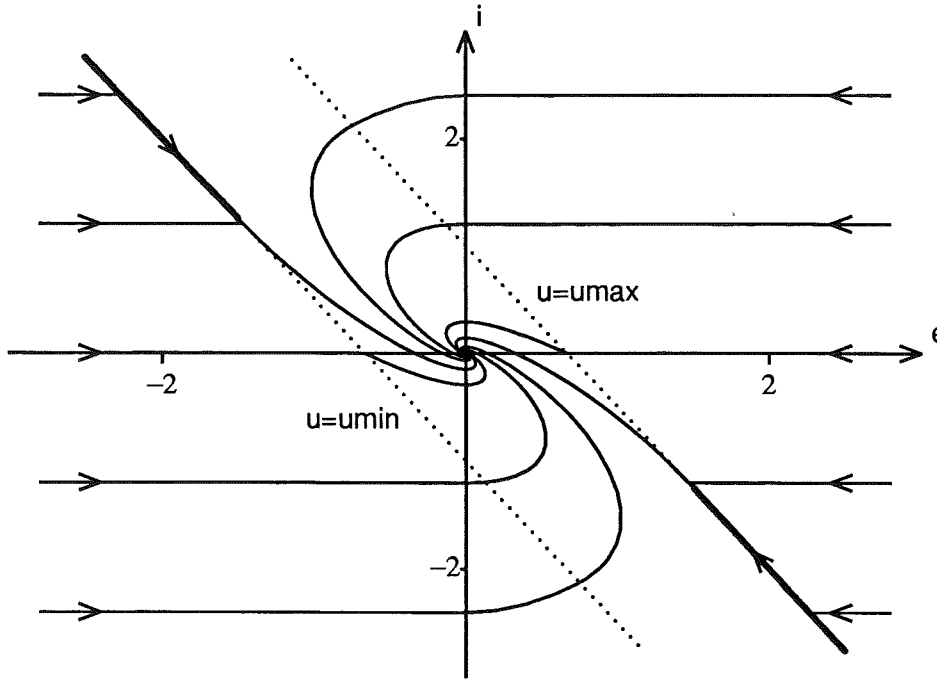


Figure 2.3 Evaluation of method C3, which suspends integration during controller saturation unless the control error is in the opposite direction, using Example 2.1. The origin is the only stationary point. The method gives chattering at the thick solid lines.

Chattering

Methods C2 and C3 have a common problem. Sliding-modes may appear if the saturation disappears for non-zero control error because the input to the integrator is discontinuous in $u - v$. The discontinuity can be removed by introducing a boundary layer which makes $\frac{di}{dt}$ continuous in both e and $u - v$. Then, e.g.,

$$\frac{di}{dt} = \begin{cases} \max\left(f_i \frac{K}{T_i} e, \frac{K}{T_i} e\right), & \text{if } v < u \\ \frac{K}{T_i} e, & \text{if } v = u \\ \min\left(f_i \frac{K}{T_i} e, \frac{K}{T_i} e\right), & \text{if } v > u \end{cases} \quad (2.4)$$

where f_i may be given by

$$f_i = 1 - \frac{\min(\varepsilon, |u - v|)}{\varepsilon} \begin{cases} = 1, & \text{if } u = v \\ < 1, & \text{if } 0 < |u - v| < \varepsilon \\ = 0, & \text{if } |u - v| \geq \varepsilon \end{cases} \quad (2.5)$$

and ε is the width of the boundary layer, a suitable fraction of $u_{\max} - u_{\min}$.

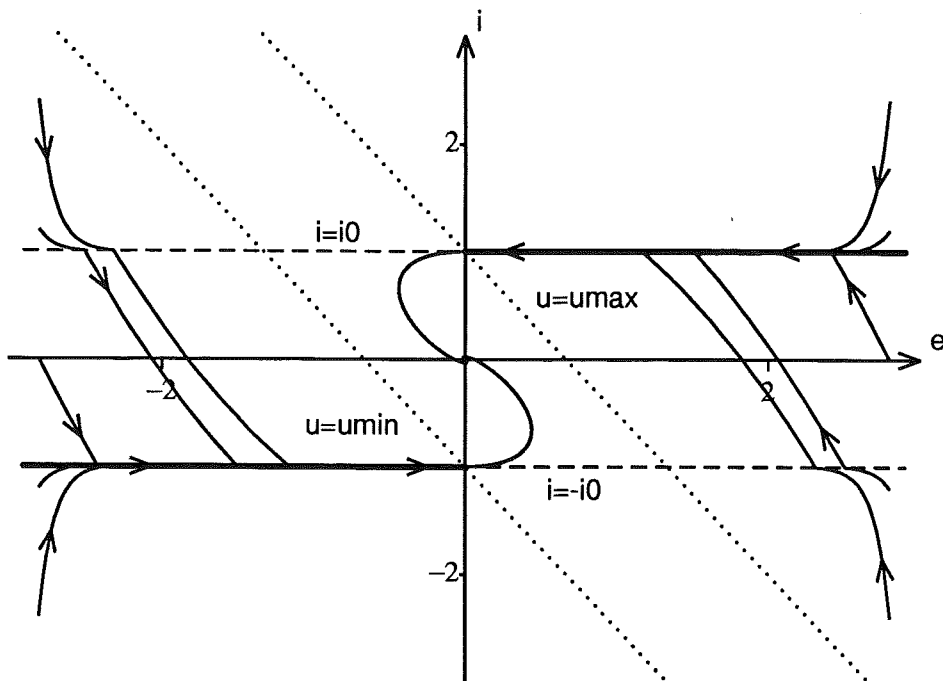


Figure 2.4 Evaluation of method C4, which limits the integrator to the interval $\pm i_0$, using Example 2.1. Hard feedback is used on i if $|i| > i_0$. The origin is the only stationary point. The method gives chattering at the thick solid lines.

In a continuous-time PID controller ε can be less than 1% of the control interval but in a discrete-time PID controller ε must be 10–20% of the interval. Otherwise chattering is not eliminated. Thus the width ε of the boundary layer is problem dependent, i.e., methods C2 and C3 has a tuning parameter, ε .

Method C4

In Figure 2.4 method C4, which limits the integrator such that $|i| < i_0$, is tested using Example 2.1. The integration limits coincide with the controller limits, i.e., $i_0 = 1$. If $|i| > i_0$ “hard” feedback brings i back to the desired interval. This method has chattering and thus requires a boundary layer. Compared with methods C2 and C3 there is a considerably smaller overshoot for cases where both e and i have large initial values, but when $i = 0$ initially, the method gives larger overshoots than methods C2–C3. Desaturation occurs when $e = 0$. Earlier desaturation and smaller overshoot is obtained for smaller i_0 , but then a load disturbance l_0 , where $u_{\max} > l_0 > i_0$, such that the load could have been balanced by the control signal, instead gives a stationary error.

It is thus clear that the limits for integration must be chosen such that the control signal u can use the full span of the actuator. If the control limits

are asymmetric or the set point y_r and the output y are weighted differently, asymmetric integration limits are required. The limits may then depend on both the set point and controller parameters, as well as the controller limits. This is noted in, e.g., French and Cox (1990), where method C4 is used in a state feedback controller with integral action. The integration limits are adjusted both by a feedforward term, based on predicted load, and a feedback term, based on control error. These enhancements make their method resemble tracking anti-windup, see Section 2.4.

Discussion of the C5 Methods

In these methods the integrator is assigned a special value when integration is suspended. In controllers with a “batch unit”, see Shinskey (1988), the preload i_0 is a value assigned to the integrator when the controller saturates. Thus the control signal is

$$v(t) = K e(t) + i_0 \quad (2.6)$$

during saturation. Separate preloads for upper and lower saturation can be given. Integration continues when the controller desaturates. Thus the preload i_0 determines when the controller desaturates. Thereby the amount of overshoot can be adjusted. Although this method has a different implementation, it is almost equivalent to method C4 in Figure 2.4 if $i_0 = u_{\max}$ at upper saturation and vice versa.

A similar approach is suggested in Thomas *et al.* (1983), where the integral part is “continuously” updated during saturation from the process output $y(t)$ and a load estimate l_0 . The exact update for the controller in (2.1) is given by

$$i(t) = \frac{y(t)}{K_p} + l_0 \quad (2.7)$$

where K_p is the (estimated) static process gain. The update formula is derived for a PI controller and first order process. The control signal during saturation is

$$v(t) = K e(t) + l_0 + \frac{y(t)}{K_p} \quad (2.8)$$

This method is practically equivalent to preload, since l_0 and K_p correspond to i_0 , and then also to method C4 in Figure 2.4.

In Kramer and Jenkins (1971) an optimal control error e^* for desaturation, and a corresponding integral part i_0^* are determined. However, since a smooth desaturation is a prerequisite in the optimization, the method turns out to be equivalent to preload in the sense that i_0^* in fact determines when the controller desaturates. The value i_0^* , however, in this approach depends

on the set point y_r , the controller limits and parameters and, finally, the process. A different i_0^* is used during rate limiting.

Rosza (1989) uses the limited integrator, method C4, with an extension for override control in a digital PID controller. The integral part is then updated such that

$$i(t) = u(t-1) \quad \text{when } u(t-1) \neq v(t-1) \quad (2.9)$$

where $u(t-1)$ and $v(t-1)$ are the override and control signals respectively of the previous sampling instant.

The “cutback” method, see Howes (1988), is used in, e.g., the Eurotherm EM-1 controller. The operator determines two values of the process output where the controller desaturates. These values are called upper and lower “cutback points”. They are used when approaching the set point from above and below respectively. The cutback method is equivalent to assigning a specified value to the integrator when the process output y is outside the cutback interval, and the method is thus equivalent to preload.

The C5 methods are primarily designed for large set-point changes. They are very similar to method C4. By choosing i_0 and (l_0, K_p) in (2.6) and (2.7) respectively the overshoot is adjusted. Methods C4–C5 have the drawback that integral action may be lost, if i_0 or (l_0, K_p) are carelessly chosen. The “cutback” method, as presented in Howes (1988), is designed for the start-up problem. Saturation and anti-windup in the presence of disturbances are not at all considered in the paper.

Summary

In Figure 2.5 methods C1–C4 are compared for one initial condition, namely $y = -2.8$ (i.e., $e = 2.8$) and $i = 2.4$ using Example 2.1. Method C1 does not resume integration for the chosen initial condition, and thus get a stationary error. Method C2 has slightly higher overshoot than method C3, because C2 does not resume integration until the controller desaturates. When method C3 is used integration resumes when the control error changes sign. Above it was pointed out that methods C1–C2 (may) have stationary point outside the origin. Thus method C3 is the best out of C1–C3.

Method C4 has the lowest overshoot and the fastest desaturation in Figure 2.5. However, comparing Figures 2.3 and 2.4, method C3 has smaller overshoot and faster desaturation if instead $i = 0$ initially. For Example 2.1, where the process is an integrator, $i = 0$ and $e \neq 0$ are the initial conditions corresponding to a regular set-point change without any disturbances. If the possible difficulties in choosing integration limits for method C4 are added, e.g., parameter and set-point dependencies, the conclusion is that method C3 is better than C4, since it is simpler and more robust. In the sequel only method C3 will be used when conditional integration is tested.

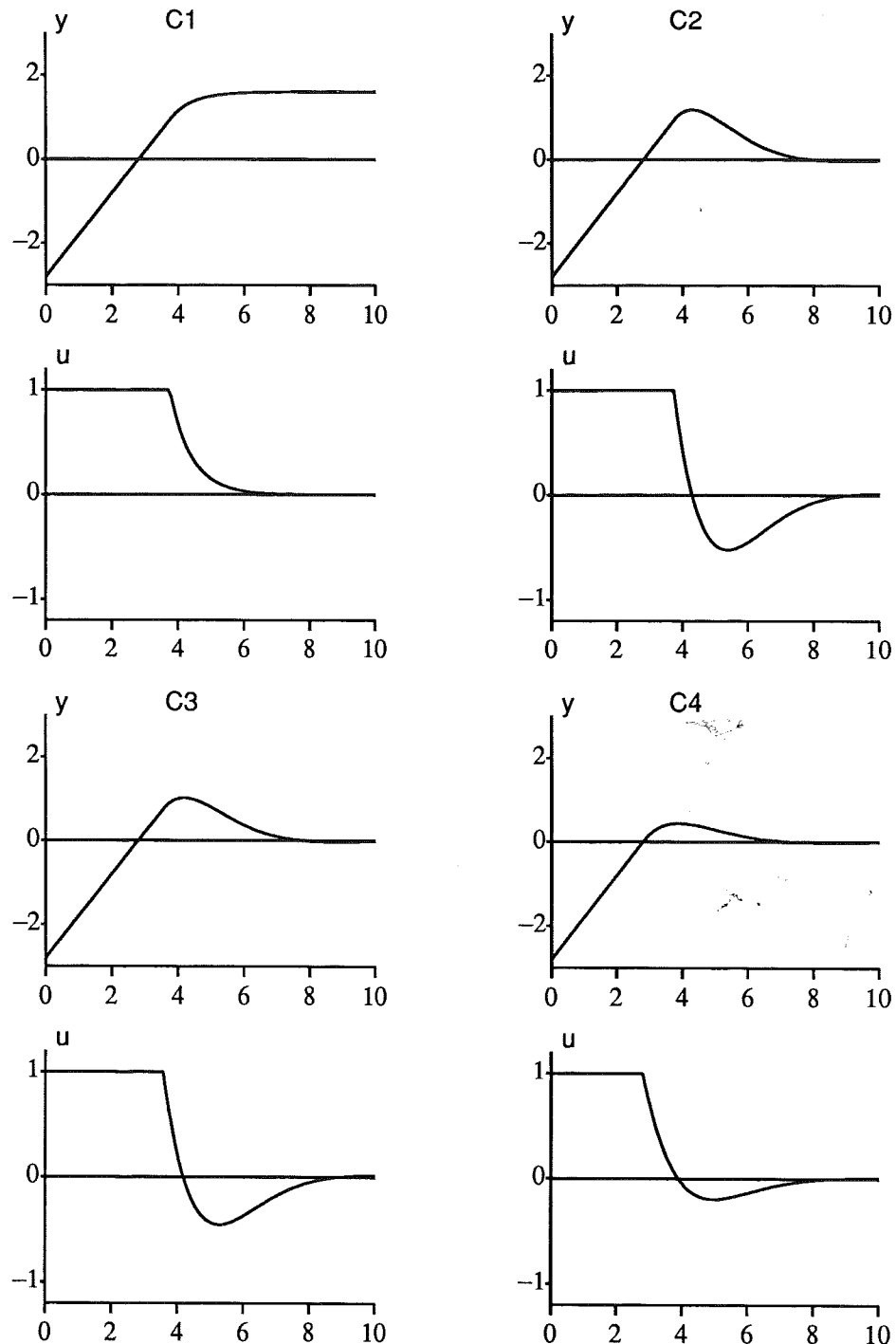


Figure 2.5 Comparison between methods C1–C4 using Example 2.1 for the initial condition $y = -2.8$ (i.e., $e = 2.8$) and $i = 2.4$. Method C1 does not resume integration, which explains the static error. Method C2 has slightly higher overshoot than C3 and method C4 desaturates faster than the other methods. For other initial values method C3 desaturates faster than method C4.

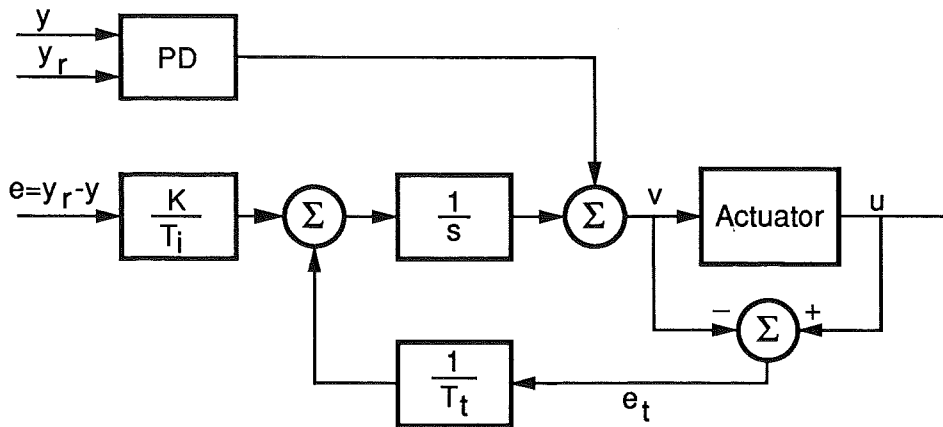


Figure 2.6 PID controller with anti-windup based on tracking.

The C5 methods are restricted to the start-up problem in (batch) processes where it is reasonable to assume that (load) disturbances at the operating point do not cause saturation. This is an important special case.

All conditional integration methods have at least *one parameter* to tune, e.g., e_0 , i_0 , etc. For methods C2–C3 a boundary layer width ε needs tuning. A boundary layer was used in method C4 as well and may be necessary in some of the C5 methods too. In Kramer and Jenkins (1971) a first order process model must be given.

2.4 Observer Methods

In this section anti-windup methods similar to state observers will be discussed. In a controller based on a state observer all controller states are stable if the observer uses the saturated control signal u and the process output y for reconstruction of process states. Thus windup will not occur in such a controller, even if the controller saturates. A general anti-windup strategy is then to treat all controllers as if they were based on a state observer.

In controllers with integral action, e.g., PID controllers, it is common practice to use nonlinear feedback from the control signal, see Figure 2.6. This is a special case of the observer interpretation of a controller. The approach is often denoted *tracking* or *back calculation* and will be discussed first.

Tracking or Back Calculation

The idea of *back calculation* was proposed by Fertik and Ross (1967) for a velocity limited incremental PI algorithm. The idea is that the controller state is recomputed such that the controller output is exactly at the saturation limit. During velocity saturation the controller thus *tracks* given inputs

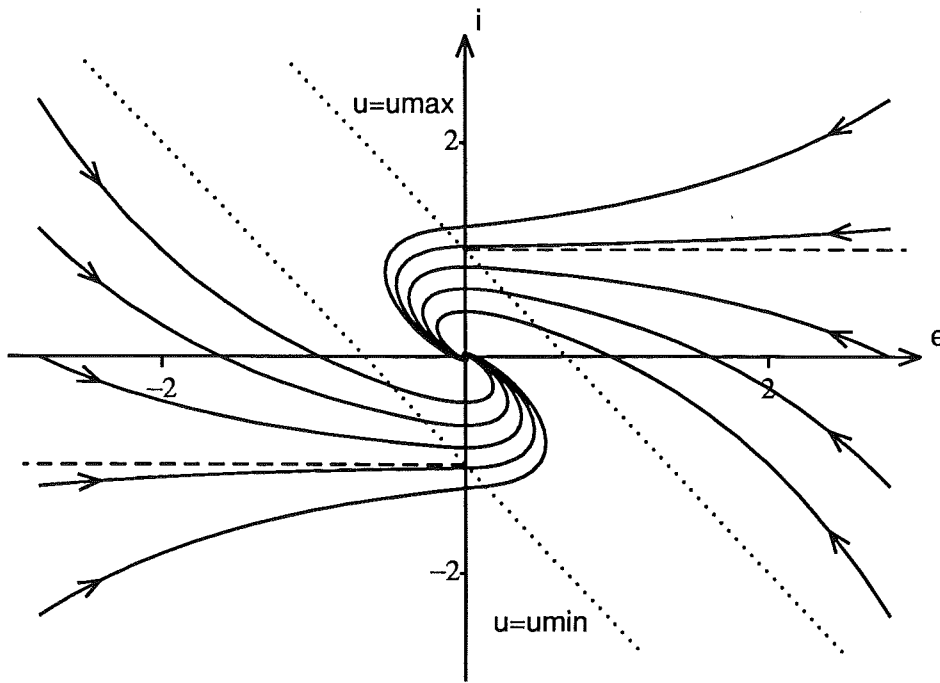


Figure 2.7 Evaluation of tracking anti-windup with $T_t = T_i$ using Example 2.1. Trajectories starting on the dashed lines remain there until desaturation. The origin is the only stationary point.

and outputs. Fertik and Ross also suggested that the controller state is kept constant during position saturation, i.e., they combine back calculation and conditional integration. Further, they found that back calculation is not a good method for (incremental) PID controllers since it “.. results in a delayed derivative action which can cause overshoot of the controlled variable ...”. Here they instead prefer conditional integration by method C3, see Section 2.3 . Back calculation and conditional integration is also combined in Dreinhoefer (1988).

For a position form PID controller back calculation recomputes the integral part to match given inputs and outputs. It was found advantageous not to reset the integrator in one sampling period but dynamically with a time constant T_t . This is in the sequel denoted *tracking*. A rule of thumb given in the literature for the choice of T_t has been $T_t \approx T_i$, where T_i is the integral time. Figure 2.6 shows a block diagram of a PID controller with tracking anti-windup. Thus the main idea in tracking (and back calculation) is to give good values to the controller states.

In Figures 2.7–2.8 tracking anti-windup is evaluated using Example 2.1. See also Figures 2.1–2.4 where conditional integration methods are evaluated. For $T_t = T_i$ the overshoot depends on the initial value of i . For larger initial values of e the trajectories converge to the asymptotic (dashed) lines.

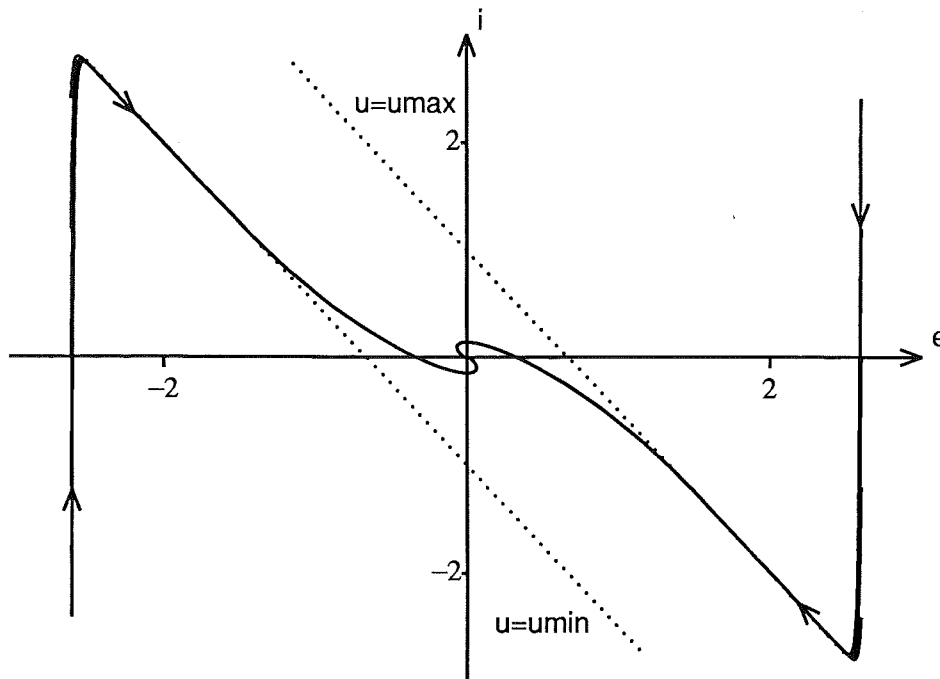


Figure 2.8 Evaluation of tracking anti-windup with $T_t = T_i/100$ using Example 2.1. All trajectories (for the chosen initial conditions) “immediately” follow the controller limits, but there is no chattering.

Then the performance is similar to the best obtainable for method C4, see Figure 2.4. For tracking anti-windup, however, $T_t < T_i$ results in earlier desaturation but disturbances are still handled well compared to method C4, since the integrator i is not restricted to stay within any predetermined interval. For $T_t = T_i/100$, see Figure 2.8, the integrator i is “immediately” given a value such that the controller is at the saturation limit, which results in an early desaturation and a small overshoot. In Figure 2.9 the time responses for $T_t = T_i$ and $T_t = T_i/100$ are compared for the initial condition $y = -2.8$ (i.e., $e = 2.8$) and $i = 2.4$ using Example 2.1. Compare Figure 2.5. For $T_t = T_i$ and method C4 the performance is almost identical. This was discussed above. When $T_t = T_i/100$ the overshoot is very small due to the fast desaturation of the controller.

The discussion indicates that a small value of T_t is advisable. However, it will later be shown that $T_t = T_i/100$ is a much too small value due to large disturbance sensitivity. Besides $T_t > 0$, for stability of the controller, there is no lower limit for T_t reported in the literature.

Controllers with tracking are discussed in, e.g., Åström (1987), Glattfelder and Schaufelberger (1983), Glattfelder *et al.* (1983), Glattfelder and Schaufelberger (1986), and Glattfelder *et al.* (1988). Kapasouris and Athans (1985) use tracking anti-windup for an integrating multivariable controller.

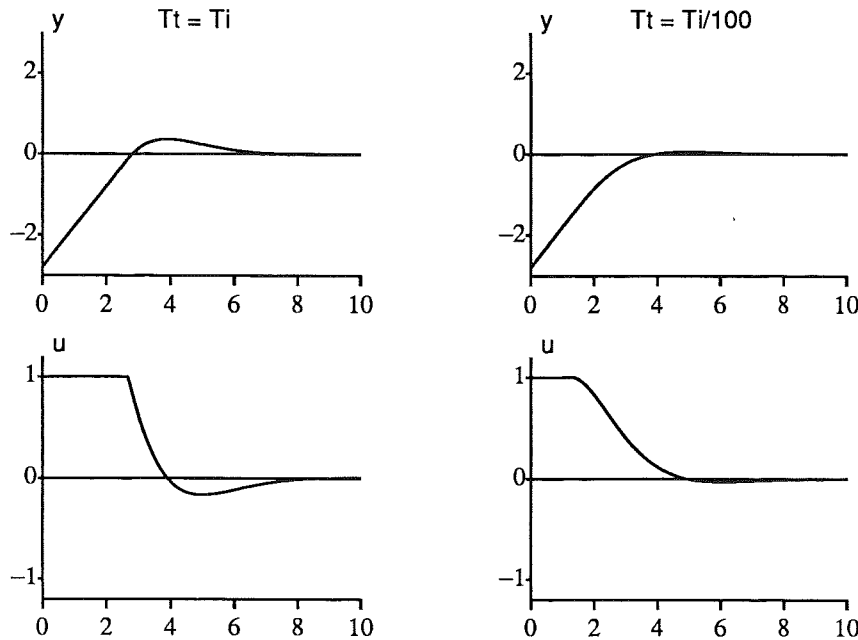


Figure 2.9 Comparison between tracking time constants $T_t = T_i$ and $T_t = T_i/100$ using Example 2.1 for the initial condition $y = -2.8$ (i.e., $e = 2.8$) and $i = 2.4$. For $T_t = T_i$ the performance is almost identical to that of method C4 in Figure 2.5. When $T_t = T_i/100$ the controller desaturates much faster and the overshoot is very small.

The Observer Approach

Now the general observer based anti-windup will be discussed. In state space formulation a feedback controller is viewed as a combination of an observer and a state feedback. This leads to ideas on how anti-windup should be included in a controller. Consider the following example.

EXAMPLE 2.2

Assume that the process is given by

$$\begin{aligned} \frac{dx}{dt} &= Ax + Bu & (2.10) \\ y &= Cx \end{aligned}$$

and that state feedback and observer gain vectors L and K respectively and the gain L_r have been computed for the controller

$$\frac{d\hat{x}}{dt} = (A - KC)\hat{x} + Bu + Ky \quad (2.11a)$$

$$v = -L\hat{x} + L_r y_r \quad (2.11b)$$

$$u = \text{sat}(v) \quad (2.11c)$$

The observer (2.11a) does not suffer from windup since \hat{x} is only updated from the process input and output. From the observer design $A - KC$ is a stable matrix. \square

The following anti-windup method was originally given in Åström (1983) and is also described in Åström and Wittenmark (1990). The idea is to resemble the structure of the observer based controller (2.11). Consider the following realization of a controller

$$\begin{aligned}\frac{dx}{dt} &= Fx + G_r y_r - G_y y \\ v &= Hx + D_r y_r - D_y y \\ u &= \text{sat}(v)\end{aligned}\tag{2.12}$$

where F may be an unstable matrix. The general way to avoid windup in (2.12) is similar to tracking anti-windup, i.e., use feedback from $u - v$. Then

$$\begin{aligned}\frac{dx}{dt} &= Fx + G_r y_r - G_y y + M(u - v) \\ &= (F - MH)x + (G_r - MD_r)y_r - (G_y - MD_y)y + Mu \\ v &= Hx + D_r y_r - D_y y \\ u &= \text{sat}(v)\end{aligned}\tag{2.13}$$

If $H = -L$, $M = B$, $F - MH = A - KC$ etc., the correspondences with (2.13) and the observer and state feedback in (2.11) are obvious. Therefore the anti-windup method in (2.13) is denoted the *observer approach*. M must be chosen such that $F - MH$ is a stable matrix.

The observer approach can be used for controllers given by transfer functions as well. Assume that the original controller is given by

$$\begin{aligned}V(s) &= G_{ff}(s)Y_r(s) - G_{fb}(s)Y(s) = (H(sI - F)^{-1}G_r + D_r)Y_r(s) \\ &\quad - (H(sI - F)^{-1}G_y + D_y)Y(s)\end{aligned}\tag{2.14}$$

Introducing anti-windup compensation by the observer approach yields

$$\begin{aligned}V(s) &= G_{ff}(s)Y_r(s) - G_{fb}(s)Y(s) + W(s)(U(s) - V(s)) \\ &= G_{ff}(s)Y_r(s) - G_{fb}(s)Y(s) + H(sI - F)^{-1}M(U(s) - V(s)) \\ u(t) &= \text{sat}(v(t))\end{aligned}\tag{2.15}$$

if the anti-windup in (2.13) and (2.15) coincides. The controller can also be given on polynomial form, e.g.,

$$R(s)V(s) = T(s)Y_r(s) - S(s)Y(s)\tag{2.16}$$

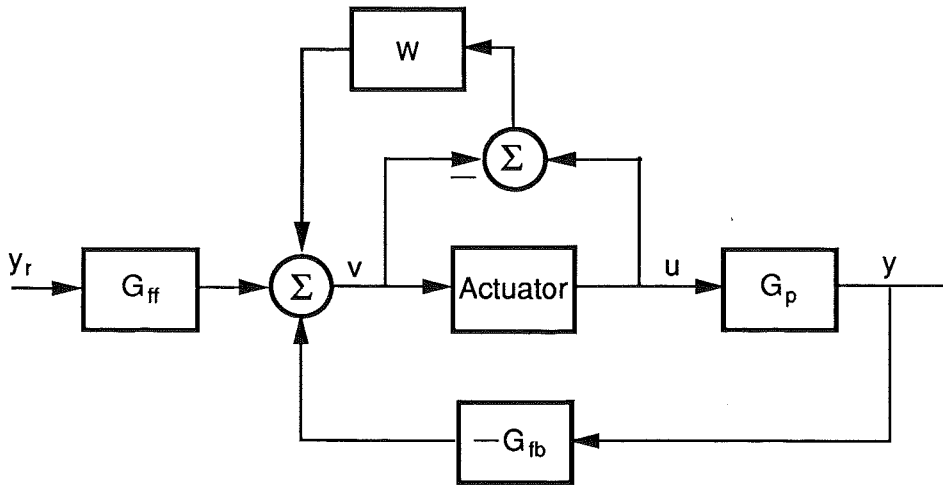


Figure 2.10 A control system with saturation and anti-windup by the observer approach. G_{ff} , G_{fb} and W are given in (2.14) and (2.15).

Introducing anti-windup compensation by the observer approach yields

$$\begin{aligned} A_o(s)V(s) &= T(s)Y_r(s) - S(s)Y(s) + (A_o(s) - R(s))U(s) \\ u(t) &= \text{sat}(v(t)) \end{aligned} \quad (2.17)$$

where the observer polynomial

$$A_o(s) = \det(sI - F + MH) \quad (2.18)$$

if the anti-windup in (2.13) and (2.17) coincides. Anti-windup by the observer approach can be described by the block diagram in Figure 2.10.

Tracking and back calculation are special cases of the observer approach where unstable states, e.g., integrators, are stabilized by feedback during saturation while stable states are left unaffected. For the PID controller in (2.1), tracking anti-windup according to Figure 2.6 is obtained if

$$M = \begin{pmatrix} \frac{1}{T_t} \\ 0 \end{pmatrix}, \quad W(s) = \frac{1}{sT_t} \quad \text{and} \quad A_o(s) = \left(s + \frac{1}{T_t} \right) \left(s + \frac{N}{T_d} \right) \quad (2.19)$$

for the state space, transfer function and polynomial forms respectively. For the PID controller $R(s) = s(s + N/T_d)$. Thus $A_o(s)$ clearly shows that tracking anti-windup moves one controller pole from 0 to $-1/T_t$ while the other pole is unaffected.

Many versions of anti-windup can be summarized in the formulas above. In Walgama and Sternby (1990) a number of different anti-windup methods for, e.g., discrete-time PID controllers have been interpreted in terms of their equivalent observer polynomials A_o .

Many anti-windup methods in the literature are special cases of the observer approach. In Parrish and Brossilow (1985) a dead-beat observer is used for a discrete-time lead/lag controller. Dead-beat observers are also used in adaptive controllers in, e.g., Abramovitch and Franklin (1987), Abramovitch *et al.* (1986) and Payne (1986). Here the dead-beat observer is a consequence of the prediction model

$$\hat{y}(t+1) = \hat{A}y(t) + \hat{B}u(t) = \hat{\theta}\varphi(t) \quad (2.20)$$

which is used in the parameter estimation. In Zhang and Evans (1988) a dead-beat observer is used for a rate constrained adaptive controller. In order to rewrite the suggested controller to the polynomial form (2.17) the saturation function must be replaced by a rate saturation function. This illustrates that the saturation can be replaced by other nonlinearities.

Segall *et al.* (1991) derive a discrete-time one-step optimal correction for a saturated controller. The resulting controller can be interpreted in terms of R , S , T and A_o polynomials (or polynomial matrices).

The conditioning technique, see Hanus *et al.* (1987), is another special case of the observer approach. The idea behind this technique is to compute the “realizable reference” \hat{y}_r , i.e., the reference value that, given the controller state x and process output y in (2.12), would just saturate the controller, i.e.,

$$u = \text{sat}(v) = Hx + D_r\hat{y}_r - D_yy \quad (2.21)$$

Then

$$u - v = D_r(\hat{y}_r - y_r) \quad (2.22)$$

If D_r is left invertible \hat{y}_r can be computed and is then used instead of y_r in the differential equation in (2.12). This is equivalent to letting $M = G_rD_r^{-1}$ in (2.13). If D_r is singular the left inverse D_r^\dagger , i.e., $D_r^\dagger D_r = I$, is used instead of D_r . The controller states x are then not directly affected by the reference signal y_r during saturation. The eigenvalues of $F - G_rD_r^{-1}H$ are equal to the transmission zeros of the controller.

The conditioning technique is also discussed in Hanus (1988) and Henrotte (1988). Banyasz *et al.* (1985) use the conditioning technique for an adaptive PID controller with error feedback.

Observer Interpretation of Back Calculation

Back calculation is a special case of the observer approach. It may be interesting to see where back calculation places the observer poles. Two cases, incremental and position PI controllers will be examined.

EXAMPLE 2.3—Incremental PI controller

Fertik and Ross (1967) discuss the velocity limited incremental PI controller

$$\begin{aligned} x(k+1) &= e(k) \\ \Delta v(k) &= -Kx(k) + K\left(1 + \frac{h}{T_i}\right)e(k) \\ \Delta u(k) &= \text{sat}(\Delta v(k)) \end{aligned} \quad (2.23)$$

with sampling interval h . A backward-difference is used when approximating the derivative. Thus the state is $x(k) = e(k-1)$. Back calculation means "adjust the state to match given inputs and outputs". Thus the state update should use the effective or realizable control error $e^*(k)$ that would just saturate the controller, i.e.,

$$x(k+1) = e^*(k) = e(k) + \frac{\Delta u(k) - \Delta v(k)}{K(1 + h/T_i)} \quad (2.24)$$

Rewriting and identifying the matrices F , H and M in (2.12) and (2.13) gives that the observer polynomial, see (2.18), is

$$A_o(z) = \det(zI - F + MH) = z - \frac{T_i}{T_i + h} \quad (2.25)$$

The observer pole, from (2.25), equals the zero in the transfer function for (2.23). Hence back calculation and the conditioning technique are equivalent for (2.23). In continuous time the corresponding time constant is $T = T_i$. \square

EXAMPLE 2.4—Position form PI controller

The corresponding position form PI controller in Fertik and Ross (1967) is

$$\begin{aligned} x(k+1) &= x(k) + K \frac{h}{T_i} e(k) \\ v(k) &= x(k) + K\left(1 + \frac{h}{T_i}\right)e(k) \\ u(k) &= \text{sat}(v(k)) \end{aligned} \quad (2.26)$$

Thus the state $x(k)$ is the integral of the control error. Back calculation means "adjust the state to match given inputs and outputs", i.e., determine the state $x^*(k)$ such that

$$u(k) = x^*(k) + K\left(1 + \frac{h}{T_i}\right)e(k) \quad (2.27)$$

and use $x^*(k)$ in the state update. Then

$$\begin{aligned} x(k+1) &= x^*(k) + K \frac{h}{T_i} e(k) = u(k) - K e(k) \\ &= x(k) + K \frac{h}{T_i} e(k) + u - v \end{aligned} \quad (2.28)$$

Identifying the matrices F , H and M in (2.12) and (2.13) gives that the observer polynomial, see (2.18), is

$$A_o(z) = \det(zI - F + MH) = z \quad (2.29)$$

i.e., a dead-beat observer. In continuous time the corresponding time constant is $T = 0$. \square

Thus the equivalent observer poles depend on which entity is back calculated. Back calculation of the integral part gives a fast observer pole while back calculation of the control error in an incremental algorithm gives a moderate speed of the observer pole.

Multivariable Extensions

There is some freedom left in the anti-windup when a multi-variable controller is unsaturated in some of the control signals. In Campo and Morari (1990) *direction preservation* combined with the conditioning technique is used on ill-conditioned multivariable plants. The direction preservation scales the control signals such that the maximum control signal is at the saturation limit while the others are proportionally scaled down. This seems to be an important issue for ill-conditioned plants which are very sensitive to changes in control signal direction.

In Hanus and Kinnaert (1989) the approach taken is to determine the “best” realizable reference which would just saturate the controller. This reference signal is then used to update the controller states by the conditioning technique. There are two suggestions for determining the reference signal, the first is a quadratic programming problem for all reference inputs and the other orders the references in increasing order of importance. If m inputs are saturated the first m (less important) references are recomputed by quadratic programming. In some cases this is an alternative way of obtaining direction preservation.

Summary

Many anti-windup methods suggested in the literature can be interpreted as observer-based anti-windup, although not all authors are aware of this interpretation. With only a few exceptions, e.g., the conditioning technique

and dead-beat observers in adaptive controllers, there are no general guide lines for how to choose the observer poles. In tracking anti-windup only one pole is placed and a rule of thumb has been to choose $-1/T_i$. In Chapters 3–4 the choice of observer poles for PID controllers anti-windup will be treated.

2.5 Input Limitation Methods

The main idea in these methods is to limit the controller input such that saturation is avoided. A simple approach is to low pass filter the reference signal, which gives a slower response, but the controller does not necessarily remain unsaturated. In order to avoid slowing down the closed-loop system for small signals a *jump-and-rate-limiter* may be used instead of a low pass filter. Small signals are not affected by the limiter, but larger signals are limited both in initial magnitude and rate of change. It is, however, still not guaranteed that saturation will not occur. Irrespective of how the reference signal is filtered, disturbances may cause saturation and thus windup.

In Pajunen and Steinmetz (1987) a time-varying reference model is used in order to combine both minimum-time and unsaturated control signals for an adaptive controller. This approach is rather similar to using a jump-and-rate limiter. In Noguchi *et al.* (1987) a time-varying moving average (MA) filter is placed between the controller and the actuator. Although the filter is not placed at the controller input the basic idea is the same. In case of large control signals the filter is supposed to “spread out” the control action such that the actuator remains unsaturated. For small control signals the filter has no influence. The filter is included in the adaptive control design. Both methods contain *ad hoc* rules and are incompletely specified with respect to the order and parameters of the filters.

Kapasouris' Method

In Kapasouris (1988), Kapasouris *et al.* (1988, 1989) a type of input limitation is used for multivariable controllers with integral action. For stable processes a diagonal gain $\lambda(t)$ is placed at the controller input, see Figure 2.11, where $0 \leq \lambda(t) \leq 1$. The value of $\lambda(t)$ is chosen such that the controller $K(s)$ never saturates. For large set-point changes the response of the system is approximately only slower than it would have been without the saturation. The method is computationally intensive and requires an on-line or off-line computation of $g(x_0)$, the maximum norm of the desired control signal $v(t)$, for $t \geq 0$ and “all” initial values x_0 of the controller when $e = 0$. Then $g(x)$ is used on-line, in block N in Figure 2.11, to determine a $\lambda(t)$ such that the control output $v(t)$ does not saturate.

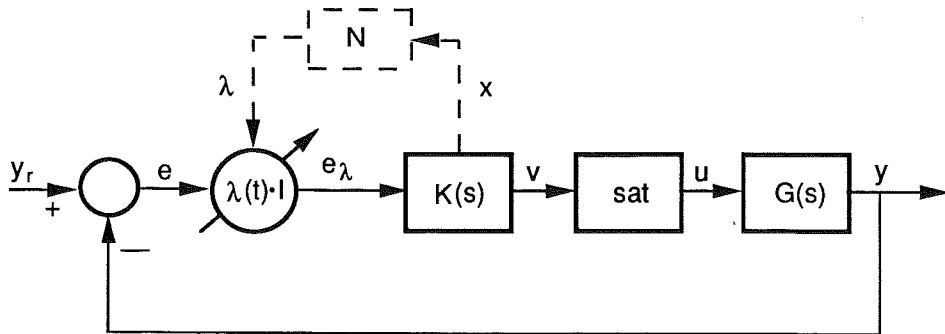


Figure 2.11 The controller structure in Kapasouris (1988) for stable processes.

2.6 Nonlinear Control Design

This section more briefly reviews a class of controller design methods and algorithms where a saturation or other nonlinearity is (more or less explicitly) accounted for. None of the methods or algorithms are evaluated and discussions are short. The main contribution in this section is a classification of the presented methods. However, the diversity of these methods makes it impossible to cover the whole area in a few pages. The intention is instead to briefly present some interesting classes of design methods and algorithms. These methods do not presume a given linear controller. Both linear and nonlinear controllers result from these methods.

Optimal Control

The linear quadratic problem

$$\begin{aligned} & \min_u \frac{1}{2} \int_0^T (x^T Q x + \varrho u^2) dt \\ & \dot{x} = Ax + Bu, \quad x(0) = x_0 \\ & |u(t)| \leq 1 \end{aligned} \tag{2.30}$$

was studied in the early 1960's, see, e.g., Rekasius and Hsia (1964) and Johnson and Wonham (1964). In Frankena and Sivan (1979) a nonlinear optimal control law is derived for a stable linear system.

The optimal control problems above does not result in controllers with integral action. If this is desirable then $\frac{du}{dt}$, or Δu in discrete time, must replace $u(t)$ in the loss function. Solving optimal control problems with saturations is far more involved than, e.g., using observer-based anti-windup. Further, the results are very restrictive and hardly ever used.

Open-Loop Optimal Feedback Methods

This is a class of controllers which is of practical use. In a number of optimization based control methods, e.g., generalized predictive control (GPC), see Tsang and Clarke (1988), and dynamic matrix control (DMC), see Cutler and Ramaker (1980), mathematical programming is used to obtain an optimal sequence of control signals. Only the first control signal is used, and then the optimization problem is solved again at the next sampling instant. This type of controller is denoted *open-loop optimal feedback* (OLOF) controller or *receding horizon* controller. Linear and quadratic programming solutions of such problems, are found in, e.g., Gutman (1982), Chang and Seborg (1983), Garcia and Morshedi (1986) and the two references above.

Both equality and inequality constraints for states and control signals can be added in the optimization. In both GPC and DMC the prediction models use control increments, Δu , thus these methods yield integral action.

Robotics Methods

An industrial robot is often supposed to follow a well defined path. Typical such applications are arc welding and gluing. Especially in the latter case robot speed is a limiting factor. Therefore a number of minimum-time approaches have been taken in order to speed up the operation of robots. In Dahl (1989) an interesting method of avoiding sensitivity for disturbances and unmodelled dynamics is used.

Quasilinearization Methods

Design methods based on describing function theory has been proposed for design of controllers for nonlinear systems. Both sinusoidal input describing functions (SIDF) and random input describing functions (RIDF) are used. Saturations are among the nonlinearities covered by these methods. In, e.g., Taylor and Strobel (1984) SIDF's are used for designing nonlinear PID controllers. In Haber *et al.* (1989) a similar PID controller is designed by a time-domain approach, using a pseudo-random binary signal. RIDF's are used by Suzuki and Hedrick (1985). The obtained PID controllers have extra nonlinearities or error dependent gains in order to compensate for the plant nonlinearities, which are not necessarily saturations.

Quantitative Feedback Theory

The quantitative feedback theory, see Horowitz (1963), has been extended to handle saturations for both stable and unstable plants. Results are reported in, e.g., Horowitz (1983) and Horowitz and Liao (1985). For linear systems a two-degree-of-freedom problem is solved resulting in a compensator G and a prefilter F . In the paper Horowitz (1983), a compensator

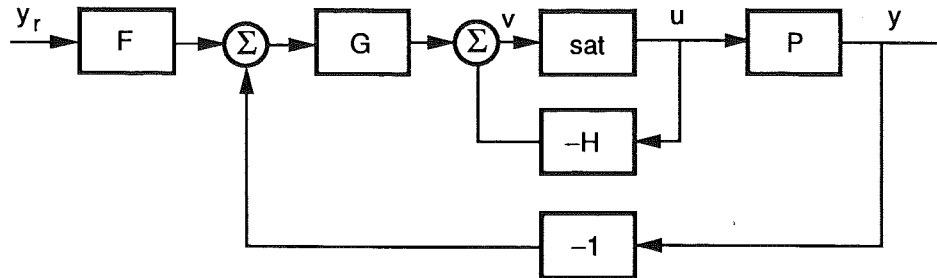


Figure 2.12 The anti-windup structure in Horowitz (1983).

H around the saturation is added, see Figure 2.12. G and H affect the loop gain $L_n = H + PG$, seen from control input to saturation, similar to observer-based anti-windup. The design idea is to make $L_n \approx K/s$, i.e., to approximate an integrator. There is one significant difference between this method and observer-based anti-windup. Here the compensator H always gives linear feedback around the saturation. In observer-based anti-windup there is nonlinear feedback which influences the closed-loop system only during saturation. The paper Horowitz and Liao (1985) deals with unstable plants and there a time-varying saturation is added in the controller in order to prevent saturation in the control signal. Thus there are similarities with Kapasouris' method, see Section 2.5.

Stabilizing Methods I

A number of design methods focus on stability despite the saturation. In Gutman and Hagander (1985) a state feedback controller is designed using Lyapunov functions. If the process is unstable a low gain stability feedback is designed, and then, based on the Lyapunov function for the stabilized system a second “high-gain” state feedback is designed. The two feedback signals are added and saturated.

Another group of methods uses the conic sector inequality

$$\left\| \text{sat}(u) - \frac{1}{2} u \right\| \leq \frac{1}{2} \|u\| \quad (2.31)$$

for a unit gain saturation. Then a standard control problem is solved for the nominal process $G(s)/2$ and finally robust stability is checked for the nominal process and controller plus perturbation. In Chen and Wang (1988) the Bellman-Grönwall Lemma is used for checking robust stability while the standard control problems are state and output feedback. In Chen and Kuo (1988) the LQG approach is used in order to find a controller for the nominal process. The controller must then also satisfy an H^∞ -condition in order to guarantee robust stability. In some cases a controller satisfying both nominal closed-loop stability and robust stability for the saturated system does not exist.

Stabilizing Methods II

Another group of methods found in the literature instead uses the strategy of designing linear state feedback controllers which never saturate. In Kosut (1983) a state feedback controller is determined such that the states never leave an *a priori* known set S . In Gutman and Cwikel (1986) a variable structure linear state feedback controller is derived. Vassilaki *et al.* (1988) and Benzaouia and Burgat (1988) also treat similar problems.

Summary

Out of the reviewed methods the OLOF methods are often used in practice, especially for control of chemical processes. One reason is simple constraint handling. Compared to the process time scale the computation time is usually sufficiently short on modern computers. In the robotics area the research activity is high in the area of minimum-time controllers.

2.7 Theory

This section contains a short resume of some of the available theory for analyzing stability of nonlinear systems. The main focus is on systems which can be separated into one linear dynamical part and a nonlinear function. Methods and theorems for single-input single-output (SISO) nonlinearities will be briefly presented. In later chapters they are used for stability analysis.

In contrast to linear systems a nonlinear system may be only locally stable, i.e., large deviations from the stationary point may yield instability. Further limit cycles and chaotic behavior may appear. The stability analysis for nonlinear systems is also harder than for linear systems. In general, only sufficient (and conservative) conditions for stability are obtained.

There are a number of different stability definitions, such as bounded-input bounded-output (BIBO) stability, asymptotic stability, uniform asymptotic stability, uniform asymptotic stability in the large, absolute stability, etc. For linear time-invariant systems some of them coincide, e.g., the different versions of asymptotic stability, but they do not necessarily coincide for nonlinear systems. A more general discussion on stability definitions is found in, e.g., Narendra and Taylor (1973).

Frequency Domain Analysis of SISO Systems

A process and controller with a saturating actuator can in many cases be reduced to a standard configuration with a linear system having nonlinear feedback. One example is the observer based anti-windup methods presented in Section 2.4. Disregarding the reference signal, they can be put in a standard

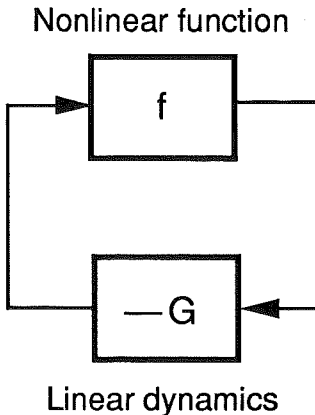


Figure 2.13 A linear system G with nonlinear feedback f in a standard configuration for stability analysis.

form with a linear system G having nonlinear feedback f , see Figure 2.13. For a unit gain saturation, (2.3), the nonlinearity obeys the sector condition

$$0 < k_1 \leq \frac{f(\sigma, t)}{\sigma} \leq k_2 = 1 \quad (2.32)$$

where σ is the input to the nonlinearity, $f(0, t) = 0$, and t is time. Then the linear system G is given by

$$G = \frac{G_{fb}G_p - W}{1 + W} \quad (2.33)$$

where G_p is the process transfer function, G_{fb} is the feedback path of the controller and W the anti-windup transfer function, see (2.14–2.15).

Note that conditional integration methods, see Section 2.3, cannot be reformulated into the structure in Figure 2.13 with a linear time-invariant system G . When integration is suspended G has lower order than normally.

For the observer-based anti-windup methods stability can be examined by the describing function method and circle criteria.

Describing function analysis is an approximate method where the nonlinearity is replaced by a describing function $N(a)$, see Atherton (1975). Here a sinusoidal-input describing function is used, where a is the amplitude of the sinusoidal input to the nonlinearity. A limit cycle in the closed-loop system or an unstable closed-loop system is predicted if

$$G(i\omega)N(a) + 1 = 0 \quad (2.34)$$

i.e., if the Nyquist curve $G(i\omega)$ intersects the curve $-1/N(a)$. For the saturation (2.3), the curve $-1/N(a)$ is the interval $(-\infty, -1]$ of the real axis. Thus, if the linear part G , (2.33), has at least one intersection with this interval, limit cycles or instability is predicted.

Circle criteria are based on Lyapunov stability and give sufficient conditions for absolute stability, see Narendra and Taylor (1973). There are a few different circle criteria, which differ in the type of nonlinearity they allow. The circle criteria are here only formulated for the saturation nonlinearity, i.e., for any time-invariant memoryless nonlinearity obeying sector condition (2.32). The Circle Criterion, which allows a time-varying nonlinear function $f(\sigma, t)$ but also gives the most conservative conditions for closed-loop absolute stability, is stated first.

THEOREM 2.1—The Circle Criterion (Narendra and Taylor (1973))

If the linear system $G(s)$ has all poles in the open left half plane and has nonlinear feedback $-f(\sigma, t)$, where $f(\sigma, t)$ obeys sector condition (2.32) the closed-loop system is absolutely stable provided that

$$\operatorname{Re} G(i\omega) + 1 > 0, \quad \forall \omega \quad (2.35)$$

□

The Popov criterion requires a time-invariant nonlinearity $f(\sigma)$.

THEOREM 2.2—The Popov Criterion (Narendra and Taylor (1973))

If the linear system $G(s)$ has all poles in the open left half plane and has time-invariant nonlinear feedback $-f(\sigma)$, where $f(\sigma)$ obeys sector conditions (2.32), the closed-loop system is absolutely stable provided that there exists a real constant α such that

$$\operatorname{Re} \left((G(i\omega) + 1)(1 + \alpha i\omega) \right) \geq 0, \quad \forall \omega \quad (2.36)$$

□

Remark. Theorem 2.2 thus requires that the Popov locus

$$\Gamma_P(\omega) = \left(\operatorname{Re} G(i\omega), \omega \operatorname{Im} G(i\omega) \right)$$

lies to the right of a line through -1 with slope α^{-1} .

□

The unit gain saturation is also monotonically non-decreasing, i.e.,

$$0 = m_1 \leq \frac{f(\sigma_1) - f(\sigma_2)}{\sigma_1 - \sigma_2} \leq m_2 = 1 \quad (2.37)$$

In Foss (1981) it is shown that the Popov criterion, the Off-Axis Circle Criterion and a third criterion from Dewey (1966) can be unified for all nonlinearities obeying (2.37). This theorem is now stated.

THEOREM 2.3—The Unified Off-Axis, Popov and Dewey Criterion

If the linear system $G(s)$ has all poles in the open left half plane and has time-invariant monotonic nonlinear feedback $-f(\sigma)$, where $f(\sigma)$ obeys condition (2.37), the closed-loop system is absolutely stable provided that there exists a real constant α such that

$$\operatorname{Re} \left((G(i\omega) + 1)(1 + \alpha i\omega^n) \right) > 0, \quad \forall \omega \quad (2.38)$$

where $n = -1, 0$ or $+1$. □

Remark. Theorem 2.3 thus requires that either of

- the Popov locus $\Gamma_P(\omega) = (\operatorname{Re} G(i\omega), \omega \operatorname{Im} G(i\omega))$
- the Nyquist locus $G(i\omega)$
- the Dewey locus $\Gamma_D(\omega) = (\operatorname{Re} G(i\omega), \operatorname{Im} G(i\omega)/\omega)$

lies to the right of a line through -1 with slope α^{-1} . □

Integrators The three circle criteria, Theorems 2.1–2.3 are only formulated for asymptotically stable processes $G(s)$. A simple pole in $s = 0$, i.e., an integrator, is allowed in Theorems 2.1–2.2 if the nonlinearity is such that $k_1 > 0$ in the sector condition (2.32). Similarly, if the nonlinearity is such that $m_1 > 0$ in (2.37) Theorem 2.3 still holds if $G(s)$ has an integrator.

Thus, since $m_1 = 0$ in (2.37) for a unit gain saturation, Theorem 2.3 cannot be used if $G(s)$ contains an integrator. Since $k_1 > 0$ in (2.32) Theorems 2.1–2.2 may be used when $G(s)$ contains an integrator.

Frequency Domain Analysis of MIMO Systems

The theorems above are not applicable for systems with multiple nonlinearities. Besides multivariable processes with nonlinear feedback this type of problem also appears in single-input single-output controllers, e.g., when the derivative or the rate of change of the control signal are limited in PID controllers. Then stability analysis must be formulated as a multiple-input multiple-output problem. Some analysis methods found in the literature are, e.g., the Moore-Anderson Theorem, (see, Narendra and Taylor (1973)), the multi-loop circle criterion, see Safonov and Athans (1981), and structured singular values, see Doyle (1982).

Time Domain Analysis

The methods used for time domain analysis of nonlinear systems aim at either deducing asymptotic stability in the large or at estimating a maximum region, denoted stability region, such that asymptotic stability holds in that region. For first and second order systems, *phase plane analysis* is a simple method for determination of the stability region.

For high-order systems other methods, e.g., the second method of Lyapunov, must be used. For the Lyapunov method the drawback is that a Lyapunov function must be found in order to prove stability. In Weissenberger (1968) and Willems (1969) the regions of asymptotic stability is estimated for systems which violate a sector condition for large inputs σ . In Wu (1986) and Wu and Schaufelberger (1988) the result from Willems (1969) is extended to handle multiple-input multiple-output nonlinearities.

2.8 Summary

This chapter contains a survey of published methods for handling control systems with saturations. The methods are classified and unified. They are divided into two main groups. The first group, *modified realizations*, starts with a given linear controller and then adds some algorithm with the purpose of giving good values to the controller states. Here the traditional PID anti-windup methods are found. The modified realizations were subdivided into *conditional integration methods*, *observer-based anti-windup methods* and *input limiting methods*. A comparison of conditional integration methods, highlighting deficiencies in the methods, is believed to be new. One of the methods, denoted C3 in Section 2.3, was judged best. The reasons were simplicity of the method and an over-all good performance. The term observer-based anti-windup unifies many published anti-windup methods, where the authors often seem to be unaware of the observer interpretation.

The other group of methods, *nonlinearly designed controllers*, is much more diverse. It is characterized by that the nonlinearity is accounted for already at the design stage or in a multi-step optimization. A major difference between the modified realizations and the nonlinearly designed controllers is the computational complexity of the latter group, either on-line or at the design stage. This explains why observer-based anti-windup and conditional integration are widely used.

Some of the methods are completely specified, e.g., the conditioning technique, see Hanus *et al.* (1987). Other methods have tuning parameters, e.g., a tracking time constant, see Section 2.4. There is a lack of design rules for how to select tuning parameters in order to achieve small deviations, short settling-times, etc. Further, in many cases only set-point performance is considered, while disturbances are neglected in evaluations.

The rest of the thesis focuses on the last two issues, namely derivation and evaluation of design rules for two observer-based anti-windup methods using two particular disturbances. The evaluation will also cover set-point changes and load disturbances. For comparison, conditional integration by method C3 will be included in the evaluation.

3

PID Control with Anti-Windup

From this chapter and onwards only PID controllers will be discussed. A large number of PID controllers in industry motivates this specialization. The simplicity of the PID controller also gives good insight into the windup problem, which may be used for anti-windup in general controllers.

After a more detailed introduction of PID controllers and anti-windup methods, stability properties of two observer-based anti-windup methods are investigated. From this investigation one may conclude that fast anti-windup is the best choice. The behavior of the controllers is also examined for impulse disturbances to the process and sinusoidal measurement disturbances. For these disturbances fast anti-windup turns out to be unfeasible. Further analysis of these cases leads to design rules for the two anti-windup methods. In the analysis and the design the noninteracting PID controller, see below, is used because it is the most general form of the PID controller.

3.1 PID Controllers

In Section 2.2 a simple PID controller, (2.1), was introduced. Now a few PID controllers, which are more practically useful, will be discussed. These controllers are treated in more detail in, e.g., Åström and Hägglund (1988) and Shinskey (1988). The first PID controller in this chapter is a slight

extension of (2.1), such that

$$V(s) = K \left\{ bY_r(s) - Y(s) + \frac{1}{sT_i} (Y_r(s) - Y(s)) - \frac{sT_d}{1 + sT_d/N} Y(s) \right\} \quad (3.1)$$

where $Y_r(s)$ is the set point, $Y(s)$ the controlled output, $V(s)$ the control signal, K the controller gain and T_i and T_d the integral and derivative times respectively. This controller is denoted the *parallel* form or the *noninteracting* PID controller, since there is no interaction between the three modes in the controller. The derivative part is filtered with a time constant T_d/N , where the filter constant N is in the range 3–20. This also limits the maximum derivative gain to N . A state space model is then

$$\begin{aligned} \frac{dx}{dt} &= \begin{pmatrix} 0 & 0 \\ 0 & -N/T_d \end{pmatrix} x + \begin{pmatrix} K/T_i \\ 0 \end{pmatrix} y_r - \begin{pmatrix} K/T_i \\ N/T_d \end{pmatrix} y \\ v &= \begin{pmatrix} 1 & -KN \end{pmatrix} x + \begin{pmatrix} Kb \\ K(1+N) \end{pmatrix} y_r - \begin{pmatrix} K(1+N) \\ 0 \end{pmatrix} y \end{aligned} \quad (3.2)$$

Compared to (2.1) the set point is no longer differentiated. Parameter b is useful for adjusting the closed-loop step response. The controller introduces a zero at $s = -1/(bT_i)$ and the choice $b = 1$ may give a too large overshoot. A lower value for b moves the zero away from the origin, which reduces the overshoot. $b = 0$ gives a controller structure known as “Integral on error only”, where the feedforward path only contains an integrator.

In commercial single-loop controllers, see Hägglund (1990), the most usual form of the PID controller is the *serial* form or the *interacting* controller, which has a PI and a PD part in series. Then

$$V(s) = K' \left(\frac{1 + sT'_i}{sT'_i} \right) \left(Y_r(s) - \frac{1 + sT'_d}{1 + sT'_d/N'} Y(s) \right) \quad (3.3)$$

where T'_i and T'_d are the interacting integral and derivative times and K' is the interacting gain. The set point is not differentiated. In this realization the three modes in the controller interact.

The interacting PID controller was simpler to implement in, e.g., pneumatic controllers. Later the same controller was translated into electronical controllers and microprocessors. Backwards compatibility was perhaps one important reason for not changing the controller structure.

When $T_i \geq 4T_d$ in (3.1) simple formulas relate the parameters in the two PID controller realizations. One way of realizing the PI part in (3.3) is by positive feedback of the actuator output, see Figure 3.1. This realization automatically gives tracking anti-windup, see Section 2.4, with $T_t = T'_i$.

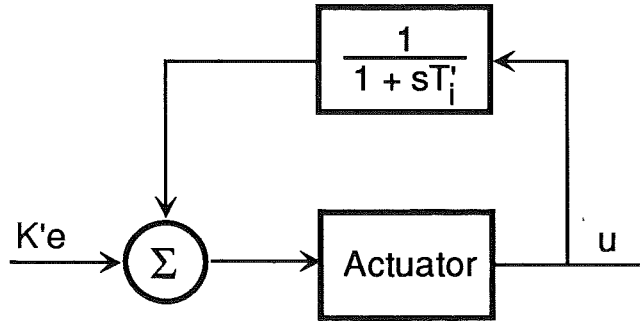


Figure 3.1 Integral action by positive feedback of the actuator output.

Discrete-Time PID Controllers

Today most PID controllers are implemented in computers. They are mostly used with sampling intervals small enough to justify continuous-time design. Using a forward-difference approximation of the integral part and a backward-difference approximation of the derivative part, the sampled version of (3.1) is

$$v(k) = K \left(b y_r(k) - y(k) + \frac{h}{T_i} \frac{1}{q-1} (y_r(k) - y(k)) - N\gamma \frac{q-1}{q-\gamma} y(k) \right) \quad (3.4)$$

where

$$\gamma = \frac{T_d}{Nh + T_d}, \quad (3.5)$$

h is the sampling interval, and q is the forward-shift operator. Other approximations are also used, but for short sampling intervals the differences between different approximations are negligible.

The velocity form PID controller is common in computer implementations. Then the control increment $\Delta v(k) = v(k) - v(k-1)$ is computed, i.e.,

$$\begin{aligned} \Delta v(k) = & K \left(b y_r(k) - y(k) + \left(\frac{h}{T_i} - b \right) q^{-1} y_r(k) \right. \\ & \left. - \left(\frac{h}{T_i} - 1 \right) q^{-1} y(k) - N\gamma \frac{\Delta^2}{1 - \gamma q^{-1}} y(k) \right) \end{aligned} \quad (3.6)$$

where q^{-1} is the backward-shift operator and $\Delta = 1 - q^{-1}$. Such algorithms are often denoted *incremental algorithms*. $\Delta v(k)$ is fed either to an actuator with built-in integral action, e.g., a stepping motor, or to a cascaded integrator which then outputs the control signal $v(k)$. Note that the velocity form cannot operate in P- or PD-mode.

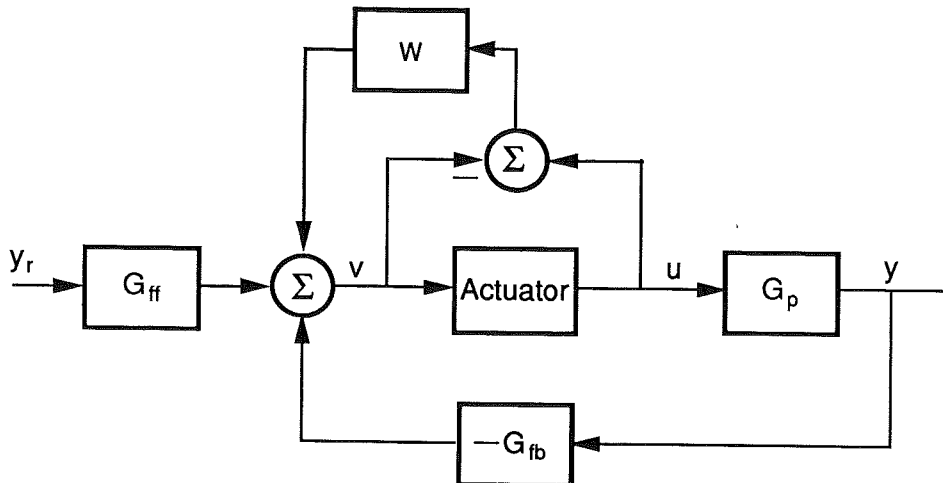


Figure 3.2 A control system with saturation and observer-based anti-windup. G_{ff} and G_{fb} are given by (3.1) and W depends on how the observer is chosen.

Discussion

As we mentioned in Section 2.2, limitations on the derivative part and on $\frac{dv}{dt}$ or $\Delta v(k)$ are sometimes used besides the saturation in PID controllers.

The PID controller must also be able to operate without derivative action, i.e., as a PI controller. In a continuous-time realization, e.g., (3.2), it is sufficient to let $N = 0$ in the computation of v . In the differential equation, however, it may be desirable to have $N/T_d > 0$ since the stable state x_2 will then continue to track $-y$, which will result in bumpless transfer from PI to PID control. A similar arrangement is necessary in a discrete-time PID controller.

Besides (3.1) and (3.3) a few other parameterizations of PID controllers are found in literature and commercial controllers. They can usually be reparameterized into the same form as (3.1) or (3.3). The same thing also holds for the discrete-time counterparts. Error feedback, i.e., equal feedback and feedforward parts, is used in some cases.

Since the noninteracting PID controller (3.1) is the more general form compared to the interacting PID controller (3.3), only (3.1) or its discrete-time counterpart (3.4) will be used in the sequel.

3.2 Anti-Windup Methods for PID Controllers

Some of the anti-windup methods described in Sections 2.3–2.4 will now be applied to PID controllers. First the observer-based anti-windup methods, see Section 2.4, and then conditional integration, see Section 2.3, will be discussed.

The realization in (3.2) of a PID controller has the same structure as (2.12). Hence observer-based anti-windup methods can be described by either the transfer function W in Figure 3.2, or equivalently by the matrix M or the observer polynomial $A_o = \det(sI - F + MH)$, see Section 2.4. A state space model of the interacting PID controller (3.3) is, using the diagonal form, almost identical to (3.2). Both F and H have identical structure for the two controllers and thus observer-based anti-windup is identically described.

Continuous-Time PID Controllers

In tracking anti-windup only the integrator pole is moved. For the PID controller (3.1–3.2) it has been found, see (2.19), that

$$M = \begin{pmatrix} \frac{1}{T_t} \\ 0 \end{pmatrix}, \quad W(s) = \frac{1}{sT_t} \quad \text{and} \quad A_o(s) = \left(s + \frac{1}{T_t}\right)\left(s + \frac{N}{T_d}\right) \quad (3.7)$$

The conditioning technique, i.e., when $M = G_r D_r^{-1}$ in (2.13), gives

$$M = \begin{pmatrix} \frac{1}{bT_i} \\ 0 \end{pmatrix}, \quad W = \frac{1}{sbT_i} \quad \text{and} \quad A_o = \left(s + \frac{1}{bT_i}\right)\left(s + \frac{N}{T_d}\right) \quad (3.8)$$

which is a special case of tracking anti-windup. However, the conditioning technique is for other controllers than (3.1), usually *not* a special case of tracking anti-windup. For the general case, the observer approach, the observer polynomial A_o is chosen such that

$$A_o = \det(sI - F + MH) = s^2 + 2\zeta\omega_0 s + \omega_0^2 \quad (3.9)$$

and then

$$M = \begin{pmatrix} \omega_0^2 T_d \\ \frac{N}{K N^2} \left(\omega_0 - \frac{N}{T_d} \right)^2 + \frac{2\omega_0}{KN} (1 - \zeta) \end{pmatrix} \quad (3.10)$$

and

$$W(s) = \frac{(2\omega_0\zeta - N/T_d)s + \omega_0^2}{s(s + N/T_d)} \quad (3.11)$$

Unless it is explicitly stated, $\zeta = 1$ in the sequel. Without derivative action (3.9–3.11) are meaningless. Instead the observer approach is equivalent to tracking anti-windup for this particular case.

Discrete-Time PID Controllers

Tracking anti-windup in a discrete-time PID controller (3.4) is described by

$$M = \begin{pmatrix} \frac{h}{T_t} \\ 0 \end{pmatrix}, \quad W = \frac{h}{T_t} \frac{1}{q-1} \quad \text{and} \quad A_o(q) = \left(q - 1 + \frac{h}{T_t} \right) (q - \gamma) \quad (3.12)$$

similarly to the continuous-time case. For the matrix M a state space realization corresponding to (3.2) is presumed. If $T_t = h$ one pole is placed in the origin. This implies that the integrator is immediately reset to a value such that the controller is exactly at the saturation limit. This is denoted back calculation, and is discussed in Section 2.4, especially in Example 2.4. The conditioning technique is equivalent to $T_t = bT_i$. A more general choice of observer poles, corresponding to (3.9), may also be used.

Incremental Algorithms

In an incremental PID controller, e.g. (3.6), there is no integral part that winds up during saturation. However, the derivative and proportional parts may give undesirable transients, see Fertik and Ross (1967). A common anti-windup implementation of (3.6) is

$$\begin{aligned} v(k) = & u(k-1) + K \left(b y_r(k) - y(k) + \left(\frac{h}{T_i} - b \right) y_r(k-1) \right. \\ & \left. - \left(\frac{h}{T_i} - 1 \right) y(k-1) - N\gamma \frac{\Delta^2}{1 - \gamma q^{-1}} y(k) \right) \end{aligned} \quad (3.13)$$

i.e., the control increment is added to the saturated control signal u . Then the excess Δv is discarded. It is easily verified that (3.13) is equivalent to $A_o(q) = q(q - \gamma)$, i.e., tracking with $T_t = h$. Other choices of observer polynomials $A_o(q)$ in discrete-time PID controllers are discussed in Walgama and Sternby (1990).

Conditional Integration

After an evaluation in Section 2.3 a conditional integration method denoted C3 was judged best. This method is used in the sequel when conditional integration is tested and discussed. In method C3 the integral part is kept constant until the control error changes sign or the controller desaturates.

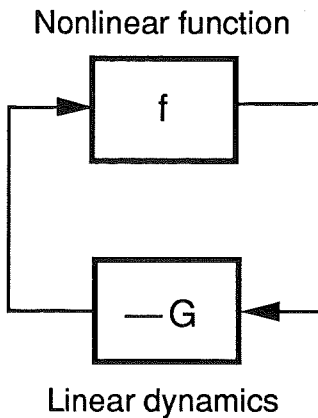


Figure 3.3 A linear system G with nonlinear feedback f in standard configuration for stability analysis.

3.3 Stability Improvements when using Anti-Windup

In this section the stability improvements using observer-based anti-windup will be analyzed. The block diagram in Figure 3.2 can be put in the standard form in Figure 3.3. The nonlinearity f is a unit gain saturation, and

$$G = \frac{G_{fb}G_p - W}{1 + W} \quad (3.14)$$

where G_p is the process transfer function, G_{fb} the feedback part of the controller, and W is the anti-windup transfer function.

The negative inverse of the describing function $N(a)$ of a unit gain saturation, see Atherton (1975), is the interval $(-\infty, -1]$ of the real axis, see Figure 3.4. If $G(i\omega)$ intersects this interval, instability or limit cycling is predicted by the describing function method. From the Off-Axis Circle Criterion it follows that it is necessary that $G(i\omega)$ does not intersect the interval $(-\infty, -1]$.

This condition is not sufficient. Although the Nyquist curve $G(i\omega)$ in Figure 3.4 does not intersect the interval $(-\infty, -1]$, the conditions for absolute stability by the Off-Axis Circle Criterion are not satisfied. Thus neither stability nor instability can be concluded. In a few test cases of this type instability was not observed even if $G(i\omega)$ was very close to -1 without intersecting $-1/N(a)$. However, an intersection of $-1/N(a)$ quickly leads to instability or limit cycles. The analysis below concentrates on avoiding $-1/N(a)$. This can be easily checked by investigating the variation of the argument of $G + 1$, where

$$G + 1 = \frac{G_{fb}G_p + 1}{1 + W} \quad (3.15)$$

3.3 Stability Improvements when using Anti-Windup

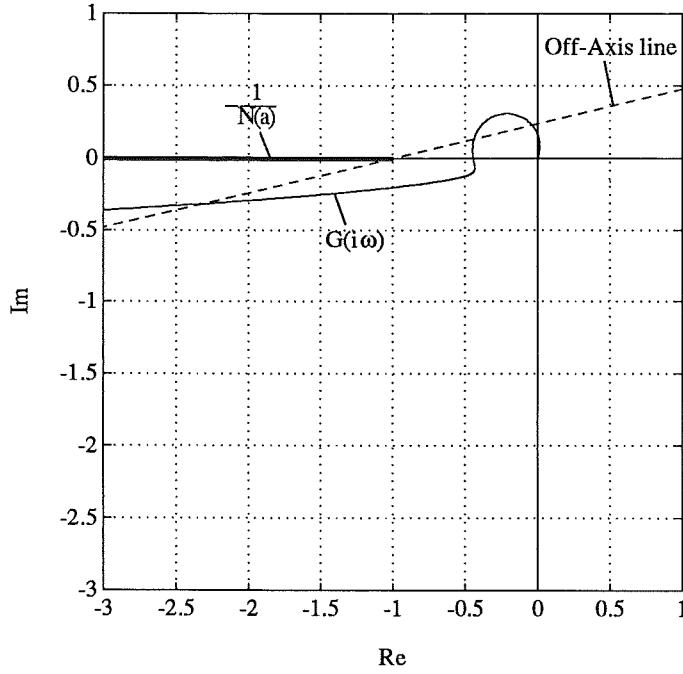


Figure 3.4 Example of a Nyquist curve $G(i\omega)$ where the describing function method does not predict instability or limit cycles, since $G(i\omega)$ and $-1/N(a)$, where $N(a)$ is the describing function for a saturation, do not intersect each other. The dashed line through -1 always intersects $G(i\omega)$. Thus sufficient conditions for stability by the Off-Axis Circle Criterion, Theorem 2.3, are not satisfied.

It suffices to examine $(1 + W(i\omega))^{-1}$ to see how $\arg(G(i\omega) + 1)$ changes with the anti-windup parameters.

From (2.15) it follows that $W = H(sI - F)^{-1}M$, where H , F and M are matrices in the state space realization (2.13) of the controller, i.e.,

$$\begin{aligned}\dot{x} &= Fx + G_r y_r - G_y y + M(u - v) \\ v &= Hx + D_r y_r - D_y y \\ u &= \text{sat}(v)\end{aligned}$$

The controller can also be written, (2.17),

$$\begin{aligned}A_o(s)V(s) &= T(s)Y_r(s) - S(s)Y(s) + (A_o(s) - R(s))U(s) \\ u(t) &= \text{sat}(v(t))\end{aligned}$$

It follows from Kailath (1980, pp. 198, 651) that

$$\frac{1}{1 + W(s)} = \frac{\det(sI - F)}{\det(sI - F + MH)} = \frac{R(s)}{A_o(s)} \quad (3.16)$$

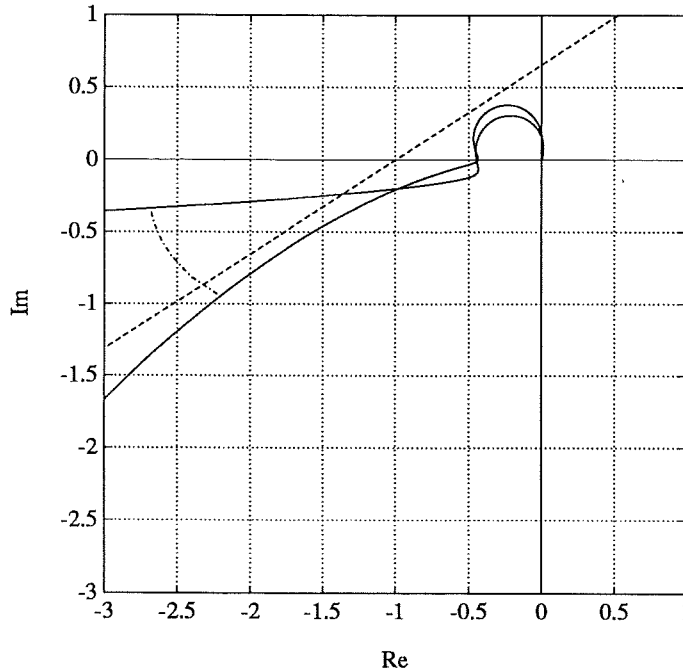


Figure 3.5 Tracking anti-windup is added to the Nyquist curve $G(i\omega)$ in Figure 3.4. Both the original curve and the curve with anti-windup is shown. For the latter curve the geometric condition for absolute stability by the Off-Axis Circle Criterion is satisfied. One point on the original Nyquist curve is traced (for constant ω) to the new Nyquist curve. The phase advance is dominant for low frequencies, while $G(i\omega)$ changes only marginally for high frequencies.

Thus $(1 + W(s))^{-1}$ is the ratio between the characteristic equations for the controller and the observer respectively.

The stability properties of $G + 1$, with respect to the negative real axis, can now simply be examined. It is often desirable that $\arg(G(i\omega) + 1)$ increases, i.e., that $\arg(1 + W(i\omega))^{-1} > 0$ in order to avoid the negative real axis. Thus it is often desirable that $\arg W(i\omega) < 0$.

Stability Improvement using Tracking Anti-Windup

In tracking anti-windup, see (2.19), the anti-windup transfer function is

$$W(s) = \frac{1}{sT_t}$$

where T_t is the tracking time constant. Note that this is valid for *all controllers* with integral action where only the integrator is “adjusted” during saturation. Hence

$$\frac{1}{1 + W} = \frac{sT_t}{1 + sT_t} \quad (3.17)$$

which always has positive phase and an amplitude less than one. In fact,

3.3 Stability Improvements when using Anti-Windup

$(1 + W(i\omega))^{-1}$ describes a semi-circle in the first quadrant with end points in 1 and 0 and thus has a phase in the interval $[0^\circ, 90^\circ]$. The following result can thus be established.

RESULT 3.1—Stability improvement using tracking anti-windup

With tracking anti-windup the argument of $G(i\omega) + 1$ increases by an amount in the interval $[0^\circ, 90^\circ]$ and $|G(i\omega) + 1|$ decreases when the tracking time constant T_t decreases from ∞ . Thus $G(i\omega)$ is moved counter clockwise away from $-1/N(a)$. \square

Result 3.1 is illustrated in Figure 3.5. The phase advance does not guarantee that stability can be proved using any of the circle criteria. If the loop gain $G_{fb}G_p$, i.e., without saturation, satisfies a number of conditions it is, however, possible to prove absolute stability for tracking anti-windup. This is shown in the following theorem.

THEOREM 3.1—Absolute stability for tracking anti-windup

The linear system (3.14) with tracking anti-windup

$$W = \frac{1}{sT_t}$$

has nonlinear feedback f . If

1. G_p is asymptotically stable
2. G_{fb} has one integrator but is otherwise asymptotically stable
3. the nonlinearity f is monotonically non-decreasing such that $f(0) = 0$ and

$$0 \leq \frac{f(\sigma_1) - f(\sigma_2)}{\sigma_1 - \sigma_2} \leq 1$$

4. there exist real constants α and β , where $\alpha\beta = -1$ and $0 < \alpha < \infty$, such that

$$\begin{aligned} \operatorname{Re} \left((G_{fb}(i\omega)G_p(i\omega) + 1)(1 + i\alpha) \right) &> 0, \quad \forall \omega \geq 0 \\ \operatorname{Re} \left((G_{fb}(i\omega)G_p(i\omega) + 1)(1 + i\beta) \right) &\geq 0 \quad \text{if } \omega \geq \omega_\beta \\ \operatorname{Re} \left((G_{fb}(i\omega)G_p(i\omega) + 1)(1 + i\beta) \right) &\leq 0 \quad \text{if } 0 \leq \omega \leq \omega_\beta \end{aligned}$$

then the closed-loop system with tracking anti-windup is absolutely stable for $0 < T_t < \infty$. \square

Proof: With tracking anti-windup the transfer function

$$G = \frac{G_{fb}G_p - W}{1 + W}$$

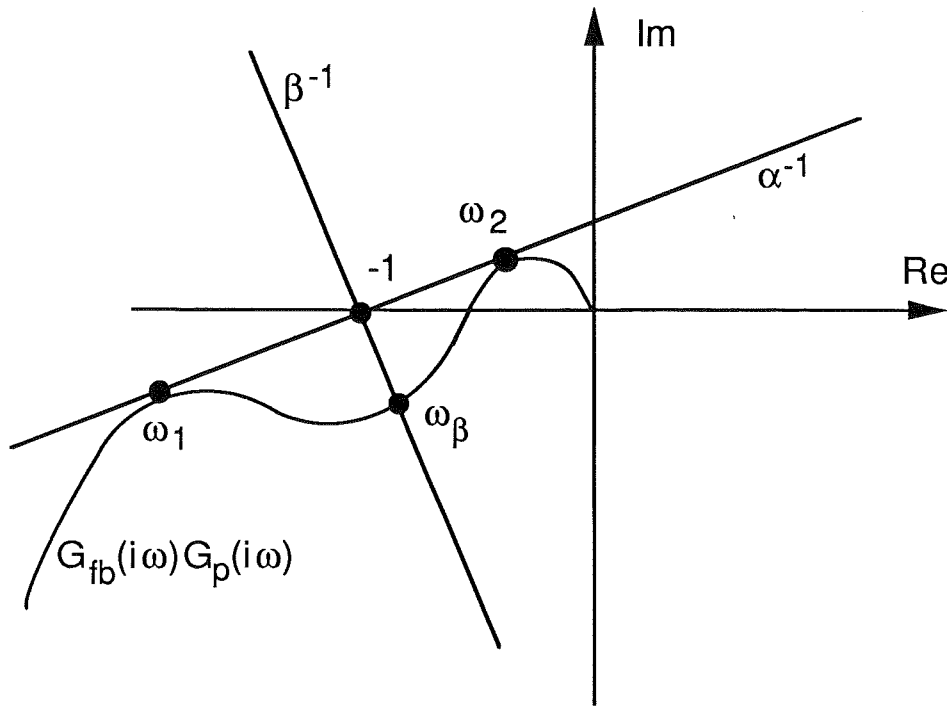


Figure 3.6 Illustration of Theorem 3.1. $G_{fb}(i\omega)G_p(i\omega)$ is the loop gain without saturation.

is asymptotically stable. To apply the Off-Axis Circle Criterion it suffices to show that

$$\operatorname{Re} \left((G(i\omega) + 1)(1 + i\gamma) \right) = \operatorname{Re} \left(\frac{G_{fb}(i\omega)G_p(i\omega) + 1}{W(i\omega) + 1} (1 + i\gamma) \right) > 0 \quad \forall \omega \quad (3.18)$$

is satisfied for $0 < T_t < \infty$ and some finite γ . From 4. it is clear that this condition is satisfied without anti-windup, i.e., when $T_t = \infty$ and $\alpha = \gamma$. In the worst case there exists $\alpha > 0$ such that $\operatorname{Re}((G(i\omega_2) + 1)(1 + i\alpha)) = \varepsilon > 0$ and $\operatorname{Re}((G(i\omega_1) + 1)(1 + i\alpha)) = \varepsilon > 0$ where ε is very small, $\omega_2 > \omega_\beta$ and $\omega_1 < \omega_\beta$, see Figure 3.6. With $T_t = \delta^{-1}$, where $\delta > 0$ is small, the variation of the argument of $G(i\omega) + 1$ is larger for ω_1 than for ω_2 since

$$\arg \frac{1}{1 + W(i\omega_1)} = \frac{\pi}{2} - \arctan \omega_1 T_t > \arg \frac{1}{1 + W(i\omega_2)} = \frac{\pi}{2} - \arctan \omega_2 T_t$$

for $\omega_2 > \omega_1$. This also holds for $\omega'_1 \approx \omega_1$ and $\omega'_2 \approx \omega_2$. Hence if

$$\operatorname{Re} \left((G(i\omega'_2) + 1)(1 + i\gamma) \right) = \varepsilon > 0$$

then $\operatorname{Re}((G(i\omega'_1) + 1)(1 + i\gamma)) > \varepsilon > 0$ where $\beta < \gamma < \alpha$. Absolute stability for $T_t = \delta^{-1}$, where δ is small, then follows from the Off-Axis Circle Criterion, since the geometric condition (3.18) is satisfied.

3.3 Stability Improvements when using Anti-Windup

In the other limit, when $T_t = \delta$, where $\delta > 0$ is small, all points of $G + 1$, except points for which ω is very large, have obtained a phase advance of $\pi/2$. Thus

$$\operatorname{Re} \left(\frac{G_{fb}(i\omega)G_p(i\omega) + 1}{1 + W(i\omega)} (1 + i\beta) \right) > 0 \quad \forall \omega$$

and then absolute stability for $T_t = \delta > 0$, where δ is small, follows from the Off-Axis Circle Criterion, since the geometric condition (3.18) is satisfied.

Since all points with $\omega < \omega_\beta$ have larger phase advance than points with $\omega > \omega_\beta$ it follows that absolute stability also holds for $\delta < T_t < \delta^{-1}$, since condition (3.18) cannot be violated. \square

Stability Improvement from Observer-Based Anti-Windup

Equation (3.16) can also be written

$$\frac{1}{1 + W(s)} = \frac{R(s)}{A_o(s)} = \prod_{i=1}^n \frac{(s + a_i)}{(s + b_i)} \quad (3.19)$$

where $-a_i$ are the controller poles and $-b_i$ are the observer poles. Tracking anti-windup, see above, can then be described by $a_1 = 0$, $b_1 = 1/T_t$ and $b_i = a_i$ for $i = 2, \dots, n$. Thus tracking anti-windup can be interpreted as if it “moves” one controller pole to an observer pole. The enumeration in (3.19) is not unique but is assumed to be such that $\sum |b_i - a_i|$ is minimum. This avoids uninteresting cases in the enumeration.

In observer-based anti-windup a pole in the origin ($a_i = 0$) is always stabilized ($b_i > 0$), which implies $\arg(1 + W)^{-1} > 0$. Other controller poles may also be moved by the anti-windup and their effects on $\arg(1 + W)^{-1}$ will now be investigated.

A single real pole If a single real pole is moved by the anti-windup the argument of $(1 + W)^{-1}$ increases by

$$\varphi(\omega) = \arg \frac{i\omega + a_i}{i\omega + b_i} = \arctan \frac{\omega}{a_i} - \arctan \frac{\omega}{b_i} \quad (3.20)$$

When $a_i < 0$ or $b_i < 0$ the principal branch of arctan is not used, but arctan instead returns values in $[\frac{\pi}{2}, \frac{3\pi}{2}]$. Thus $b_i > a_i \Leftrightarrow \varphi(\omega) \geq 0 \quad \forall \omega > 0$, i.e., if the pole is moved “to the left” by anti-windup the argument increase of $(1 + W)^{-1}$ is non-negative, see Figure 3.7.

If a number of real poles are to be moved, it is seen from Figure 3.7 that it is advantageous to first move the poles closest to the origin (or the unstable poles). Then a large phase advance is obtained for small ω (low frequencies) while high ω does not give much difference in the argument.

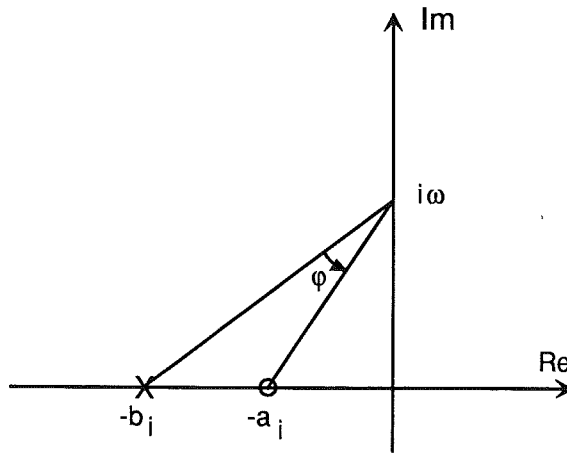


Figure 3.7 Graphical proof of positivity of (3.20). $\varphi \geq 0$ when $b_i \geq a_i$ and $\omega \geq 0$.

Complex-conjugated poles When stable complex-conjugated controller poles (including double poles) are moved by anti-windup the argument of $(1 + W)^{-1}$ increases in two simple cases:

1. The poles are moved radially away from the origin, i.e., constant relative damping ζ_0 and increasing natural frequency ω_0 .
2. The poles are moved away from the origin, parallel to the imaginary axes.

Graphical proofs, similar to Figure 3.7, are easily constructed. In these two cases the relative damping is non-increasing. A condition for obtaining relative damping 1 without argument decrease of $(1 + W)^{-1}$ will now be given.

LEMMA 3.1—A circle for argument increase of $(1 + W)^{-1}$

Complex-conjugated controller poles, with natural frequency ω_0 and relative damping ζ_0 , can be moved by anti-windup to the point $-\omega_r$ on the real axis without argument decrease of $(1 + W)^{-1}$, provided

$$\omega_r \geq \frac{\omega_0}{\zeta_0} \quad (3.21)$$

All poles (ω_0, ζ_0) which satisfy equality in (3.21) for a fixed ω_r are located on a circle with radius $\omega_r/2$ centered in $(-\omega_r/2, 0)$.

Proof: The lemma is proved for the special case $\omega_0 = 1$. The general case is obtained by rescaling. Let $x = \omega_r/\zeta_0$, $y = \omega/\zeta_0$, $\psi = \sqrt{1 - \zeta_0^2}/\zeta_0$ and $\omega_0 = 1$. Then, for $s = i\omega$ and $0 < \zeta_0 \leq 1$,

$$\arg \frac{s^2 + 2\zeta_0 s + 1}{(s + \omega_r)^2} = \varphi(y) = \arctan(y + \psi) + \arctan(y - \psi) - 2 \arctan \frac{y}{x} \quad (3.22)$$

where

$$\varphi(0) = \varphi(\infty) = 0 \quad (3.23)$$

Further

$$\frac{d\varphi}{dy}(y) = \frac{1}{1+(y+\psi)^2} + \frac{1}{1+(y-\psi)^2} - \frac{2x}{x^2+y^2} \quad (3.24)$$

i.e.,

$$\frac{d\varphi}{dy}(0) = \frac{2}{1+\psi^2} - \frac{2}{x} \quad (3.25)$$

which is positive if $x > 1 + \psi^2$. If $x < 1 + \psi^2$ then $\varphi(y) < 0$ for small y . $\varphi(y)$, (3.22), has local extrema with respect to $y = \sqrt{z}$ if

$$z^2 - \frac{(x-1)^2 + \psi^2(2x+1)}{x-1} z = \frac{x(1+\psi^2)(x-1-\psi^2)}{x-1} \quad (3.26)$$

If $x > 1 + \psi^2 = \zeta_0^{-2}$, i.e., $\omega_r > \zeta_0^{-1}$, then (3.26) has only one positive solution z_1 , i.e., there is only one positive solution y_1 to

$$\frac{d\varphi}{dy}(y) = 0 \quad (3.27)$$

From (3.23) and (3.25) it now follows that $\varphi(y) \geq 0 \ \forall y \geq 0$, since $\varphi(y)$ is continuous and there is only one local extremum, which then must be positive. In the general case, when $\omega_0 \neq 1$, it thus required that

$$\omega_r \geq \frac{\omega_0}{\zeta_0}$$

in order to get non-negative $\varphi(y)$.

Other poles, which satisfy equality in (3.21), have real and imaginary parts

$$\left(-\omega_0 \zeta_0, \pm \omega_0 \sqrt{1 - \zeta_0^2} \right) = \left(-\omega_r \zeta_0^2, \pm \omega_r \zeta_0 \sqrt{1 - \zeta_0^2} \right) \quad (3.28)$$

It is easily verified that $\left(-\omega_r \zeta_0^2, \pm \omega_r \zeta_0 \sqrt{1 - \zeta_0^2} \right)$ describes a circle with radius $\omega_r/2$ centered in $(-\omega_r/2, 0)$. \square

All anti-windup methods do not move all poles away from the origin. This is illustrated in an example.

EXAMPLE 3.1—The observer approach for PID controllers

From (3.11)

$$W(s) = \frac{(2\omega_0 - N/T_d)s + \omega_0^2}{s(s + N/T_d)}$$

i.e.,

$$\frac{1}{1 + W(s)} = \frac{s(s + N/T_d)}{(s + \omega_0)^2}$$

If $\arg(1 + W(i\omega))^{-1} > 0$ is desired, it is necessary that $\omega_0 > N/(2T_d)$. In many cases, see Chapter 4, ω_0 is instead chosen such that $\omega_0 < N/(2T_d)$, i.e., $\arg(1 + W(i\omega))^{-1} < 0$ for some frequencies. The closed-loop systems are usually stable unless ω_0 is very small. \square

Most of the points on $G(i\omega) + 1$ can tolerate phase decrease without causing instability due to intersection of the negative real axis. To guarantee that $G(i\omega) + 1$ does not intersect the negative real axis it is sufficient that

$$\max \arg(W(i\omega) + 1) < \pi + \min \arg(G_p(i\omega) \cdot G_{fb}(i\omega) + 1) \quad (3.29)$$

Summary

The main result in this section has been rules for how to choose observer poles for a controller, such that the variation of the argument of $G + 1$ is non-negative. Thus instability or limit cycles, due to intersections between $G(i\omega)$ and $-1/N(a)$, where $N(a)$ is the describing function for a saturation, can be avoided. However, absolute stability by any of the circle criteria is not guaranteed, except in special cases.

When a non-negative variation of the argument for $G(i\omega) + 1$ is desired, the derived anti-windup rules all say: “move the poles farther away from the origin”. However, in the next few sections, where disturbances are considered, this will not always be a good choice.

3.4 Disturbances

The discussion in previous section focused on stability issues when anti-windup is used. The results indicate that a small tracking time constant T_t or a fast observer is the best choice. Then limit cycles are avoided although absolute stability cannot always be proved.

However, experiments in the laboratory show that, e.g., a small tracking time constant T_t is not a good choice when there are disturbances. Fast anti-windup may lead to a highly undesirable result in such cases. This is illustrated for two different disturbances.

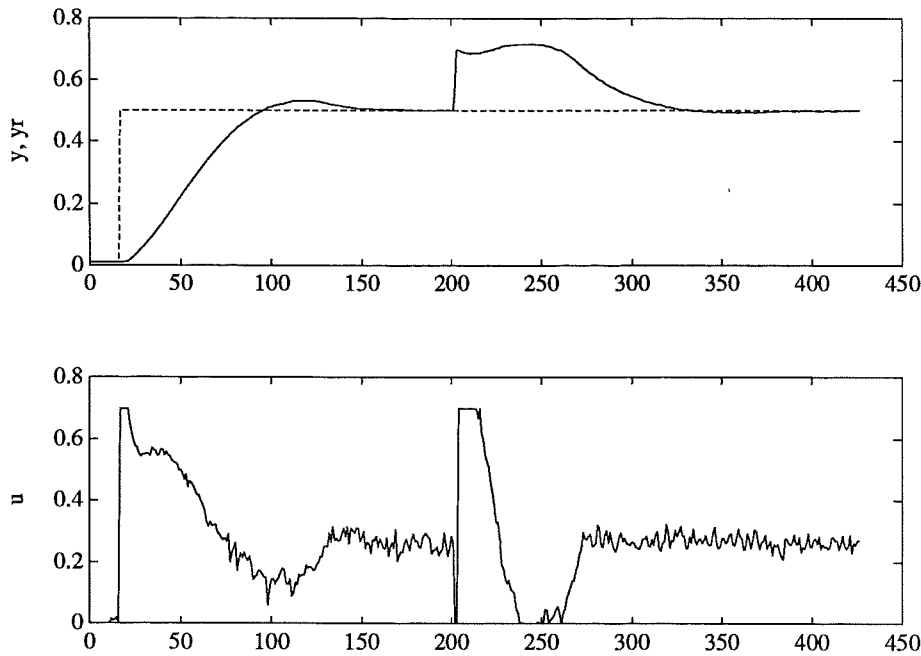


Figure 3.8 Set-point change and impulse disturbance response for the laboratory double-tank process in Example 3.2. Notice that after the disturbance the control signal first saturates at the lower limit, and then quickly desaturates and resaturates at the upper limit. This causes the tank level (y) to remain well over the set point for a while, before it decays to the set point.

EXAMPLE 3.2—Impulse disturbance

A PID controller with tracking anti-windup is used for control of the lower level in a laboratory double-tank process, consisting of two cascaded tanks, see also Section 4.1. If a cup of water is quickly poured into the lower tank, a very undesirable response is obtained when a small tracking time constant T_t is used, see Figure 3.8. The reason is that when T_t is small the integrator in the PID controller is adjusted too fast, which for this particular disturbance makes the controller resaturate at the wrong controller limit. The disturbance is well approximated by an impulse. \square

EXAMPLE 3.3—Measurement noise

A PID controller with fast tracking anti-windup is used for position control of a DC servo, see also Section 4.2. If a measurement disturbance, in this case a high-frequency sinusoidal disturbance, is added to the position measurement when the controller is close to saturation, a position offset is obtained, see Figure 3.9. The reason is that the disturbance saturates the controller during one part of the period. During the saturated part of the period the value of the integrator is quickly adjusted, due to fast anti-windup, but during the unsaturated part of the period the integrator value changes much slower. A larger tracking time constant would give smaller offset. \square

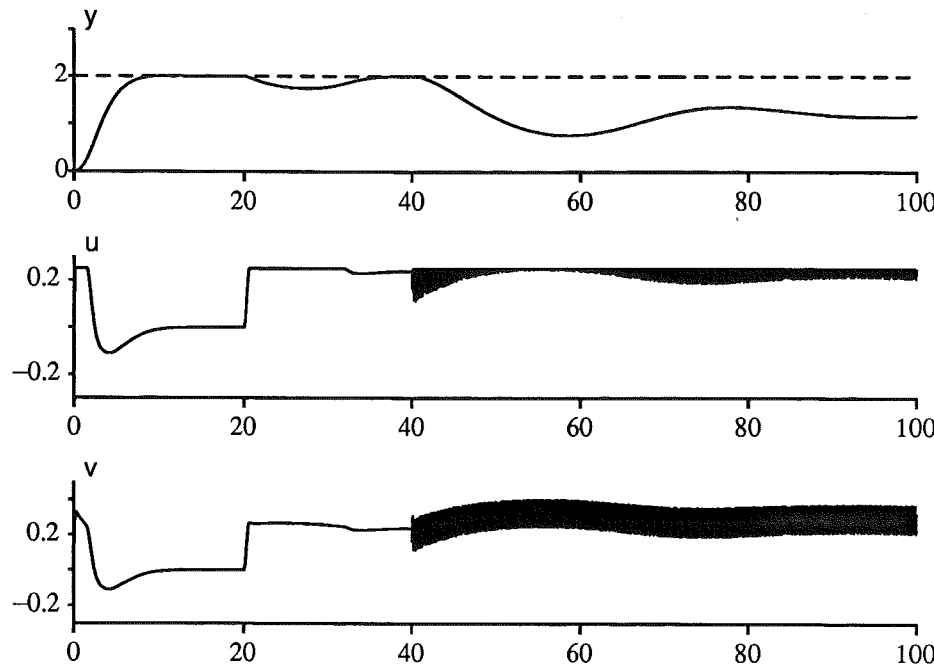


Figure 3.9 Simulation of set-point change, load and measurement disturbances for the DC servo in Example 3.3. During the load disturbance the controller is close to saturation in stationarity. Then a sinusoidal measurement disturbance, partially saturates the controller and causes an offset in the process output y .

The two examples clearly show that fast anti-windup may lead to undesirable results when disturbances occur. Note that in Example 3.3 both the set-point change and the load disturbance was handled well with a small tracking time constant. Thus the sensitivity for the impulse disturbance and the measurement noise in the two examples cannot be predicted when only set-point changes and load disturbances are used for evaluation of the anti-windup. Instead special investigations are required, which will be presented in the next two sections. The insight obtained from these investigations will be used for derivation of design rules for anti-windup, e.g., limits for the choice of tracking time constant T_t .

3.5 Impulse Disturbances and Anti-Windup Design

In previous section it was demonstrated that the effects of disturbances may be highly undesirable if the anti-windup is too fast. In this section the effects of impulse disturbances will be analyzed. The analysis will give insight into the combined effects of PID control with anti-windup and impulse disturbances. From this insight design criteria may be formulated. The criteria then lead to design rules for the anti-windup, e.g., limits for the tracking time

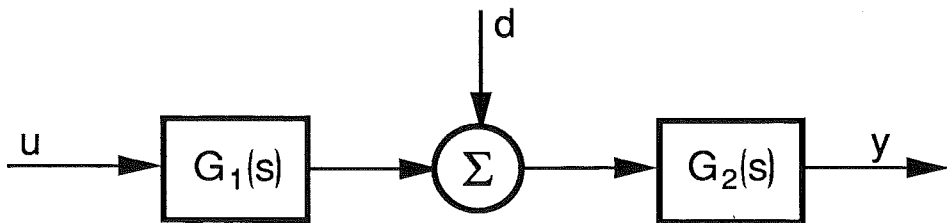


Figure 3.10 The process $G_p = G_1 G_2$ is separated in two parts. Disturbances d act only on G_2 .

constant T_t . A drawback with this approach is that closed-loop stability is not guaranteed, but has to be checked separately. The main results in this section are the insight on the effects of impulse disturbances, and design rules for anti-windup parameters.

Problem Formulation

The impulse disturbance is a good model of a relatively fast disturbance, see, e.g., Example 3.2. For mechanical systems a collision may be modeled by an impulse.

The effects of impulse disturbances will now be analyzed. The disturbance is assumed to enter as shown in Figure 3.10. Two cases are studied.

Case A Relative degree one disturbance influence

Assume that the relative degree of G_2 is one, and G_2 is scaled such that

$$\lim_{s \rightarrow \infty} s G_2(s) = 1 \quad (3.30)$$

A simple example is

$$G_2(s) = \frac{1}{s + a_1} \quad (3.31)$$

An impulse disturbance $d(t) = d_0 \cdot \delta(t)$ then results in an immediate change d_0 in the process output y .

Case B Relative degree two disturbance influence

Assume that the relative degree of G_2 is two, and G_2 is scaled such that

$$\lim_{s \rightarrow \infty} s^2 G_2(s) = 1 \quad (3.32)$$

A simple example is

$$G_2(s) = \frac{1}{(s + a_1)(s + a_2)} \quad (3.33)$$

An impulse disturbance $d(t) = d_0 \cdot \delta(t)$ then gives an immediate derivative change d_0 in the process output y .

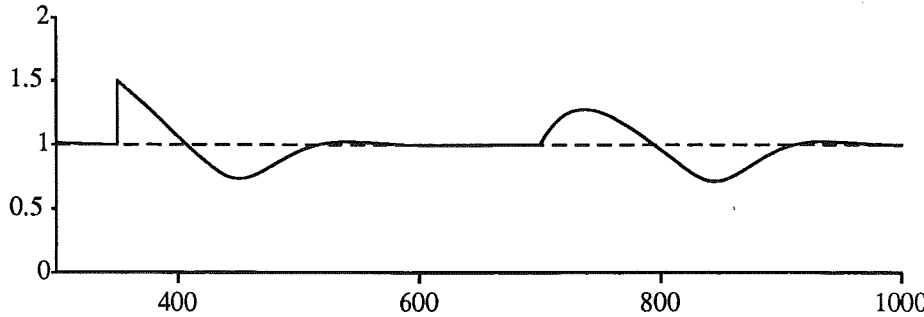


Figure 3.11 The two cases of impulse disturbances, i.e., (3.31) and (3.33) respectively, are shown in a simulation of the double-tank process from Example 3.2. Case A corresponds to pouring a cup of water in the lower tank, and case B to pouring the cup in the upper tank. The integral of the control error is zero for both disturbances when anti-windup is not in effect.

The process transfer function $G_p = G_1 \cdot G_2$ is assumed to have a relative degree of at least two. If the relative degree of G_p is one there is usually not much use for the derivative part in the PID controller. The assumption of a relative degree of at least two also simplifies the analysis immediately after the impulse disturbance.

Let the state space representation of the process in Figure 3.10 be

$$\begin{aligned}\dot{x} &= Ax + Bu + Ed \\ y &= Cx\end{aligned}\tag{3.34}$$

The impulse response from the disturbance input is

$$h_2(t) = Ce^{At}E = CE + CAEt + \dots = \sum_1^{\infty} \beta_i \frac{t^{(i-1)}}{(i-1)!}\tag{3.35}$$

where $\beta_i = CA^{i-1}B$ are the Markov parameters. In case A, $CE = 1$ and in case B, $CE = 0$ and $CAE = 1$. Similarly, $CB = 0$ since the relative degree of G_p is at least two. The two disturbances are shown in Figure 3.11. When a PID controller is used the integral of the control error is zero both in the unsaturated case and in the saturated case without anti-windup, provided that the closed-loop system is stable. In the latter case the response usually has large overshoots.

The approach taken in the analysis and design is to study the control signal $v(t)$ in the following case. Assume that the set point $y_r = 0$, the controller limits $u_{\min} < 0$ and $u_{\max} > 0$, and that all initial conditions are zero. Further, assume that a positive impulse $d_0\delta(t)$ to the process G_p immediately saturates the controller at the lower limit u_{\min} . Since all feedback, except the anti-windup in the controller, is broken, the block diagram in Figure 3.2 can

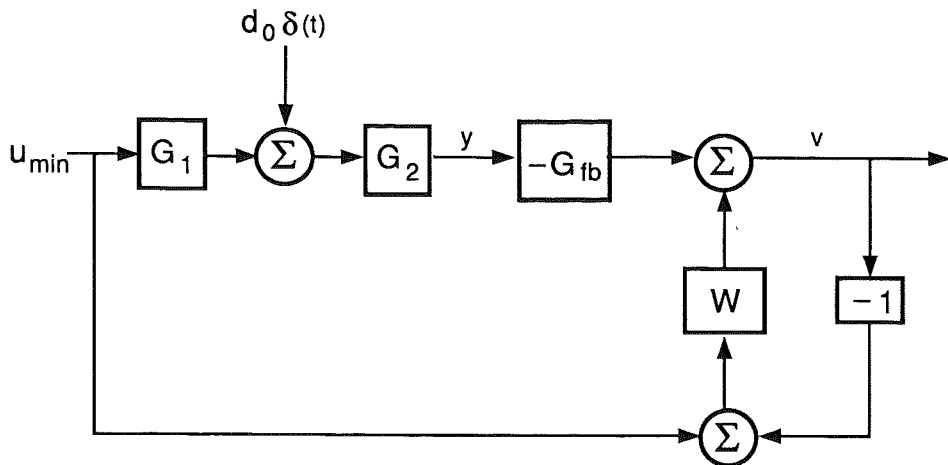


Figure 3.12 When $y_r = 0$, $d(t) = d_0 \delta(t)$ and the controller is saturated at the lower limit u_{min} the block diagram in Figure 3.2 can be redrawn into this block diagram.

be redrawn as shown in Figure 3.12 provided that the process G_p is separated as shown in Figure 3.10. The control signal $v(t)$ will be studied in cases A and B. The idea is to choose the anti-windup such that $v(t)$ satisfies some design criteria which will be formulated below.

Formulation of Design Criteria

The design criteria for anti-windup are based on the insight gained from the following example.

EXAMPLE 3.4—Tracking anti-windup for case A

A simulation of the double-tank process, see Example 3.2, and PID control with tracking anti-windup is tested with an impulse disturbance. Process outputs y and control signals v for different tracking time constants T_t are shown in Figure 3.13. A rather large value of N , the derivative filter constant, is used in these simulations. The PID controller is then close to an ideal PID controller which has $N = \infty$.

Initially $v(t)$ resembles a negative impulse, which is caused by the derivative part in the controller. Immediately after the impulse, the value of v depends on the tracking time constant T_t . In the worst case the controller is immediately desaturated, see the dotted line in Figure 3.13. Compare also Example 3.2. For larger values of T_t the desaturation is not immediate and for very large values of T_t the desaturation comes very late, see the dashed line in Figure 3.13. Note the under- and overshoots in y respectively for small and large T_t . \square

From Figure 3.13 it is thus clear that a moderate value of the tracking time constant T_t gives a good performance. Small and large values of T_t do not

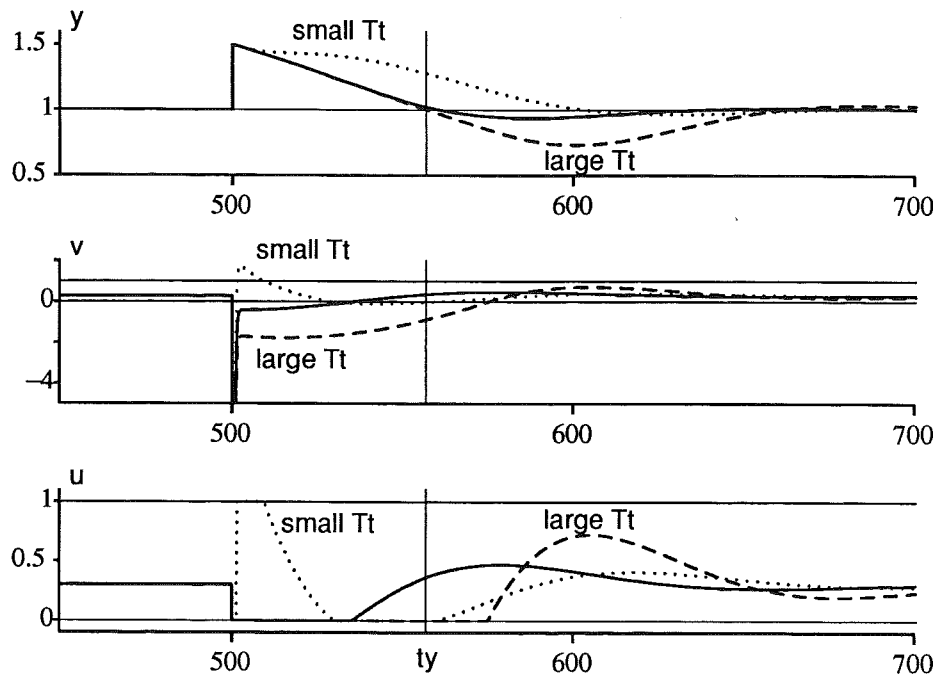


Figure 3.13 Simulation of three cases of tracking anti-windup performance for an impulse disturbance in case A. For large tracking time constants T_t the control signal desaturates too late, which causes excessive overshoot. For a too small tracking time constant the control signal instead resaturates at the opposite limit, which causes undershoot. For a moderate tracking time constant the two extreme cases can be avoided and good performance is obtained. The process is a simulation of the double-tank process from Example 3.2. A large derivative filter constant, $N = 50$, was used in this simulation. Time t_y will be defined later.

give good performances. An immediate desaturation gives undershoot and if desaturation occurs after the control error has changed sign a larger overshoot may be expected.

For case B there is no step change in the process output and thus no impulse from the derivative part in the controller. Then the anti-windup does not affect the initial value of the controller. However, the choice of, e.g., T_t , affects the desaturation time for the controller.

The design criteria for anti-windup are chosen as follows.

Design criterion 1 The control signal must not desaturate immediately after the impulse disturbance. This demand is relevant only in case A. \square

Design criterion 2 The control signal must desaturate before the control error changes sign for the first time after the impulse disturbance. \square

Before proceeding to the analysis of anti-windup, the design criteria will be slightly reformulated in order to get practical and simple test quantities. The phrase “immediately after the impulse disturbance” implies that the right

3.5 Impulse Disturbances and Anti-Windup Design

limit value $v(0_+)$ of $v(t)$ at time $t = 0$ is the interesting quantity when design criterion 1 is checked. Assume that the Laplace transform of $v(t)$ is

$$V(s) = v_0 + v_1 s + v_2 s^2 + \cdots + V_p(s) \quad (3.36)$$

where $V_p(s)$ is strictly proper. The right limit value $v(0_+)$ is given by the initial value theorem

$$v(0_+) = \lim_{s \rightarrow \infty} s V_p(s) \quad (3.37)$$

see, e.g., Kailath (1980). If $V(s)$ is not strictly proper $v(t)$ contains impulses $\delta(t)$, etc., at time $t = 0$.

Design criterion 1 can be written: $v(0_+) < u_{\min}$. \square

The following criterion is usually simpler to evaluate, but it is not sufficient.

Design criterion 1' The control signal must at least satisfy the inequality $v(0_+) < 0$. \square

As long as the controller remains saturated after the impulse disturbance, the control signal is

$$V = -\frac{G_{fb}}{1 + W} Y + \frac{W}{1 + W} \frac{u_{\min}}{s} \quad (3.38)$$

see Figure 3.12. The process output is

$$Y = G_p \frac{u_{\min}}{s} + G_2 d_0 \quad (3.39)$$

or in time domain

$$y(t) = H(t)u_{\min} + h_2(t)d_0 \quad (3.40)$$

where $H(t)$ is the step response of G_p and $h_2(t)$ the impulse response of G_2 .

DEFINITION 3.1—Time t_y

When the saturated control signal $u(t) = u_{\min}$, see the dashed lines in Figure 3.13, the control error changes sign for the first time at time $t = t_y$. Thus t_y is implicitly given by the equation

$$y(t_y) = H(t_y)u_{\min} + h_2(t_y)d_0 = 0 \quad (3.41)$$

If this equation has more than one positive solution, t_y is chosen as the smallest of these solutions. \square

If the desaturation time is t_d , i.e., t_d is the smallest positive solution to $v(t_d) = u_{\min}$, design criterion 2 requires $t_d \leq t_y$. Both t_d and t_y are, however, rather complicated to determine since two nonlinear equations must be solved. This can be done numerically, but little insight is gained and the design rules are not easily formulated.

It is, however, in many cases possible to evaluate $v(t)$, given by (3.38), at time $t = t_y$ and still satisfy design criterion 2, provided a few assumptions are valid. In fact, time t_y does not even have to be determined. It is sufficient to know that $y(t_y) = 0$ and $\frac{dy}{dt}(t_y) < 0$ provided $u = u_{\min}$. Then, presuming $u = u_{\min}$, $v(t_y)$ is given by relatively simple expressions. Note that $v(t)$ computed in this way does not give the correct value of the control signal after desaturation at time t_d . However, if $v(t_d) = u_{\min}$ then it is clear that for $v(t)$ given by (3.38), i.e., when $u = u_{\min}$

$$\begin{cases} v(t) \geq u_{\min} \\ t_d \leq t \leq t_y \end{cases} \Leftrightarrow v(t_y) \geq u_{\min} \quad (3.42)$$

See the solid signal $v(t)$ in Figure 3.13.

Design criterion 2' The control signal $v(t)$, given by (3.38), must satisfy $v(t_y) \geq u_{\min}$ where t_y is defined in Definition 3.1. \square

Remark. If $v(t)$ oscillates then resaturation may occur in the interval $[t_d, t_y]$. Design criterion 2' is not valid for such control signals. \square

Analysis and Design of Tracking Anti-Windup

Now (3.38), i.e.,

$$V = -\frac{G_{fb}}{1+W}Y + \frac{W}{1+W} \cdot \frac{u_{\min}}{s}$$

will be further analyzed for tracking anti-windup in a PID controller. Then, see Sections 3.1–3.2,

$$G_{fb} = K \frac{(N+1)s^2 + (N/T_d + 1/T_i)s + N/(T_i T_d)}{s(s + N/T_d)}$$

$$W = \frac{1}{sT_t}$$

To simplify the analysis for tracking anti-windup the PID controller is for the moment assumed to be ideal, i.e., the derivative filter is neglected by letting $N \rightarrow \infty$. This approximation is reasonable when $T_t > 3T_d/N$. Then

$$\begin{aligned} \frac{G_{fb}}{1+W} &= K \frac{T_d s^2 + s + 1/T_i}{s + 1/T_t} \\ &= K \left(T_d s + \left(1 - \frac{T_d}{T_t}\right) + \frac{f(T_t)}{1 + sT_t} \right) \end{aligned} \quad (3.43)$$

where

$$f(T_t) = \frac{T_d}{T_t} - 1 + \frac{T_t}{T_i} \quad (3.44)$$

and the control signal $v(t)$, from (3.38), is

$$\begin{aligned} v(t) &= -KT_d \frac{dy}{dt}(t) - K\left(1 - \frac{T_d}{T_t}\right)y(t) \\ &\quad - Kf(T_t) \int_0^t \frac{1}{T_t} e^{-(t-s)/T_t} y(s) ds + (1 - e^{-t/T_t})u_{\min} \end{aligned} \quad (3.45)$$

The design idea is to choose T_t such that design criteria 1 (or 1') and 2' are satisfied for $v(t)$. Recall that

$$\begin{aligned} y(t) &= H(t)u_{\min} + h_2(t)d_0 \\ \frac{dy}{dt} &= h(t)u_{\min} + \frac{dh_2}{dt}(t)d_0 \end{aligned} \quad (3.46)$$

where $H(0) = h(0) = 0$ since the relative degree of G_p is at least 2. Further, in case A

$$\begin{aligned} h_2(t) &= CE + CAEt + \dots = 1 - \alpha_1 t + \dots \\ \frac{dh_2}{dt}(t) &= CE\delta(t) + CAE + CA^2t + \dots = \delta(t) - \alpha_1 + CA^2Et + \dots \end{aligned} \quad (3.47)$$

where $CAE = -\alpha_1$ has been introduced. Hence

$$y(0_+) = d_0 \quad \text{and} \quad \frac{dy}{dt}(0_+) = -\alpha_1 d_0$$

If $\alpha_1 > 0$ then $y(t)$ has a negative derivative for small t , see, e.g., Figure 3.13. For $t \approx 0$ in case A, the control signal is

$$v(t) = -KT_d(\delta(t) - \alpha_1)d_0 - K\left(1 - \frac{T_d}{T_t}\right)d_0 \quad (3.48)$$

i.e., there is a negative impulse in the control signal at time $t = 0$. The impulse comes from the derivative part in the controller and affects the integrator via the anti-windup. Hence the right limit value of the control signal is

$$v(0_+) = K\left(\frac{T_d}{T_t} + T_d\alpha_1 - 1\right)d_0 \quad (3.49)$$

To satisfy design criterion 1, i.e., no immediate desaturation or $v(0_+) < u_{\min}$, it is required that

$$T_t > \frac{T_d}{1 - \alpha_1 T_d + u_{\min}/(Kd_0)} \quad (3.50)$$

Here the lower limit for T_t depends on both u_{\min} and the impulse magnitude d_0 . Design criterion 1', i.e., $v(0_+) < 0$, corresponds to the limiting case when $u_{\min} \rightarrow 0$ or $d_0 \rightarrow \infty$. Since $v(0_+)$ is already obtained by an approximation, i.e., $N = \infty$, the simpler design rule implied by design criterion 1' is chosen.

RESULT 3.2—Design limit for tracking anti-windup in case A

For satisfaction of design criterion 1', i.e., $v(0_+) < 0$, it is necessary that

$$T_t > \frac{T_d}{1 - \alpha_1 T_d} \quad (3.51)$$

where $\alpha_1 = -CAE$, and C , A and E are defined in (3.34). \square

Design criteria 1 or 1' can never be satisfied when the following Result holds.

RESULT 3.3—Immediate desaturation

If $1 - \alpha_1 T_d < 0$ the controller desaturates immediately, irrespective of how T_t is chosen, since then $v(0_+) > 0$, see (3.49). \square

The continued analysis in this section requires that at least $1 - \alpha_1 T_d > 0$ but Result 3.2 must also be satisfied. Cases where $1 - \alpha_1 T_d < 0$ will be studied in simulations in Chapter 4.

The simplicity of Results 3.2–3.3 depends on the approximation $N = \infty$ in G_{fb} . If N is finite (3.43) and (3.45) also contain the pole $-N/T_d$ and the mode e^{-tN/T_d} respectively instead of only $-1/T_t$ and e^{-t/T_t} . Further, $v(0_+) = -K(N + 1)d_0$ which is independent of T_t .

According to design criterion 2', $v(t_y) - u_{\min} \geq 0$ is required. Thus, using (3.45) and (3.41)

$$v(t_y) - u_{\min} = -KT_d \frac{dy}{dt}(t_y) - Kf(T_t) \int_0^{t_y} \frac{1}{T_t} e^{-(t_y-s)/T_t} y(s) ds - e^{-t_y/T_t} u_{\min} \quad (3.52)$$

Since $u_{\min} < 0$, $\frac{dy}{dt}(t_y) < 0$ and $y(t) > 0$ for $0 < t < t_y$ it is clear that $v(t_y) - u_{\min} \geq 0$ if $f(T_t) \leq 0$. Thus the sign of $f(T_t)$, (3.44), has to be checked, where

$$f(T_t) = \frac{T_d}{T_t} - 1 + \frac{T_t}{T_i}$$

which has the local minimum

$$f_{\min} = \sqrt{\frac{4T_d}{T_i}} - 1 \quad \text{for} \quad T_t = \sqrt{T_i T_d} \quad (3.53)$$

and if $T_i \geq 4T_d$

$$f = 0 \quad \text{for} \quad T_t = \frac{T_i}{2} \left(1 \pm \sqrt{1 - \frac{4T_d}{T_i}} \right) \quad (3.54)$$

If $T_i \geq 4T_d$ the obvious choice is to make $f(T_t) \leq 0$.

RESULT 3.4—Design limits for tracking anti-windup

Design criterion 2', i.e., $v(t_y) \geq u_{\min}$, is satisfied when $T_i \geq 4T_d$ and T_t is chosen such that

$$\frac{T_i}{2} \left(1 - \sqrt{1 - \frac{4T_d}{T_i}} \right) \leq T_t \leq \frac{T_i}{2} \left(1 + \sqrt{1 - \frac{4T_d}{T_i}} \right) \quad (3.55)$$

Without derivative action the design limits are $0 < T_t \leq T_i$. \square

In case A Result 3.2 must also be considered. However, it may happen that

$$\frac{T_d}{1 - \alpha_1 T_d} > T_i$$

also when $T_i \geq 4T_d$. If then $T_t > T_d/(1 - \alpha_1 T_d) > T_i$ the controller will not surely desaturate either at time $t = 0$ or at time $t = t_y$. Design criterion 2' is then not surely satisfied. A possible conclusion is that T_t must always be less than (or equal) to T_i even if Result 3.2 is violated.

RESULT 3.5—Revised design limits for tracking anti-windup

It is necessary that T_t is chosen such that

$$0 < T_t \leq T_i \quad (3.56)$$

If possible Results 3.2 and 3.4 must also be followed. \square

If $T_i < 4T_d$ it is still possible that $v(t_y) \geq u_{\min}$ for some T_t , but it is difficult to prove in the general case. A possible strategy is to approximately minimize the integral term in (3.52), which now is positive. Neglecting initial conditions

$$\begin{aligned} I &= f(T_t) \int_0^{t_y} \frac{1}{T_t} e^{-(t_y-s)/T_t} y(s) ds \\ &= f(T_t) \cdot \left(y(t_y) - T_t \frac{dy}{dt}(t_y) + T_t^2 \frac{d^2y}{dt^2}(t_y) - \dots \right) \end{aligned} \quad (3.57)$$

The following observations can then be made

1. If $y(t_y) = 0$ and $\frac{dy}{dt}(t) < 0$ is constant, minimization of $f(T_t) \cdot T_t$, i.e., choosing $T_t = T_i/2$, minimizes I .
2. In other cases the minimizing T_t depends on $y(t)$. The second best choice is then to minimize $f(T_t)$, the coefficient in front of the integral, i.e., to choose $T_t = \sqrt{T_i T_d}$.

When $T_i \geq 4T_d$ both $T_t = T_i/2$ and $T_t = \sqrt{T_i T_d}$ satisfy Result 3.4. When $T_i < 4T_d$ then $\sqrt{T_i T_d} > T_i/2$. Hence $T_t = \sqrt{T_i T_d}$ is a “safer” choice in case A, when Result 3.2 also must be satisfied.

RESULT 3.6—Design rules for tracking anti-windup

The two design rules

$$T_t = \sqrt{T_i T_d} \quad (3.58)$$

$$T_t = \frac{T_i}{2} \quad (3.59)$$

both satisfy Result 3.4 when $T_i \geq 4T_d$. When $T_i < 4T_d$ the two choices approximately minimize the integral (3.57). If $y(t)$ has a constant derivative at time $t = t_y$ then $T_t = T_i/2$ minimizes the integral. The choice $T_t = \sqrt{T_i T_d}$ minimizes the coefficient in front of the integral in (3.57) and is better when Result 3.2 must be satisfied. \square

Small values of T_t In the results above small values of T_t are excluded, since the derivative filter in the controller cannot be neglected when $T_t < 3T_d/N$. In case A T_t is also limited by Result 3.2. In case B it may, however, be possible to use small values of T_t . This will now be investigated.

Above the derivative filter was neglected when $T_t > 3T_d/N$. For small values of T_t it is instead reasonable to neglect the “integrator” dynamics when $T_t < T_d/(3N)$, i.e., letting $sT_t \rightarrow 0$. Then the control signal, (3.38), is

$$\begin{aligned} V &= -\frac{G_{fb}}{1+W}Y + \frac{1}{1+W} \frac{u_{\min}}{s} \\ &= -KT_t \left((N+1)s + \left(\frac{1}{T_i} - \frac{N^2}{T_d}\right) + \frac{N^3}{T_d^2} \frac{1}{s + N/T_d} \right) Y + \frac{1}{s} u_{\min} \end{aligned} \quad (3.60)$$

Hence

$$\begin{aligned} v(t) &= -KT_t \left((N+1)\frac{dy}{dt}(t) + \left(\frac{1}{T_i} - \frac{N^2}{T_d}\right)y(t) \right. \\ &\quad \left. + \frac{N^3}{T_d^2} \int_0^t e^{-(t-s)N/T_d} y(s) ds \right) + u_{\min} \end{aligned} \quad (3.61)$$

3.5 Impulse Disturbances and Anti-Windup Design

Integration by parts gives

$$\frac{N^3}{T_d^2} \int_0^t e^{-(t-s)N/T_d} y(s) ds = \frac{N^2}{T_d} y(t) - N \frac{dy}{dt}(t) + T_d \int_0^t e^{-(t-s)N/T_d} \frac{d^2y}{dt^2}(s) ds \quad (3.62)$$

which yields

$$v(t) = -K \frac{T_t}{T_i} y(t) - K T_t \frac{dy}{dt} - K T_t T_d \int_0^t e^{-(t-s)N/T_d} \frac{d^2y}{dt^2}(s) ds + u_{\min} \quad (3.63)$$

Evaluated at time t_y , when $y(t_y) = 0$ and $\frac{dy}{dt}(t_y) < 0$,

$$v(t_y) - u_{\min} = -K T_t \frac{dy}{dt}(t_y) - K T_t T_d \int_0^{t_y} e^{-(t-s)N/T_d} \frac{d^2y}{dt^2}(s) ds \quad (3.64)$$

If $\frac{d^2y}{dt^2} \leq 0$, at least during the last part of the time interval $[0, t_y]$, design criterion 2' is satisfied, i.e., the controller desaturates before the control error changes sign.

RESULT 3.7—Fast tracking anti-windup in case B

Fast tracking anti-windup, i.e.,

$$0 < T_t < \frac{T_d}{3N} \quad (3.65)$$

is in case B a sufficient condition for desaturation according to design criterion 2', provided

$$\frac{d^2y}{dt^2} \leq 0 \quad \text{for} \quad 0 < t \leq t_y$$

or at least during the last part of the interval, e.g., for $t_y - 3T_d/N < t \leq t_y$. \square

Synthesis of design rules Now Results 3.2–3.7 will be synthesized into design rules for tracking anti-windup in cases A and B respectively. In the synthesis a result from Section 3.6 is also considered. There it is shown that larger tracking time constants T_t are preferable.

RESULT 3.8—Design rule for tracking anti-windup in case A

Choose

$$T_t = \begin{cases} \min\left(T_i, \max\left(\sqrt{T_i T_d}, \frac{T_i}{2}, \frac{T_d}{1 - \alpha_1 T_d}\right)\right) & \text{when } 1 - \alpha_1 T_d > 0 \\ T_i & \text{when } 1 - \alpha_1 T_d \leq 0 \end{cases} \quad (3.66)$$

Normally this rule chooses the largest value of $\sqrt{T_i T_d}$ and $T_i/2$, but when $\alpha_1 T_d$ grows Results 3.2 and 3.5 are applied. When $\alpha_1 T_d \geq 1$ immediate desaturation is obtained and the analysis was discontinued, but $T_t = T_i$ is suggested for this case too. \square

RESULT 3.9—Design rule for tracking anti-windup in case B

Choose

$$T_t = \min\left(T_i, \max\left(\sqrt{T_i T_d}, \frac{T_i}{2}\right)\right) \quad (3.67)$$

Now immediate desaturation need not be considered. However, due to the result in Section 3.6 small values for T_t , see Result 3.7, are omitted. \square

These rules are valid if $T_t > 3T_d/N$, when one controller mode may be neglected. When $T_i \geq 4T_d$ the design criteria are satisfied (sufficient conditions), except when Result 3.2 demands a value of T_t outside the interval in (3.55). This completes the analysis and design of tracking anti-windup with respect to impulse disturbances.

Analysis and Design of Anti-Windup by the Observer Approach

The observer approach anti-windup will be analyzed similar to tracking anti-windup. Thus the control signal, i.e., (3.38),

$$V = -\frac{G_{fb}}{1+W} Y + \frac{W}{1+W} \cdot \frac{u_{\min}}{s}$$

will be studied in case A and B when

$$G_{fb} = K \frac{(N+1)s^2 + (N/T_d + 1/T_i)s + N/(T_i T_d)}{s(s + N/T_d)}$$

$$W(s) = \frac{(2\omega_0 - N/T_d)s + \omega_0^2}{s(s + N/T_d)}$$

see Section 3.1–3.2. In the observer approach both controller poles are moved to $-\omega_0$ by the anti-windup. The process output is given by (3.39), i.e.,

$$Y = G_p \frac{u_{\min}}{s} + G_2 d_0$$

In contrast to tracking anti-windup the derivative filter cannot initially be neglected in the analysis. The transfer function

$$\frac{G_{fb}}{1+W} = K \left(N + 1 + \frac{g_0 s + g_1}{(s + \omega_0)^2} \right) \quad (3.68)$$

3.5 Impulse Disturbances and Anti-Windup Design

is proper and

$$\begin{aligned} g_0 &= \frac{N}{T_d} + \frac{1}{T_i} - 2(N+1)\omega_0 \\ g_1 &= \frac{N}{T_i T_d} - (N+1)\omega_0^2 \end{aligned} \quad (3.69)$$

Since (3.68) is proper it follows that $V(s)$ is strictly proper, i.e., $v(t)$ does not contain impulses at time $t = 0$.

In case A the controller is immediately saturated if

$$v(0+) = -K(N+1)d_0 < u_{\min} \quad (3.70)$$

In case B the controller is not immediately saturated. However, for small times t when the controller has not yet saturated

$$\frac{dv}{dt}(t) \approx -K(N+1)d_0 \quad (3.71)$$

Thus, if d_0 is sufficiently large, the controller quickly saturates. For simplicity this case is treated as if the controller saturated at time $t = 0$.

Further analysis of $v(t)$ for $t \approx 0$ is deferred until later. For the continued analysis it is assumed that $v(t)$ remains saturated for a while. Then it follows from (3.38) and (3.68) that

$$\begin{aligned} v(t) - u_{\min} &= -K(N+1)y(t) - Kg_0 \int_0^t (1 - \omega_0 s)e^{-\omega_0 s} y(t-s) ds \\ &\quad - Kg_1 \int_0^t s e^{-\omega_0 s} y(t-s) ds \\ &\quad - \left(\left(\frac{N}{T_d} - \omega_0 \right) t + 1 \right) e^{-\omega_0 t} u_{\min} \end{aligned} \quad (3.72)$$

From design criterion 2' this quantity should be positive at time $t = t_y$.

From the definition of time t_y , see (3.41), it is clear that $y(t) > 0$ for $0 < t < t_y$ and $y(t_y) = 0$ in both cases of impulse disturbances. Thus $v(t_y) - u_{\min} \geq 0$ if

$$\omega_0 \leq \frac{N}{T_d}, \quad g_1 \leq 0 \quad \text{and} \quad g_0 = 0 \quad (3.73)$$

since then all terms are zero or negative. Thus it is required that

$$\begin{aligned}\omega_0 &\leq \frac{N}{T_d} \\ \omega_0 &\geq \sqrt{\frac{N}{N+1} \cdot \frac{1}{T_i T_d}} \approx \frac{1}{\sqrt{T_i T_d}} \\ \omega_0 &= \frac{1}{2(N+1)} \left(\frac{N}{T_d} + \frac{1}{T_i} \right) \approx \frac{1}{2T_d}\end{aligned}\tag{3.74}$$

All conditions may be satisfied if $T_i \geq 4T_d$ and $N > 1/2$.

RESULT 3.10—Design rule 1 for anti-windup using the observer approach Design criterion 2', i.e., $v(t_y) \geq u_{\min}$, is satisfied when $T_i \geq 4T_d$, $N > 1/2$, and ω_0 is chosen such that

$$\omega_0 = \frac{1}{2(N+1)} \left(\frac{N}{T_d} + \frac{1}{T_i} \right) \approx \frac{1}{2T_d}\tag{3.75}$$

□

If $T_i < 4T_d$ it is still possible, but in general hard to prove, that $v(t_y) - u_{\min} \geq 0$. It is, however, possible to approximately minimize the integral terms in (3.72), compare tracking anti-windup. Neglecting initial conditions

$$\begin{aligned}I &= \int_0^{t_y} \left(g_0(1 - \omega_0 s) + g_1 s \right) e^{-\omega_0 s} y(t-s) ds \\ &= \frac{1}{\omega_0^2} \left(g_1 y(t_y) + \left(g_0 - \frac{2}{\omega_0} g_1 \right) \frac{dy}{dt}(t_y) + \left(\frac{3}{\omega_0^2} g_1 - \frac{2}{\omega_0} g_0 \right) \frac{d^2 y}{dt^2}(t_y) + \dots \right)\end{aligned}\tag{3.76}$$

The following observations are made.

1. If $y(t_y) = 0$ and $\frac{dy}{dt}(t_y) < 0$ is constant, $2g_1 \leq \omega_0 g_0$, i.e., $\omega_0 \geq 2/T_i$, makes $I \leq 0$ and design criterion 2' is satisfied.
2. In other cases the minimizing ω_0 depends on $y(t)$.

Thus three quantities, $1/(2T_d)$, $1/\sqrt{T_i T_d}$ and $2/T_i$, are lower limits or exact conditions for ω_0 . When $T_i \geq 4T_d$ then $1/(2T_d)$ is the larger of the three quantities, otherwise $2/T_i$ is largest.

RESULT 3.11—Design rule 2 for anti-windup using the observer approach The general design rule

$$\omega_0 = \max \left(\frac{1}{2T_d}, \frac{2}{T_i} \right)\tag{3.77}$$

satisfies Result 3.10 when $T_i \geq 4T_d$. When $T_i < 4T_d$ design criterion 2' is satisfied for the special case when $y(t_y) = 0$ and $y(t)$ has a constant derivative.

□

3.5 Impulse Disturbances and Anti-Windup Design

If $y(t)$ is not well approximated by a straight line the following design rule may be better to use.

RESULT 3.12—Design rule 3 for anti-windup by the observer approach
Choose

$$\omega_0 = \max\left(\frac{1}{\sqrt{T_i T_d}}, \frac{1}{2T_d}\right) \quad (3.78)$$

When $T_i \geq 4T_d$ Result 3.10 is satisfied. When $T_i < 4T_d$ then at least $g_1 = 0$ but $g_0 > 0$ in (3.72). \square

For large ω_0 the controller desaturates rather quickly. There is, however, one significant difference compared to tracking anti-windup. The initial value of the controller is $v(0_+) = -K(N+1)d_0$ in case A, irrespective of ω_0 . This value does not give any upper limit for ω_0 similar to the lower limit for T_t in Result 3.2, i.e., $T_t > T_d/(1 - \alpha_1 T_d)$. However, for large ω_0 and relatively small times t a minor result is obtainable from an investigation of $v(t)$ in case A.

Assume that $\omega_0 > N/T_d$. Then

$$\frac{G_{fb}}{1 + W} \rightarrow K(N+1) \frac{s^2}{(s + \omega_0)^2} \quad (3.79)$$

$$\frac{W}{1 + W} \rightarrow \frac{2\omega_0 s + \omega_0^2}{(s + \omega_0)^2} \quad (3.80)$$

Further, neglect $H(t)u_{\min}$ in $y(t)$, i.e., consider only the disturbance impulse response $h_2(t)d_0$ in case A, see (3.40). This is reasonable if time t is relatively small. Then from (3.38),

$$V - \frac{u_{\min}}{s} = -\left(K(N+1)G_2d_0 + \frac{u_{\min}}{s}\right) \frac{s^2}{(s + \omega_0)^2} \quad (3.81)$$

If the impulse response $h_2(t)d_0$ is almost constant for small t , i.e., $h_2(t)d_0 \approx d_0$, then

$$V - \frac{u_{\min}}{s} = -\left(K(N+1)d_0 + u_{\min}\right) \cdot \frac{s}{(s + \omega_0)^2} \quad (3.82)$$

i.e.,

$$v(t) - u_{\min} = -\left(K(N+1)d_0 + u_{\min}\right) \cdot (1 - \omega_0 t) e^{-\omega_0 t} \quad (3.83)$$

Thus desaturation occurs for time $t_d = \omega_0^{-1}$, if the simplifications above are valid. In Figure 3.14 this is tested and verified for a simulation of the

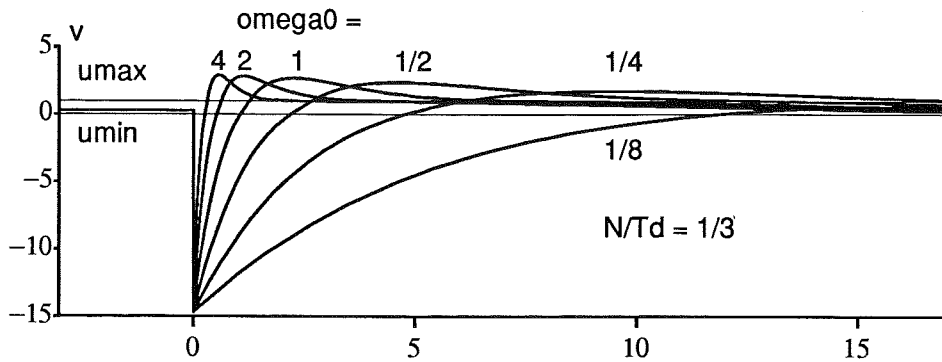


Figure 3.14 Anti-windup by the observer approach for a simulation of the double-tank process in Example 3.2. The desired control signal $v(t)$ is shown for different large ω_0 . When $\omega_0 > N/T_d$ it is seen that the desaturation time t_d is such that $\omega_0 t_d \approx 1$. When $\omega_0 < N/T_d$ then $\omega_0 t_d$ is larger. For large ω_0 $v(t)$ resaturates and then remains at $v = u_{\max}$ a while before the final desaturation.

double-tank process in Example 3.2. For $\omega_0 > N/T_d$ it thus seems possible to estimate the desaturation time t_d from the relation $t_d \omega_0 \approx 1$. When $\omega_0 < N/T_d$ the product $t_d \omega_0 > 1$ in Figure 3.14. If a minimum value for the desaturation time t_d is specified, it is thus possible to get an approximate upper bound for ω_0 .

RESULT 3.13—Design limit for the observer approach in case A

A desaturation time $t_d > t_0$, where t_0 is some predetermined or desired value, is approximately obtained if

$$\omega_0 < \frac{1}{t_0} \quad (3.84)$$

□

Remark. When $\omega_0 < N/T_d$ the upper limit in (3.84) is probably conservative.

RESULT 3.14—A lower limit for the desaturation time in case A

For a given value of ω_0 , the desaturation time t_d is (approximately) such that

$$t_d \geq \frac{1}{\omega_0} \quad (3.85)$$

□

Design rules Two general design rules, see Results 3.11–3.12, suggesting

$$\omega_0 = \max \left(\frac{1}{2T_d}, \frac{2}{T_i} \right) \quad \text{and} \quad \omega_0 = \max \left(\frac{1}{2T_d}, \frac{1}{\sqrt{T_i T_d}} \right)$$

have been derived for the observer approach. Their performance are, however, not predicted but has to be evaluated in simulations and experiments. In case A the design limit in Result 3.13 may be used.

Summary

In this section anti-windup by tracking and the observer approach have been analyzed for process impulse disturbances. Design criteria for the anti-windup methods have been formulated and design rules have been derived. When $T_i \geq 4T_d$ sufficient conditions for satisfaction of design criteria were obtained. When $T_i < 4T_d$ the obtained conditions may be sufficient in the special case when the process output has constant derivative. In other cases the conditions have to be evaluated in simulations or by experiments.

When $T_i \geq 4T_d$ the noninteracting PID controller can be converted to the interacting PID controller (3.3). Hence corresponding design rules for anti-windup in an interacting PID controller are always sufficient for satisfaction of design criterion 2. However, it may in some cases be necessary to make an exact parameter conversion for finite N instead of the simplified conversion which only holds for infinite N .

The obtained anti-windup design rules will be tested in simulations and experiments on a number of different processes in Chapter 4. The evaluation will also reveal if the design criteria are well chosen.

3.6 Sinusoidal Measurement Disturbances

If the measurement signal y is contaminated by a sinusoidal disturbance large enough to cause partial controller saturation the *anti-windup mechanism* will cause an offset in the output y . This is most noticeable when the controller is close to saturation, and was demonstrated in Example 3.3. The size of the offset depends on the speed of the anti-windup, e.g., the tracking time constant T_t or the observer bandwidth ω_0 .

One immediate way of eliminating the disturbance is to filter the measurement signal. This is, however, feasible only when the disturbance frequency $\omega_d \gg \omega_c$, the crossover frequency. If ω_d is relatively close to ω_c , say $\omega_d < 5\omega_c$, then the filter cannot both damp the disturbance well and be negligible in the loop gain. This is the type of situation considered, although a high disturbance frequency is assumed in the derivation below. If the controller is not close to saturation then the amplitude n_1 and the frequency ω_d are assumed to be such that the resulting oscillations in u and y are insignificant, and there is no offset in the process output y if the controller has integral action.

PID Controllers and High Frequencies

For high frequencies the feedback controller transfer function (3.1), has the property

$$\lim_{\omega \rightarrow \infty} G_{fb}(i\omega) = K(N + 1) \quad (3.86)$$

which is assumed to be valid for $\omega > 3N/T_d$. For discrete-time PID controllers, however, the high-frequency behavior also depends on the choice of the sampling interval h . To avoid aliasing only frequencies $\omega \leq \pi/h$ are considered. For high frequencies the feedback path of a discrete-time PID controller, (3.4), is

$$\lim_{\omega \rightarrow \pi/h} G_{fb}(e^{i\omega h}) = K \left(1 - \frac{h}{2T_i} + N \cdot \frac{2\gamma}{1+\gamma} \right) \quad (3.87)$$

where, from (3.5),

$$\gamma = \frac{T_d}{Nh + T_d}$$

Thus, if $h \rightarrow 0$, then $\gamma \rightarrow 1$, and (3.87) will coincide with (3.86). The two equations are assumed to be sufficiently close if both

$$\frac{h}{2T_i} < 5\% \quad \text{and} \quad 1 - \frac{2\gamma}{1+\gamma} = \frac{Nh}{2T_d} < 5\% \quad (3.88)$$

i.e., if

$$h < \min \left(\frac{T_i}{10}, \frac{T_d}{10N} \right) \quad (3.89)$$

Usually $T_i \gg T_d/N$, thus it is the derivative part that limits the choice of sampling interval h . The limit in (3.89) is slightly conservative. E.g., in Åström and Wittenmark (1990) a 2–6 times larger sampling interval is suggested.

When (3.89) is satisfied continuous-time and discrete-time PID controllers thus have the same high-frequency behavior. The anti-alias filter in the discrete-time PID controller can then be discussed in the same way as the filter above. Thus a disturbance with frequency ω_d may both be insufficiently damped by the anti-alias filter and have a high frequency with respect to the controller parameters.

One goal with the derivation below is, loosely speaking, to be able to avoid controllers with a large “high-frequency gain” close to saturation. The high-frequency sinusoidal disturbance is a good tool for this purpose. The exact meaning of “high-frequency gain” will become clear later.

Derivation of Output Offset

The effects of one-sided (upper) saturation, as illustrated in Figure 3.15, will now be investigated. Consider deviations from a stationary point close to upper saturation, i.e., let $y_r = y = u = v = 0$ before the noise disturbance has been applied. Further, $u_{\max} \geq 0$ is small and $u_{\min} = -\infty$ since only one-sided saturation is considered. With obvious changes partial lower saturation

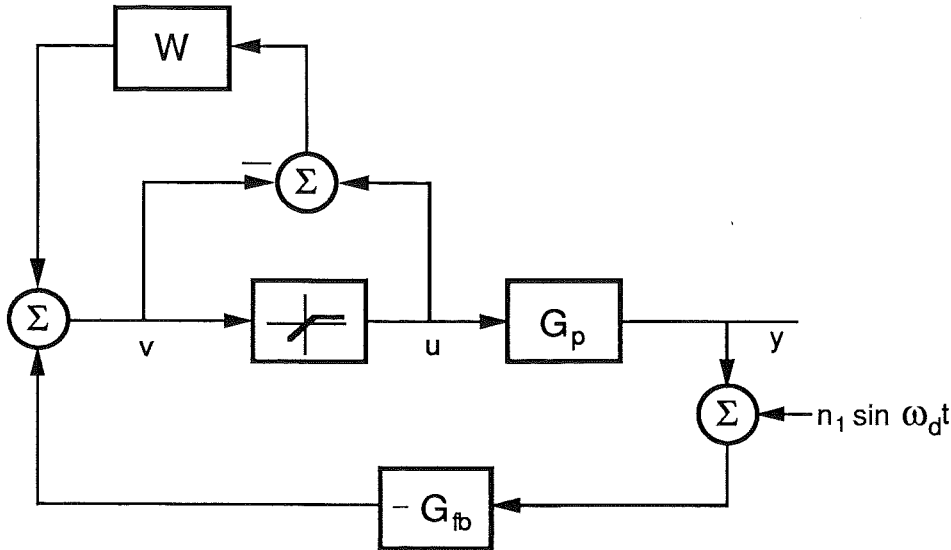


Figure 3.15 Block diagram for the one-sided saturation problem. G_p is the process transfer function, G_{fb} is the feedback path of the controller and W is the anti-windup transfer function.

can be treated. The disturbance frequency ω_d is assumed to be high, such that $G_p(i\omega_d) \approx 0$, $G_{fb}(i\omega_d) \approx K(N + 1)$ and $W(i\omega_d) \approx 0$.

The goal of the derivation below is to obtain an estimate of the bias y_0 in the process output $y(t)$, which is caused by a sinusoidal measurement disturbance $n = n_1 \sin \omega_d t$. It is an application of the SBDF (sinusoidal+bias describing function) method, see Atherton (1975). The input to the nonlinearity in Figure 3.15 is

$$v(t) = v_0 + v_1 \sin(\omega_d t) \quad (3.90)$$

where $v_1 = K(N + 1)n_1$ if the sign change in $-G_{fb}$ is neglected. The output from the nonlinearity is

$$u(t) = u_0 + u_1 \sin(\omega_d t) + u_2 \sin(2\omega_d t) + \dots \quad (3.91)$$

In the SBDF method only the bias and first harmonic are considered, and the output is then written

$$\hat{u}(t) = N_0 v_0 + N_1 v_1 \sin(\omega_d t) \quad (3.92)$$

where N_0 and N_1 both depend on v_0 and v_1 . N_0 is the gain of the bias and N_1 is the gain of the first harmonic. When determining the output offset only the bias term is necessary, since $G_p(i\omega_d) \approx 0$. Thus

$$u_0 = N_0 v_0 = v_0 + v_1 \Phi_0 = v_0 + v_1 \left(\left(\frac{1}{2} - \frac{\phi}{\pi} \right) \sin \phi - \frac{1}{\pi} \cos \phi \right) \quad (3.93)$$

where

$$\phi = \arcsin \frac{u_{\max} - v_0}{v_1} \quad (3.94)$$

At the limit of saturating at all $u_{\max} = v_1$ and $v_0 = 0$, i.e., $\phi = \pi/2$. If $u_{\max} = 0$ then $v_0 = v_1$, i.e., $\phi = -\pi/2$. Thus $\Phi_0 \in [-1, 0]$. For low frequencies

$$G_{fb}(s) = \frac{K}{sT_i} \quad \text{and} \quad W(s) = \frac{1}{sT_w} \quad (3.95)$$

where $T_w = T_t$ for tracking anti-windup and $T_w = N/(\omega_0^2 T_d)$ for the observer approach, see Sections 3.1–3.2. The low frequency gain of the process, $G_p(0)$, may be infinite. Thus, for zero frequency

$$\begin{aligned} y_0 &= G_p(0) u_0 \\ v_0 &= \int \left(-\frac{K}{T_i} y_0 + \frac{1}{T_w} (u_0 - v_0) \right) dt \\ u_0 &= v_0 + v_1 \Phi_0 \end{aligned} \quad (3.96)$$

When v_0 is constant

$$\frac{KT_w}{T_i} y_0 = u_0 - v_0 = v_1 \Phi_0 \quad (3.97)$$

and the offset may be computed.

RESULT 3.15—Stationary offset for sinusoidal disturbance

During partial upper saturation caused by a sinusoidal disturbance the bias v_0 in $v(t)$ is determined from the nonlinear equation.

$$v_0 + v_1 \Phi_0(v_0, v_1) \Phi_p = 0 \quad (3.98)$$

where

$$\Phi_p = 1 - \frac{T_i}{KT_w G_p(0)} \quad (3.99)$$

and Φ_0 is given in (3.93). When v_0 (and thus Φ_0) is known the estimated stationary offset is

$$\hat{y}_0 = \frac{T_i}{KT_w} \Phi_0 v_1 = \frac{T_i(N+1)}{T_w} \Phi_0 n_1 \quad (3.100)$$

Since $-1 \leq \Phi_0 \leq 0$ it follows that $y_0 \leq 0$ and bounded at partial upper saturation. \square

Solving the Nonlinear Equation (3.98)

In order to estimate the offset y_0 (3.98) must be solved numerically. From the structure of (3.98) an iterative solution is appealing.

ALGORITHM 3.1—Iterative solution of (3.98)

Let

$$v_1 = K(N+1)n_1$$

$$\Phi_g = \frac{G_p(0)KT_w}{G_p(0)KT_w - T_i}$$

$$v_{0,0} = u_{\max}$$

Then iterate from $k = 0$ until convergence

$$\phi_k = \arcsin \frac{u_{\max} - v_{0,k}}{v_1}$$

$$\Phi_{0,k} = \left(\frac{1}{2} - \frac{\phi_k}{\pi} \right) \sin \phi_k - \frac{1}{\pi} \cos \phi_k$$

$$v_{0,k+1} = -\frac{v_1}{\Phi_g} \Phi_{0,k}$$

Having found $v_0 = v_{0,\infty}$ and thus $\Phi_0 = \Phi_{0,\infty}$ the offset estimate \hat{y}_0 is given by (3.100). \square

The stability of Algorithm 3.1 is now to be examined.

LEMMA 3.2—A bounded derivative

With v_1 , Φ_0 and ϕ from (3.93)

$$\frac{d}{dv_0}(v_1 \Phi_0) = \frac{\phi}{\pi} - \frac{1}{2} \in [-1, 0]$$

Proof: Straightforward differentiation yields

$$\begin{aligned} \frac{d}{dv_0}(v_1 \Phi_0) &= v_1 \frac{d\Phi_0}{d\phi} \cdot \frac{d\phi}{dv_0} \\ &= v_1 \left(\left(\frac{1}{2} - \frac{\phi}{\pi} \right) \cos \phi \right) \cdot \left(-\frac{1}{v_1 \cos \phi} \right) \\ &= \frac{\phi}{\pi} - \frac{1}{2} \in [-1, 0] \end{aligned} \quad (3.101)$$

\square

LEMMA 3.3—Stability of Algorithm 3.1

The iteration in Algorithm 3.1 is stable if

$$\frac{KT_w G_p(0)}{T_i} > \frac{1}{2}$$

Proof: The iteration can be described by $v_{0,k+1} = f(v_{0,k})$. From numerical analysis it is well known that the iteration converges if $| \frac{df}{dv_0} | < 1$. Using

Lemma 3.2

$$\left| \frac{df}{dv_0} \right| = \left| \frac{\phi}{\pi} - \frac{1}{2} \right| \cdot |\Phi_p| \leq |\Phi_p| = \left| 1 - \frac{T_i}{KT_w G_p(0)} \right| < 1$$

if the given condition is true. \square

If the condition in Lemma 3.3 is not true, then Algorithm 3.1 is not stable if $|\Phi_0|$ is sufficiently large. Due to the structure of (3.98) there is no obvious way of “iterating in the other direction”. Instead (3.98) is then most easily solved by some algorithm for finding roots in an interval or by squaring and finding the local minimum. Such algorithms cover all cases for Φ_p , and can be found in, e.g., Forsythe *et al.* (1976). They are also included in, e.g., Matlab.

A Test Quantity

From (3.100) it follows that

$$|\hat{y}_0| = \frac{T_i(N+1)}{T_w} |\Phi_0| n_1 \quad (3.102)$$

where Φ_0 is the solution of (3.98).

DEFINITION 3.2—High-frequency to DC gain

The high-frequency to DC gain K_{HD} is defined as

$$K_{HD} = \frac{|\hat{y}_0|}{n_1} = \frac{T_i(N+1)}{T_w} |\Phi_0| \quad (3.103)$$

Since $|\Phi_0| \leq 1$ with equality for $u_{\max} = 0$ and $G_p(0) = \infty$, the maximum high-frequency to DC gain is

$$K_{HD,\max} = \frac{T_i(N+1)}{T_w} \quad (3.104)$$

\square

Remark 1. From (3.104) it is clear that both N and T_w can be used for reducing $K_{HD,\max}$ without affecting the nominal design parameters K , T_i , and T_d . \square

Remark 2. Without anti-windup, i.e., $W(s) = 0$, and $T_w = \infty$, it is easily seen from (3.96) that $y_0 = 0$. Thus, it is clear that the offset is caused by the anti-windup mechanism (if the disturbance is present). \square

Remark 3. Consider a process with at least one integrator, i.e., $G_p(0) = \infty$. Without saturation the control error is $e = 0$ in stationarity. If the controller is saturated in stationarity, then $|e| \rightarrow \infty$. However, in the case considered in this section a constant $e \neq 0$ is obtained in stationarity. \square

Remark 4. For the interacting PID controller (3.3) the results above hold if K is replaced by K' , T_i by T'_i and $N + 1$ by N' , where the prime indicates parameters in the interacting controller. \square

For tracking anti-windup $T_w = T_t$, i.e.,

$$K_{HD,\max} = \frac{T_i(N+1)}{T_t} \quad (3.105)$$

This quantity is reduced by choosing the largest possible T_t and a small value of N . The design rules (3.66–3.67) give $T_i/2 \leq T_t \leq T_i$, and then

$$N+1 \leq K_{HD,\max} \leq 2(N+1)$$

Hence the ratio between the estimated offset \hat{y}_0 and the disturbance amplitude n_1 may become as large as $2(N+1)$. E.g., if $N = 20$, $T_t = T_i/2$, $G_p(0) = \infty$ and $u_{\max} = 0$ a 1 % disturbance amplitude gives an estimated offset \hat{y}_0 of 42 %. If $u_{\max} > 0$ and the process has finite static gain, then smaller offsets are obtained.

For the observer approach $T_w = N/(\omega_0^2 T_d)$, i.e.,

$$K_{HD,\max} = \omega_0^2 T_d T_i \frac{N+1}{N} \approx \omega_0^2 T_d T_i \quad (3.106)$$

If the design rule $\omega_0 = \max((2T_d)^{-1}, 2/T_i)$, i.e., (3.77), is used, then

$$K_{HD,\max} \geq 1$$

with equality when $T_i = 4T_d$. If $\omega_0 = 1/\sqrt{T_i T_d}$, i.e., (3.78), then $K_{HD,\max} = 1$.

Comparison Thus the observer approach usually gives a controller where the maximum noise sensitivity is much smaller compared to tracking anti-windup. Note that when $T_i = 4T_d$ and the design rules are followed, then the observer approach has minimum noise sensitivity ($= 1$) while tracking anti-windup has maximum sensitivity ($= 2(N+1)$). However, when $T_i \gg 4T_d > 0$ the observer approach also has high noise sensitivity, when the design rule in (3.77) is used. When $\omega_0 = 1/\sqrt{T_i T_d}$ the observer approach always has a low noise sensitivity.

Summary

As will be demonstrated in Chapter 4, the estimated output offset \hat{y}_0 , in (3.100), is very accurate provided the disturbance frequency ω_d is sufficiently high. Then the feedback through W is eliminated for high frequencies, see Figure 3.15. A rule of thumb is that if $|W(i\omega_d)| < 0.25$ the feedback from W is negligible. Since the input to the nonlinearity then is sinusoidal the describing function gives an accurate estimate of the DC component in the output from the nonlinearity. For lower frequencies, when W is not negligible, a smaller offset $|\hat{y}_0|$ is obtained.

3.7 Summary

After an introduction of PID controllers and some anti-windup methods a number of design rules and results for anti-windup by tracking and the observer approach have been derived. The rules and results are based on performance for process impulse disturbances and sinusoidal measurement noise. Stability properties have also been investigated.

In Section 3.3 it was found that if the anti-windup moves controller poles away from the origin then better stability properties are obtained. This is partially in conflict with the results based on disturbances, since they may require the opposite. The different design rules and results will now be briefly summarized. In Chapter 4 they will be tested in simulations and experiments.

Tracking Anti-Windup

In Result 3.1 it is shown that when T_t decreases from ∞ , the Nyquist curve, (2.33),

$$G(i\omega) = \frac{G_{fb}(i\omega)G_p(i\omega) - W(i\omega)}{1 + W(i\omega)}$$

moves away counter clockwise from the interval $(-\infty, -1]$ of the real axis. Thus limit cycles can be avoided. Further, tracking anti-windup mainly affects the low-frequency part of $G(i\omega)$. It is in general not guaranteed that closed-loop stability can be proved by, e.g., circle criteria. However, Theorem 3.1 proves absolute stability for $0 < T_t < \infty$ when $G(i\omega)$ satisfies a few special conditions.

A test quantity for noise sensitivity close to saturation is $K_{HD,\max}$, the maximum high-frequency to DC gain, see Definition 3.2, which for tracking anti-windup is

$$K_{HD,\max} = \frac{T_i(N+1)}{T_t}$$

This quantity is reduced by choosing the largest possible T_t and a small value of N .

In Section 3.5 two design rules for T_t were derived. In case A, (3.66),

$$T_t = \begin{cases} \min\left(T_i, \max\left(\sqrt{T_i T_d}, \frac{T_i}{2}, \frac{T_d}{1 - \alpha_1 T_d}\right)\right) & \text{when } 1 - \alpha_1 T_d > 0 \\ T_i & \text{when } 1 - \alpha_1 T_d \leq 0 \end{cases}$$

and in case B, (3.67),

$$T_t = \min\left(T_i, \max\left(\sqrt{T_i T_d}, \frac{T_i}{2}\right)\right)$$

When $T_i \geq 4T_d$ the design criteria are satisfied.

The Observer Approach

In Example 3.1 it was noted that when $\omega_0 < N/(2T_d)$ then $G(i\omega)$, (2.33), loses phase with respect to the point -1 for sufficiently large ω . Sufficiently small ω_0 may result in a closed-loop system that either limit cycles or is unstable. If $\omega_0 > N/(2T_d)$ the stability properties are similar to those of tracking anti-windup. Thus limit cycles are avoided, but closed-loop stability may not be guaranteed by circle criteria.

The noise sensitivity close to saturation is given by the maximum high-frequency to DC gain, see Definition 3.2, which for the observer approach is

$$K_{HD,\max} = \omega_0^2 T_d T_i \frac{N+1}{N} \approx \omega_0^2 T_d T_i$$

This quantity is reduced by choosing the smallest possible ω_0 . At the cost of changing the linear performance T_d and T_i may also be reduced.

Using impulse disturbances, see Section 3.5, the following design rules have been derived.

$$\omega_0 = \max \left(\frac{1}{2T_d}, \frac{2}{T_i} \right) \quad \text{and} \quad \omega_0 = \max \left(\frac{1}{2T_d}, \frac{1}{\sqrt{T_i T_d}} \right)$$

When $T_i \geq 4T_d$, i.e., $\omega_0 = (2T_d)^{-1}$, the design criteria are satisfied. When $\omega_0 = 2/T_i$, the design criteria are satisfied in a special case.

In case A , it is possible to approximately limit the desaturation time from below. Then $\omega_0 \leq 1/t_o$ gives a desaturation time $t_d \geq t_o$, where t_o is a prescribed minimum desaturation time.

Without derivative action the observer approach coincides with tracking anti-windup, since there is only one controller pole. The design rules for ω_0 are, however, not valid.

Comparison

From stability point of view $T_t < \infty$ and $\omega_0 > N/(2T_d)$, respectively, guarantee increased phase and thus less risk for limit cycles. The impulse based design rules for the observer approach, however, gives reduced phase, while there is no such conflict for tracking anti-windup.

When the design rules for impulse disturbances are used the noise sensitivity close to saturation is considerable smaller for the observer approach compared to tracking anti-windup. The performance for impulse disturbances will be compared in simulations and experiments.

4

Evaluation of Anti-Windup for PID Controllers

In this chapter the design rules and design criteria from Chapter 3 for tracking anti-windup and the observer approach will be tested on different processes. For comparison conditional integration (method C3) is also tested. The processes covered are, e.g., inverse-response processes, time-delay processes and unstable processes. The first two processes, a double tank and a DC servo are “nice processes” where a PID controller is sufficient to get arbitrary pole-placement. For the other processes arbitrary pole-placement cannot be obtained by a PID controller. However, several of them are examples of process types which often are controlled by PID controllers. The analysis and evaluation is more extensive for the first three processes, while the rest of the processes are discussed more briefly.

4.1 The Double-Tank Process

The double-tank process, see Figure 4.1, consists of two identical cylindrical cascaded tanks and is used for basic experiments in the control laboratory in Lund, see Åström and Östberg (1986). In this section the double-tank process will be used for evaluation of the anti-windup design rules in case A, i.e., the relative degree one case. The control signal is pump speed, which determines

4.1 The Double-Tank Process

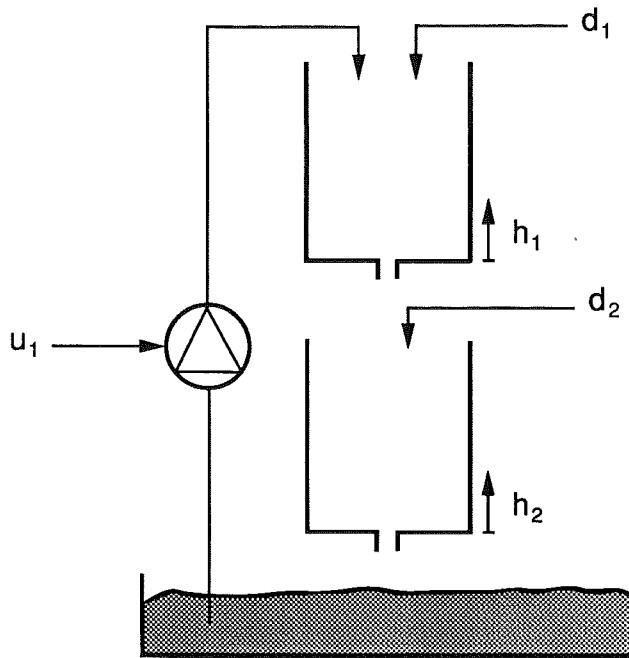


Figure 4.1 The double-tank process.

the flow rate into the upper tank, and the process output is the level of the lower tank. The double-tank process has been used in Example 3.2 and when the design criteria for impulse disturbances were established, see Section 3.5. Thus it is reasonable to expect that the design criteria are well chosen for this process and that anti-windup which satisfies these criteria also gives good performance.

After linearization the transfer function from pump speed to the level in the lower tank is

$$G_p(s) = \frac{\beta\alpha}{(s + \alpha)^2} \quad (4.1)$$

Parameters $\alpha \approx 0.015 (\text{s}^{-1})$ (at approximately 50% level) and $\beta \approx 0.05 (\text{s}^{-1})$, thus the time constant for one tank is approximately 70 seconds.

An impulse disturbance $d_2 = d_0\delta(t)$ is a good model for pouring a cup of water in the lower tank. The disturbance transfer function is, with appropriate scaling,

$$G_2(s) = \frac{1}{s + \alpha} \quad (4.2)$$

In Section 3.5 this case, where the relative degree of G_2 is one, was denoted case A. Case B, which corresponds to pouring a cup of water in the upper tank will not be treated. The reason is that the upper tank is not large enough. Not even a full upper tank gives a derivative of the lower level which is large enough to saturate the controller. This is partly due to the nonlinear

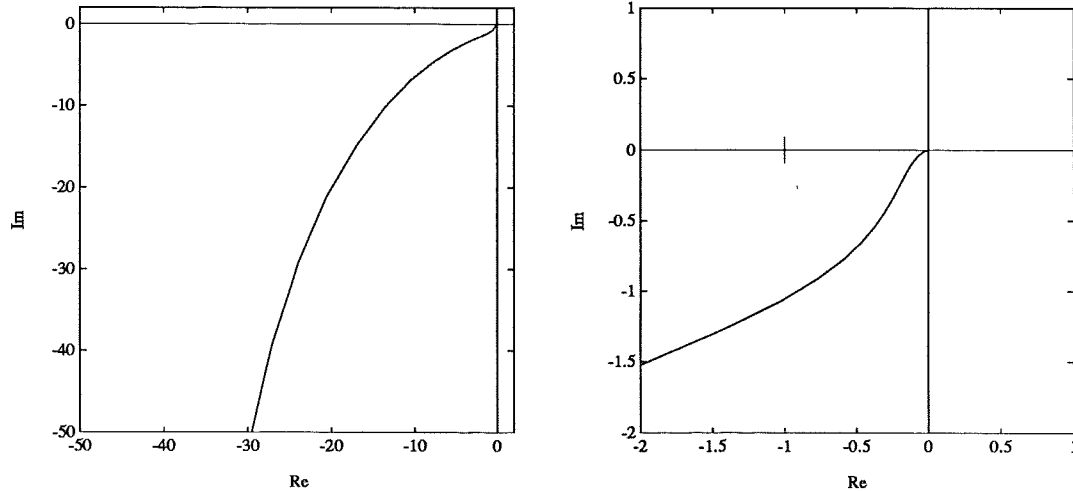


Figure 4.2 The Nyquist curve of the loop gain $G_{fb}(i\omega)G_p(i\omega)$ for the double-tank process shown in two different scales.

tank dynamics where the flow rate out of a tank is proportional to the square root of the level.

The double-tank process is controlled by a PID controller, (3.1), which has parameters $K = 5$, $T_i = 40$ s, $T_d = 15$ s and $N = 5$. To get an overshoot of 10 % the set-point weighting $b = 0.3$. The dominating closed-loop poles are -0.057 and $-0.026 \pm 0.039i$. The complex-conjugated poles have natural frequency 0.046 and relative damping 0.56.

Stability

When tracking anti-windup and the observer approach are used the system can be divided into a linear system G with nonlinear feedback. Thus circle criteria, see Section 2.7, may be used to investigate stability. From (2.33), the linear system is

$$G = \frac{G_{fb}G_p - W}{1 + W}$$

where G_p is the process transfer function (4.1), G_{fb} is the feedback path in the controller and W is the anti-windup transfer function, see Sections 3.1–3.2. The conditions for using Theorem 2.3, e.g., the Off-Axis Circle Criterion, are satisfied if G has no integrator. Thus $T_t < \infty$, for tracking, and $\omega_0 > 0$, for the observer approach, are necessary conditions for using the theorem. The stability results now follow.

Tracking anti-windup The Nyquist curve for the loop gain $G_{fb}G_p$, is shown in Figure 4.2. Since G_{fb}, G_p and the Nyquist curve $G_{fb}(i\omega)G_p(i\omega)$ satisfies the conditions in Theorem 3.1, the closed-loop system is absolutely

stable for $0 < T_t < \infty$. The closed-loop system is thus always stable with tracking anti-windup.

The observer approach The Off-Axis Circle Criterion is satisfied for $0.012 \text{ rad/s} < \omega_0 < 2.9 \text{ rad/s}$ and then absolute stability holds. For $\omega_0 < 0.012 \text{ rad/s}$ $G(i\omega)$ has two intersections with the negative real axis to the left of -1 . Describing function analysis then predicts a “hard-excited” limit cycle, which also has been observed in simulation. For $\omega_0 > 2.9 \text{ rad/s}$ the closed-loop system is not necessarily unstable, and instability has not been observed either. It is thus necessary that ω_0 is neither too small nor too large in the observer approach. Otherwise stability is not guaranteed.

The Anti-Windup Experiment

A standard experiment is used to test the anti-windup methods. In simulations the linear tank model (4.1) is used with a control signal $u \in [0, 1]$. The process and controller starts at stationarity with all signals zero. The experiment is as follows:

1. Start-up: at time $t = t_s = 0$ the reference $y_r = 1$.
2. Impulse disturbance: at time $t = t_i$ the disturbance $d_2(t) = 0.5 \delta(t - t_i)$ changes the process output to $y = 1.5$. This is a model of quickly pouring a cup of water into the lower tank.
3. Load disturbance: at time $t = t_l$ a load on the upper tank, $d_1 = -0.65$, is introduced.
4. Noise disturbance: at time $t = t_n$ a high frequency sinusoidal disturbance $(0.004 \cdot \sin t)$ is added to $y(t)$.

The four parts of the anti-windup experiment have been designed to saturate the control signal in one or both directions. The first two experiments are also performed experimentally on the double-tank process. Then corresponding discrete-time PID controllers and anti-windup methods are used. Experiments 2 and 4 are used for evaluation of the results in Sections 3.5–3.6.

A simulation of the anti-windup experiment is shown in Figure 4.3. Notice that without anti-windup the overshoots are large. Further, the measurement noise hardly influences the process output. This observation confirms Result 3.15, and a later remark, that the steady-state offset is zero without anti-windup.

Tracking Anti-Windup

Combining the design limits in Result 3.2 and 3.5, T_t must satisfy the inequality

$$\frac{T_d}{1 - \alpha_1 T_d} = 19.4 \text{ s} < T_t \leq T_i = 40 \text{ s} \quad (4.3)$$

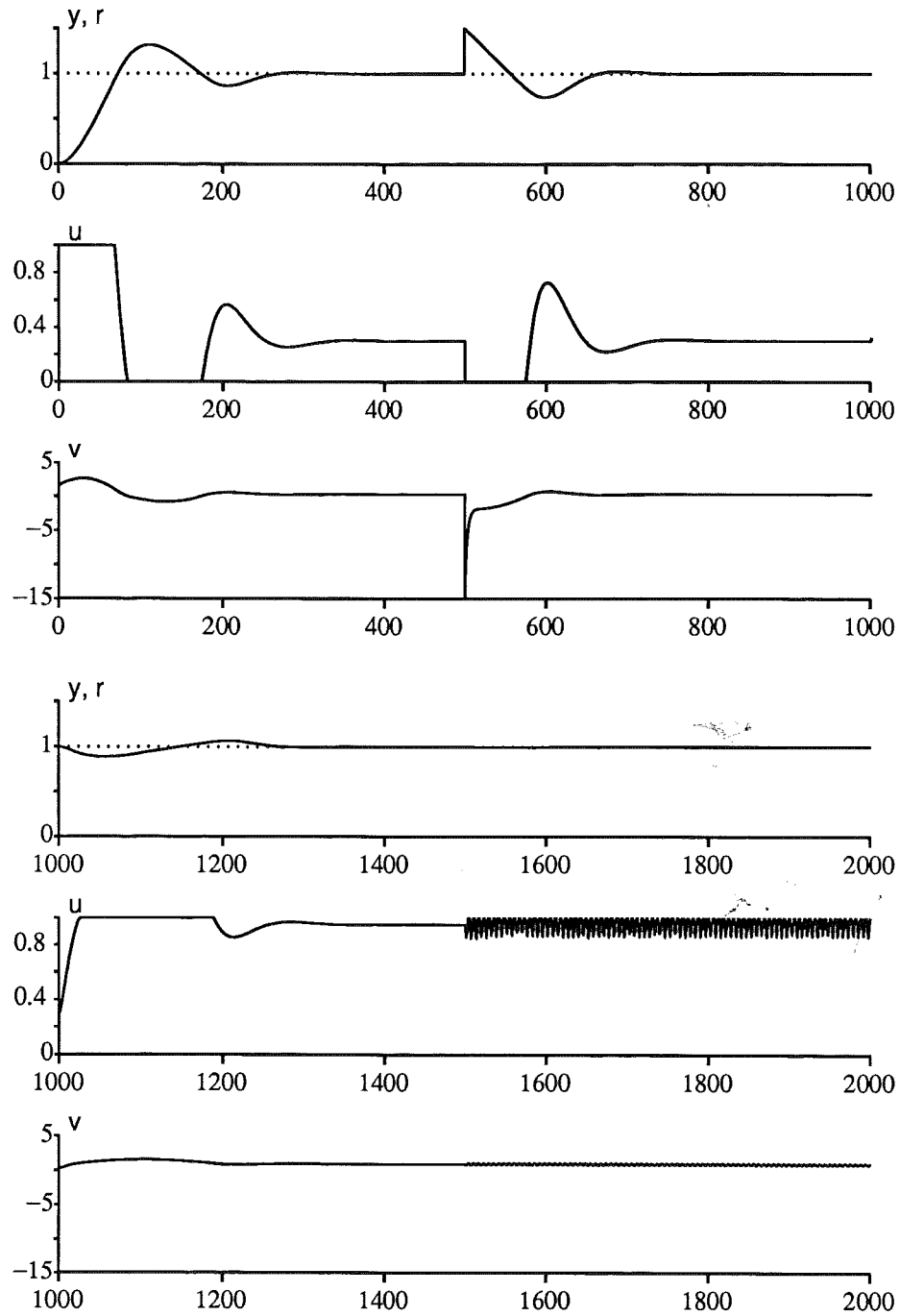


Figure 4.3 A simulation of the standard experiment without anti-windup gives large overshoots due to integrator windup. To facilitate comparisons with later simulations the longer settling times without anti-windup are compensated by a longer simulation time on the same time scale. The measurement noise does not give any steady-state offset of the process output.

where $\alpha_1 = \alpha = 0.05$. Since $T_i < 4T_d$ design criterion 2' is not surely satisfied. The general design rule for tracking anti-windup, (3.66), yields $T_t = \sqrt{T_i T_d} = 24.5$ s. The value $T_t = T_i/2 = 20$ s from Result 3.6 will also be tested. For the conditioning technique $T_t = bT_i = 12$ s, which is below the lower limit in (4.3).

The high-frequency to DC gain, see Definition 3.2, which for tracking anti-windup has the maximum value (3.105), i.e.,

$$K_{HD,\max} = \frac{T_i(N+1)}{T_t} = \frac{240}{T_t}$$

also limits T_t from below if $K_{HD,\max}$ is limited from above. When the design rules are followed $K_{HD,\max} \approx 2N = 10$, i.e., the stationary offset may in the worst case be about 10 times larger than the disturbance amplitude.

In Example 3.2 fast tracking (equivalent to back calculation) with $T_t = T_i/40 = 1$ s has been demonstrated. For the impulse disturbance fast tracking anti-windup gives a deteriorated behavior, see Figure 3.8.

In Figure 4.4 the tracking time constant $T_t = 24.5$ s is tested in simulation together with $T_t = T_d = 15$ s, which is too small according to Result 3.2. Both cases desaturate well before the control error changes sign and thus design criterion 2' is satisfied. When $T_t = 24.5$ s and $T_t = 20$ s the results are very similar. When $T_t = 15$ s the control signal has a high peak value shortly after desaturation. The result is then a slightly prolonged settling time for the process output, but it is not as bad as when $T_t = 1$ s in Figure 3.8.

Conclusion The design rules $T_t = \sqrt{T_i T_d}$, and $T_t = T_i/2$ both result in good performance for case A of the impulse disturbance on the double-tank process. If Result 3.2 is violated, i.e., when $T_t < 19.4$ s, an unnecessarily long settling time is obtained. When $T_t \ll 19.4$ s, see Figure 3.8, the deterioration is severe for the impulse disturbance. \square

In Table 4.1 offsets y_0 during the noise disturbance are given for a few values of T_t . Both predicted offsets \hat{y}_0 , see Result 3.15, and obtained offsets y_0 are given. Due to the load disturbance $u_{\max} = 0.05$. In this evaluation $\omega_d = 10$ rad/s and the amplitude $n_1 = 0.004$, compare the last part of the experiment. For lower frequencies ω_d smaller offsets are obtained. The predicted and obtained values of y_0 thus agree well.

The Observer Approach

Since the process output y is well approximated by a straight line when $u = u_{\min}$ after the impulse disturbance, see Figure 4.3, it is reasonable to apply Result 3.11 which for this particular case gives sufficient conditions for desaturation before the control error changes sign. Thus $\omega_0 = 2/T_i = 0.050$ rad/s. If a minimum desaturation time t_d is specified then Result 3.13

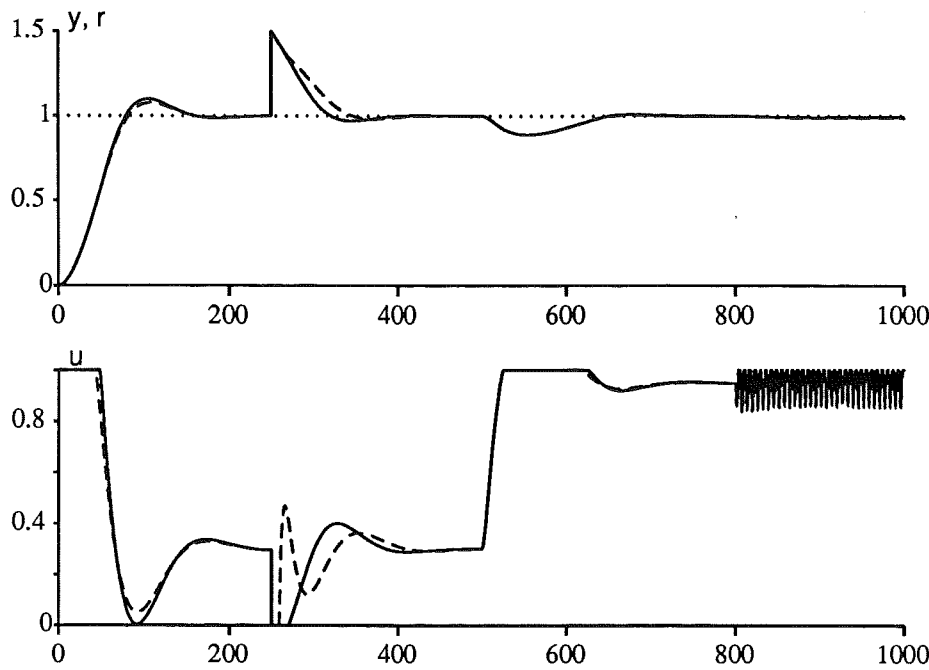


Figure 4.4 Simulation of the anti-windup experiment for tracking anti-windup with $T_t = \sqrt{T_i T_d} = 24.5$ s (solid), and $T_t = T_d = 15$ s (dashed), on the double-tank process. Except for the impulse disturbance the performances are almost identical. When $T_t = 15$ s the control signal has a high peak value after desaturation and the process output has a prolonged settling time. When $T_t = 24.5$ s the performance is good all over. For $T_t = 20$ s and $T_t = 24.5$ s the performances are very similar.

Table 4.1 Comparison between predicted offset \hat{y}_0 and obtained offset y_0 during a noise disturbance $0.004 \cdot \sin(10t)$ for tracking anti-windup.

T_t	y_0	\hat{y}_0
$T_i = 40$	-0.00528	-0.00530
$T_i/10 = 4$	-0.0391	-0.0390
$T_i/100 = 0.4$	-0.128	-0.129

gives the upper limit $\omega_0 < 1/t_d$. In Figure 4.4, for tracking anti-windup, the controller desaturates after about 10 s in the fastest case. Thus $\omega_0 < 0.100$ rad/s will not give faster desaturation in the observer approach either.

In Figure 4.5 the choices $\omega_0 = 2/T_i = 0.05$ rad/s and $\omega_0 = 0.100$ rad/s are compared in simulation. The design criteria are satisfied in both cases, but when $\omega_0 = 0.100$ rad/s the desaturation and prolonged settling time is similar to the case $T_t = T_d = 15$ s for tracking anti-windup. However, the

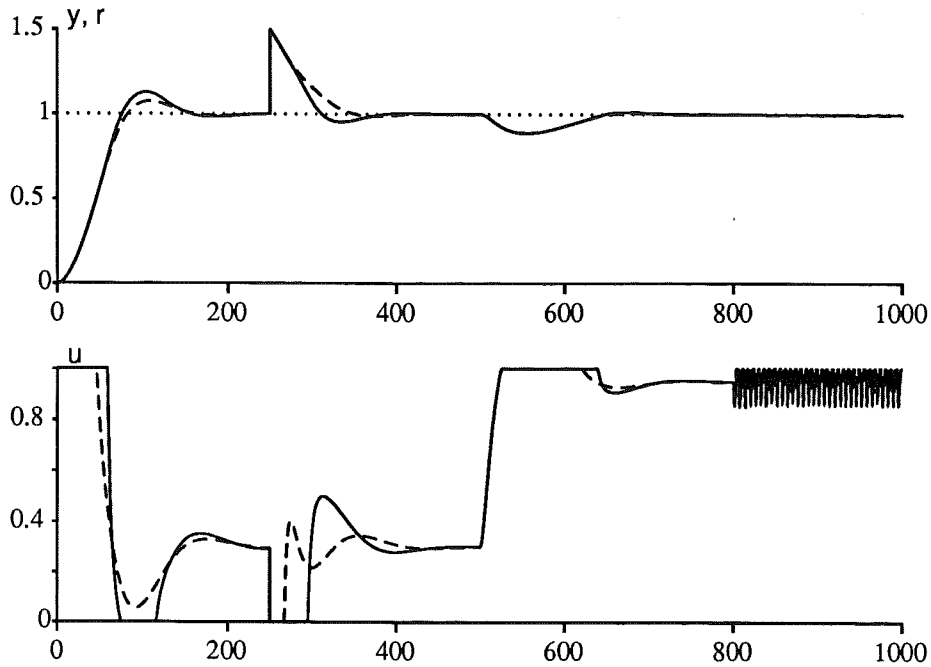


Figure 4.5 Simulation of the anti-windup experiment with anti-windup by the observer approach for $\omega_0 = 2/T_i = 0.050$ rad/s (solid) and $\omega_0 = 0.100$ rad/s (dashed). When $\omega_0 = 0.050$ rad/s the design criteria are satisfied, but $\omega_0 = 0.100$ rad/s is a slightly too high value for ω_0 since an unnecessarily long settling time and relatively fast desaturation is obtained for the impulse disturbance. The design criteria are, however, satisfied also in this case.

desaturation now occurs after almost 20 s while it was after about 10 s when $T_t = 15$ s for tracking anti-windup. Anyhow, it is clear that $\omega_0 < 0.100$ rad/s avoids prolonged settling time.

In Result 3.12 two other design choices for ω_0 are given. It is not shown in any figure, but for the choice $\omega_0 = 1/(2T_d) = 0.0333$ rad/s the demand on desaturation before the control error changes sign, i.e., design criterion 2, is not satisfied. Further, the choice $\omega_0 = 1/\sqrt{T_i T_d} = 0.041$ rad/s is just at the limit of satisfying this demand.

Conclusion The design rule $\omega_0 = 2/T_i$ results in good performance for case A of the impulse disturbance on the double tank process. It is also clear that ω_0 should not be chosen very much larger than $2/T_i$. \square

In Table 4.2 the offsets y_0 during the noise disturbance are given for some values of ω_0 . Both predicted offsets \hat{y}_0 , see Result 3.15 with $T_w = N/(\omega_0^2 T_d)$, and obtained offsets y_0 are given. Just as for tracking anti-windup, see Table 4.1, the disturbance has frequency $\omega_d = 10$ rad/s and amplitude $n_1 = 0.004$. Due to the load disturbance $u_{\max} = 0.05$. The predicted and obtained values of y_0 agree well when the observer approach is used.

Table 4.2 Comparison between predicted offset \hat{y}_0 and obtained offset y_0 during a noise disturbance $0.004 \cdot \sin(10t)$ for anti-windup by the observer approach.

ω_0	y_0	\hat{y}_0
0.025	-0.00042	-0.00041
0.033	-0.00072	-0.00073
0.041	-0.00109	-0.00111
0.050	-0.00163	-0.00164
0.100	-0.00626	-0.00630

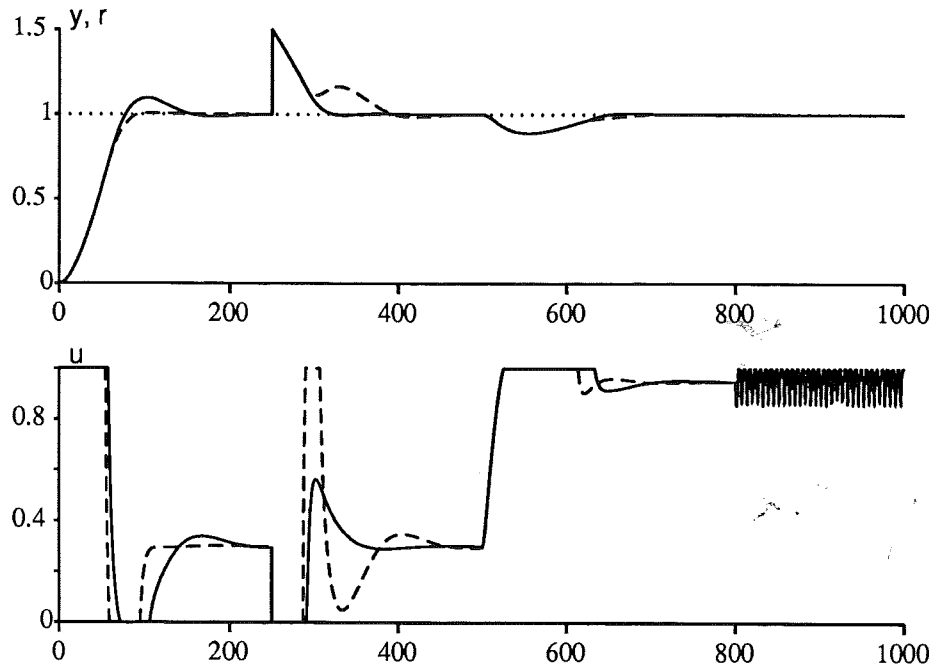


Figure 4.6 A simulation of the anti-windup experiment with observer anti-windup. The case $(\omega_0, \zeta) = (0.051, 0.78)$ (solid) is IAE-optimal for the impulse disturbance and the case $(\omega_0, \zeta) = (0.056, 0.32)$ (dashed) is IAE-optimal for the set-point change. The latter case has an almost time-optimal performance for the set-point change but a deteriorated performance for the impulse disturbance. The first case has an over-all good performance.

General pole-placement in the observer approach The pole-placement in the observer approach has so far been rather restrictive. This simplifies the derivation of design rules, but does not lead to the best possible performance. By means of optimization it is, however, quite straightforward to obtain other observer poles which give “better” performance for either the set-point change or the impulse disturbance. In Figure 4.6 two Integral-Absolute-Error (IAE) optimal observer pole-placements are tested in sim-

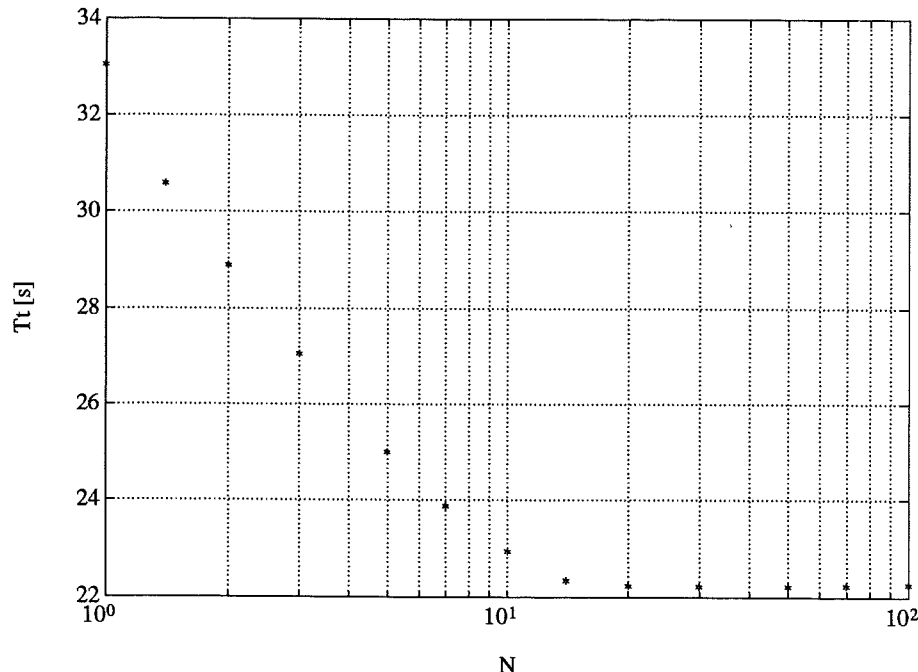


Figure 4.7 The disturbance IAE optimal tracking time constant T_t versus the filter factor N .

ulation. The choice $(\omega_0, \zeta) = (0.051, 0.78)$ is IAE optimal for the impulse disturbance. The performance for the other parts in the experiment is also good. The choice $(\omega_0, \zeta) = (0.0055, 0.32)$ is IAE optimal for the set-point change. The control signal is similar to the time-optimal bang-bang solution for the set-point change. For the impulse disturbance this pole-placement gives a deteriorated performance.

Sensitivity

The evaluations above may depend on, e.g., the impulse magnitude, set point, controller limits, etc. Therefore the sensitivity for a few parameter variations will be tested. Controller parameters K , T_i and T_d are not changed in this evaluation. The filter factor N and the impulse magnitude d_0 were chosen as test parameters. Larger values of N has a small influence on the linear closed-loop system and the impulse magnitude d_0 is usually unknown.

The filter factor N determines the initial control signal

$$v(0_+) = -K(N + 1)d_0$$

see, e.g., (3.70), and then also the amount of “reset” of the integrator. Therefore N may influence the choice of anti-windup speed. In Figure 4.7 it is shown, for the impulse disturbance, how the IAE optimal tracking time constant T_t depends on the filter factor N when other parameters are constant.

Table 4.3 IAE optimal values of T_t and ω_0 for impulse disturbances of different magnitudes.

Impulse magnitude	Tracking T_t [s]	Observer ω_0 [rad/s]
0.7	22.1	0.065
0.5	25.0	0.064
0.3	27.5	0.065
0.1	25.5	0.078

For small values of N , i.e., less reset of the integrator, larger T_t values are optimal but for higher values of N the optimal T_t converges to a constant value between $\sqrt{T_i T_d} = 24.5$ s and $T_i/2 = 20$ s.

In applications the magnitude of the impulse disturbance is usually unknown in advance. Therefore the IAE optimal T_t and ω_0 are determined for a number of different impulse magnitudes. The result is shown in Table 4.3. As expected the optimal pole locations vary with the impulse magnitude. For tracking the optimal time constants are rather close to $\sqrt{T_i T_d} = 24.5$ s. For the observer approach the optimal natural frequency ω_0 is, with one exception, close to 0.064 rad/s $\approx 2.5/T_i$.

Thus the design rules for tracking anti-windup and the observer approach give reasonable values for T_t and ω_0 respectively, also in terms of a small Integral-Absolute-Error (IAE) for impulse disturbances of different magnitude and for different filter factors N .

Conditional Integration

Conditional integration anti-windup is tested in an experiment in Figure 4.8. The method handles start-up and disturbances properly. A closer look at a corresponding simulation reveals that at start-up the performance is close to what is obtained from back calculation, i.e., $T_t \approx 0$, and for the impulse disturbance the performance is close to that of $T_t = T_i$ and $\omega_0 = 2/T_i$ for tracking and the observer approach respectively. Thus the design criteria are satisfied. In simulation the offset y_0 during the noise disturbance is -0.00218 .

Other Anti-Windup Methods

It will now be demonstrated that fast tracking anti-windup combined with a limited derivative part or a limited rate of change of the control signal do not improve performance sufficiently for the impulse disturbance. For the limited derivative, see Figure 4.9, the impulse disturbance requires a very

4.1 The Double-Tank Process

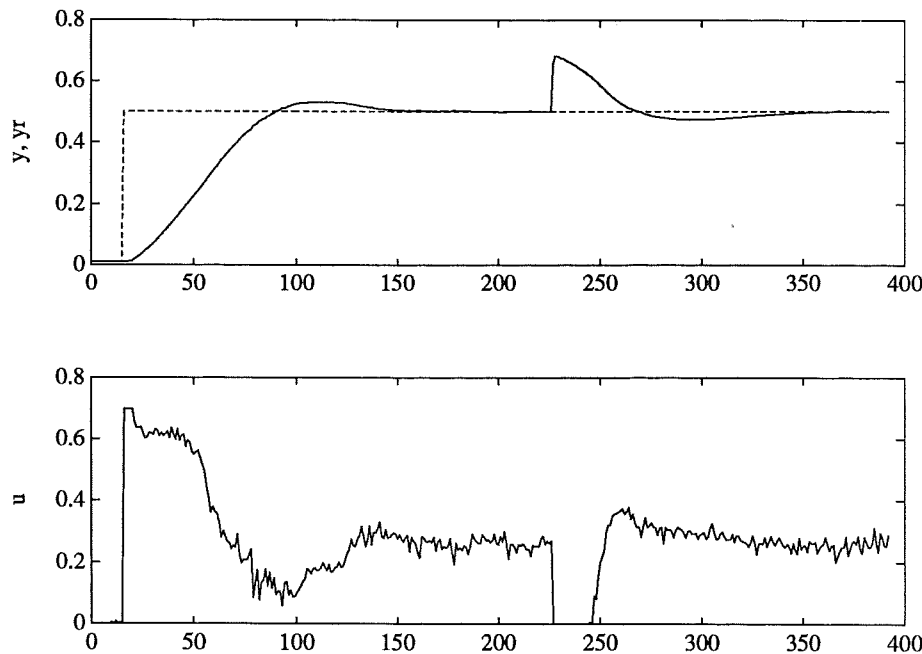


Figure 4.8 Experiment with start-up and impulse disturbance on the double-tank process with conditional integration anti-windup (method C3) in the PID controller. The reference signal is dashed.

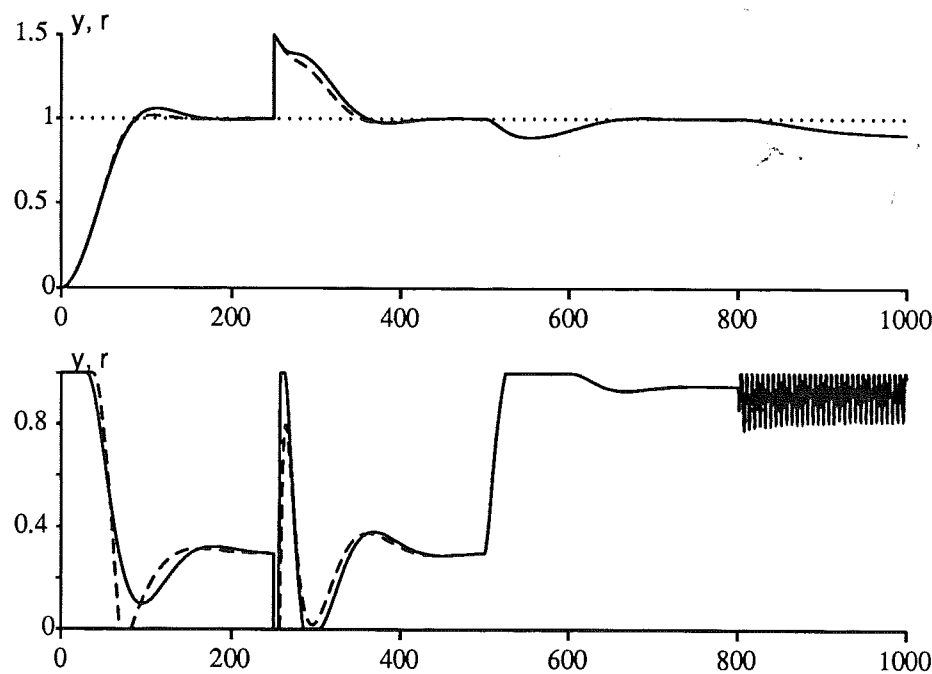


Figure 4.9 A simulation of the anti-windup experiment with $T_t = T_i/100$ and limited derivative action. The limitations $\max |d(t)| \leq 1.5$ (solid line) and $\max |d(t)| \leq 0.5$ (dashed line) are tested.

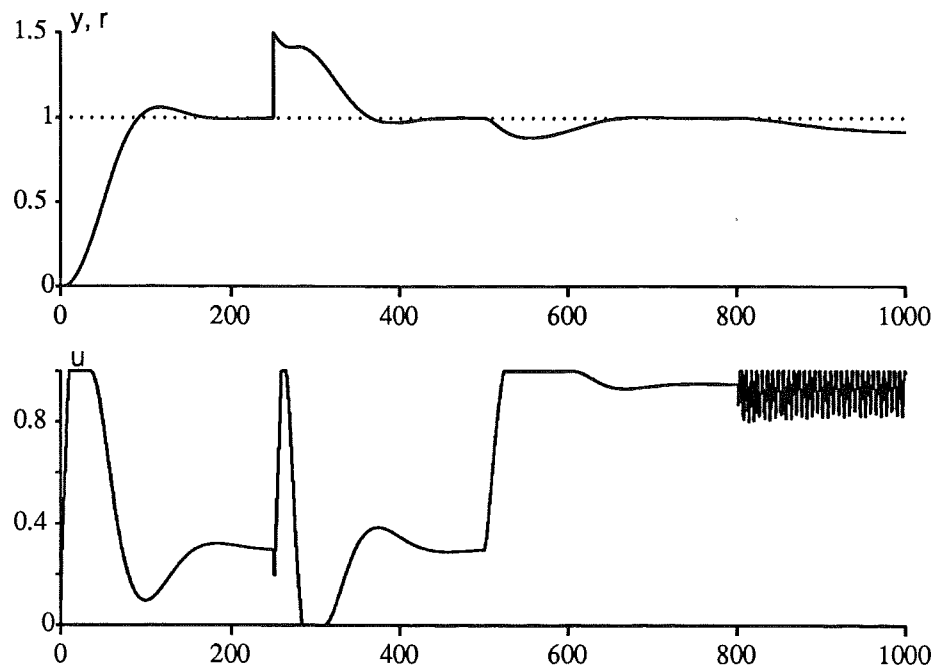


Figure 4.10 A simulation of the anti-windup experiment with $T_t = h = 1\text{s}$ for a discrete-time PID controller. The control signal has a limited rate of change such that $\max |\Delta u(t)| \leq 0.1 \cdot (u_{\max} - u_{\min}) \cdot h$, i.e., 10% per second.

small derivative limit for a satisfactory response. Then the controller would practically be a PI controller, which is unfeasible during normal control. For the limited rate of change of the control signal, see Figure 4.10, the result is similar. The use of a discrete-time PID controller in this simulation is motivated by the easier implementation of a rate limit for the control signal. Then back calculation, i.e., tracking with $T_t = h$, was used as anti-windup. These two methods are thus not capable of giving a satisfactory performance for case A of impulse disturbances.

Comparison of the Anti-Windup Methods

The three anti-windup methods, i.e., tracking anti-windup, the observer approach and conditional integration (method C3), all satisfy the design criteria with respect to impulse disturbances. Parameters must of course be chosen according to the design rules. In order to make a more refined comparison the methods are compared by their minimal Integral-Absolute-Error (IAE) for the impulse disturbance and the set-point change. The IAE:s and corresponding optimal parameters are shown in Table 4.4, together with parameter values and IAE:s for the design rules. The values of the IAE:s for conditional integration are shown for comparison.

4.1 The Double-Tank Process

Table 4.4 IAE values for set-point change and impulse disturbance for the best cases of the compared anti-windup methods. CI denotes conditional integration.

Method	Case	Parameter	IAE impulse	IAE set point
CI			17.7	49.0
Tracking	set point	$T_t = 8 \text{ s}$	30.6	48.9
	impulse	$T_t = 25 \text{ s}$	16.9	49.9
	design rule	$T_t = 24.5 \text{ s}$	16.9	49.9
Observer	set point	$\omega_0 = 0.14 \text{ rad/s}$	24.7	48.8
	impulse	$\omega_0 = 0.064 \text{ rad/s}$	16.2	49.6
	design rule	$\omega_0 = 0.050 \text{ rad/s}$	17.0	51.0

The optimal cases for the set-point change result in faster anti-windup, i.e., faster observer poles, compared to the optimal cases for the impulse disturbance. Notice that the disturbance optimal parameters, i.e., $T_t = 25 \text{ s}$ and $\omega_0 = 0.064 \text{ rad/s}$, result in a relatively small increase of the IAE for the set-point change. On the other hand the set-point optimal parameters, i.e., $T_t = 8 \text{ s}$ and $\omega_0 = 0.14 \text{ rad/s}$, cause a high increase of the IAE for the impulse disturbance. The reason is the fast desaturation after the impulse disturbance.

It is thus clear that optimizing or tuning the anti-windup with respect to set-point changes may give an unsatisfactory result for disturbances. This is similar to standard controller tuning rules, see Hang (1989). Tuning the anti-windup with respect to the impulse disturbances gives only a negligible reduction of performance for set-point changes.

It is also noticeable that the anti-windup design rules, i.e., $T_t = 24.5 \text{ s}$ and $\omega_0 = 0.05 \text{ rad/s}$, result in parameter values relatively close to the disturbance optimal parameters. Further, conditional integration anti-windup results in good performance for both the set-point change and the impulse disturbance.

The offsets for the noise disturbances can also be compared. From Tables 4.1–4.2 it is clear that predicted offsets \hat{y}_0 agree well with obtained offsets y_0 . Further, the offsets are smaller when the observer approach is used, which confirms the discussion in Section 3.7. Conditional integration gives an offset y_0 between the offsets for tracking and the observer approach.

Summary

For tracking anti-windup the design criteria are not necessarily satisfied when $T_i < 4T_d$. However, the result of the general design rule, i.e., $T_t = \sqrt{T_i T_d} = 24.5$ s, turns out to satisfy the design criteria and also gives a relatively small Integral-Absolute-Error for the impulse disturbance.

For the observer approach the design rule $\omega_0 = 2/T_i = 0.050$ rad/s is confirmed for the case when the response of the disturbance impulse is well approximated by a straight line. Conditional integration anti-windup also performs well. The offsets for noise disturbances close to saturation are small for all three methods.

4.2 A DC Motor

The DC motor in this section is a mechanical system with position/angle control where the control signal is electrical torque. Physically relevant impulse disturbances are torque impulses, i.e., the DC motor is an example of case B with a relative degree two disturbance impulse response. Thus the output is continuous for impulse disturbances. This particular process and the chosen controller also has the property of being closed-loop unstable for large signals when the controller has a saturation but not any windup, see Figure 4.11. This process has also been discussed in Yang and Leu (1989).

A DC motor has inertia J and damping D . Neglecting fast dynamics the transfer function from electrical torque u to measured angle y is

$$G_p(s) = \frac{1}{s(Js + D)} \quad (4.4)$$

In order to satisfy the scaling requirement in (3.32) the transfer function from torque disturbances is $G_2(s) = JG_p(s)$.

Parameter $J = 1$ and $D = 0.01$. The motor is controlled by a PID controller (3.1) with $K = 3$, $T_i = 3$ s, $T_d = 2.99/3$ s ≈ 1 s, $N = 5$ and $b = 0$, i.e., an "Integral on error only" PID. Neglecting the derivative filter the closed-loop poles are all in -1 .

Stability

The stability analysis for the DC motor with PID control is similar to the analysis for the double tank. The nonlinear feedback is a unit gain saturation and the linear dynamics is, (2.33),

$$G(s) = \frac{G_{fb}G_p - W}{1 + W} = \frac{G_0 - W}{1 + W}$$

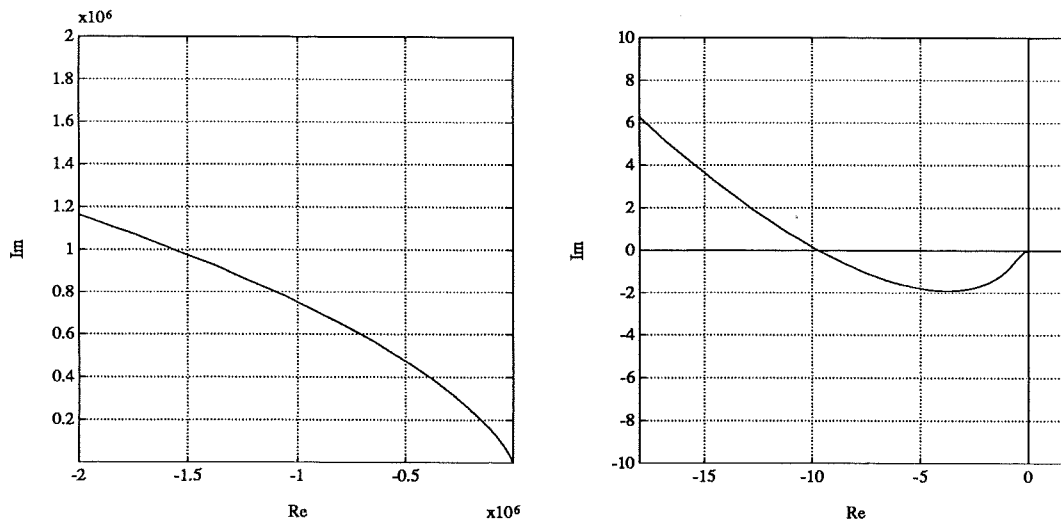


Figure 4.11 The Nyquist curve $G_0(i\omega)$ for the loop gain without anti-windup shown in two scales. $\text{Im } G(i\omega) > 0$ for $\omega < 0.57 \text{ rad/s}$ and vice versa.

where G_{fb} is the feedback path in the controller, G_p the process, and W is given by (3.2). $G_0 = G_p G_{fb}$ is the loop gain without anti-windup.

The Nyquist curve $G_0(i\omega)$, see Figure 4.11, intersects the negative real axis at approximately -9 for $\omega = 0.57 \text{ rad/s}$. If a saturation nonlinearity is introduced in the loop describing function analysis predicts an unstable limit cycle. Thus the closed-loop system is stable for small signals but goes unstable for sufficiently large signals, see Figure 4.12.

Tracking anti-windup From Result 3.1 it is known that tracking anti-windup gives a phase increase (with respect to the critical point -1) in the interval $0 - 90^\circ$. A sufficiently small T_t will thus eliminate intersections with the interval $(-\infty, -1]$ for $G(i\omega)$. However, since $\arg G_0(i\omega) < -180^\circ$ for $\omega < 0.57 \text{ rad/s}$, it is impossible to make $\text{Re } G(i\omega) + 1 > 0$ for all ω . Since G_p has one integrator, only the Popov criterion remains if absolute stability is to be proven. However, the endpoints of the Popov curve, given by

$$\begin{aligned}\Gamma_P(0) &= \frac{KT_t}{D} \left(1 - \frac{T_t}{T_i} - \frac{J}{DT_i} - i \frac{1}{T_i} \right) - 1 \\ \Gamma_P(i\infty) &= i \frac{1}{T_t}\end{aligned}\tag{4.5}$$

violate the stability condition if $T_i < J/D$. This is clearly the case for the given parameters and thus absolute stability cannot be proven by available theorems.

For $3.70 < T_t < \infty$ the Nyquist curve $G(i\omega)$ has two intersections with the negative real axis. The describing function method predicts a “hard-

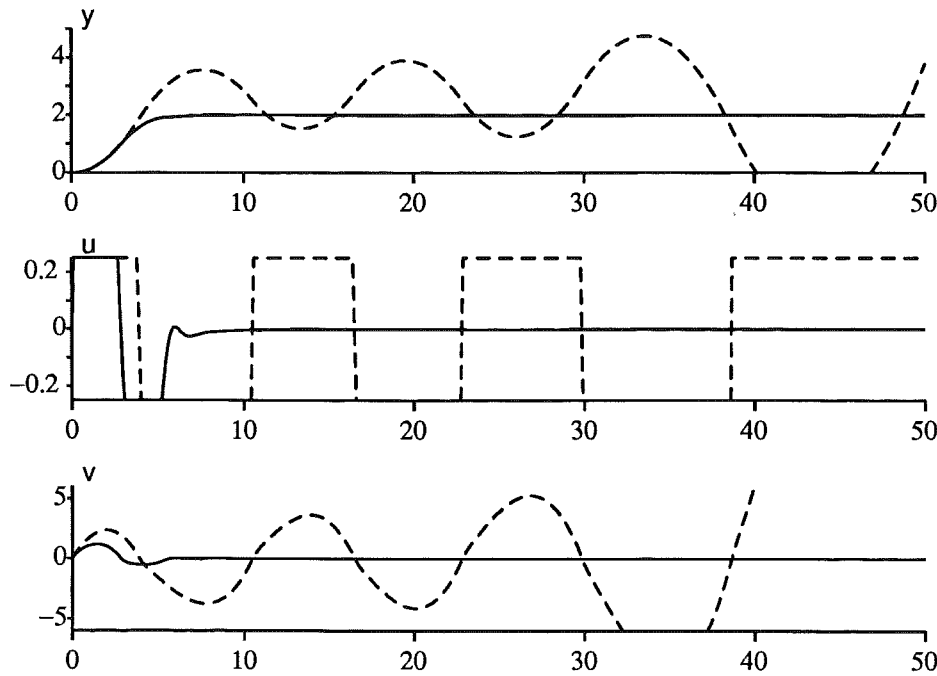


Figure 4.12 Outputs and control signals for the saturated case without anti-windup. The saturated control signal is limited such that $|u(t)| \leq 0.25$. The set points are $y_r = 2$ (solid), which gives a stable response, and $y_r = 2.7$ (dashed), which gives an unstable response. The stability limit for set-point changes is $y_r \approx 2.65$.

excited” limit cycle, i.e., sufficiently large signals result in a stable limit cycle. The existence of limit cycles has been verified in simulations for $T_{t_1} \geq 3.85$.

The observer approach For $0.57 \text{ rad/s} < \omega_0 < 2.5 \text{ rad/s}$ absolute stability is proved by the Popov criterion. The endpoint $\Gamma_P(i\infty) = i(2\omega_0 - N/T_d)$ has negative imaginary part if $\omega_0 < N/(2T_d)$. When the rest of the curve $\Gamma_P(i\omega)$ has negative imaginary part this upper limit for ω_0 is a sufficient limit for absolute stability. For $\omega_0 < 0.57 \text{ rad/s}$ the describing function method predicts “hard-excited” limit cycles, which have been verified.

The Anti-Windup Experiment

The anti-windup experiment for the DC-servo is very similar to the double tank experiment, see Section 4.1.

1. Set-point change at time $t = t_s = 0$, where $y_r = 2$.
2. Impulse disturbance at time $t = t_i$, where $d(t) = -\delta(t - t_i)$.
3. Load disturbance at time $t = t_l$, where $d(t) = -0.24$. With a load $d = -0.24$ the effective input $u + d$ to the DC motor is in $[-0.49, 0.01]$.

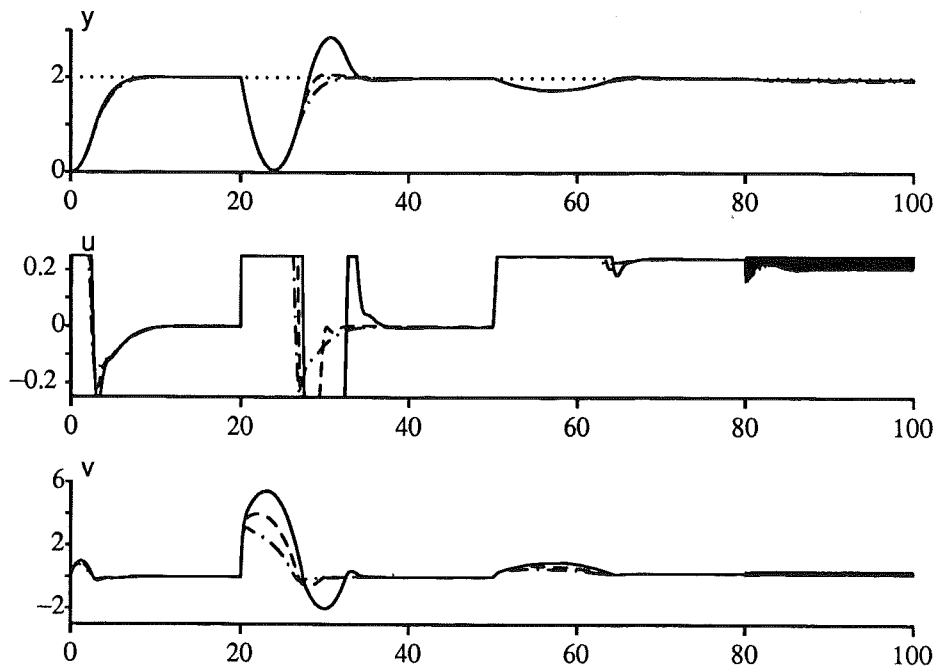


Figure 4.13 Experiment with tracking anti-windup, where $T_t = T_i = 3$ s (solid), $T_t = \sqrt{T_i T_d} = 1.73$ s (dashed) and $T_t = T_d = 1$ s (dash-dotted).

4. Noise disturbance at time $t = t_n$, a sinusoidal disturbance $0.005 \sin(30t)$ is added to the measurement $y(t)$.

Without anti-windup the impulse disturbance gives an unstable solution and the load disturbance results in a solution close to a limit cycle.

Tracking Anti-Windup

According to Result 3.5 T_t must satisfy $0 < T_t \leq T_i = 3$ s. Since $T_i < 4T_d$ design criterion 2' is not surely satisfied. The general design rule in (3.67) gives $T_t = \sqrt{T_i T_d} = 1.73$ s

In Figure 4.13 the tracking time constants $T_t = T_i = 3$ s, $T_t = \sqrt{T_i T_d} = 1.73$ s and $T_t = T_d = 1$ s are tested. All three choices of T_t satisfy design criterion 2', i.e., an early enough desaturation, but the choice $T_t = T_i = 3$ s gives a significant overshoot for the impulse disturbance. The other two cases have an acceptable performance.

In Table 4.5 the offsets y_0 during the noise disturbance are given for some values of T_t . Both predicted offsets \hat{y}_0 , see Result 3.15 with $T_w = T_t$, and obtained offsets y_0 are given. Due to the load disturbance $u_{\max} = 0.01$. Except for $T_t = 0.1$ s the predicted and obtained values of y_0 agree well. For small values of T_t the obtained offsets are smaller than the predicted offsets, since the disturbance frequency is then not sufficiently high.

Table 4.5 Comparison between predicted offset \hat{y}_0 and obtained offset y_0 during a noise disturbance $0.005 \sin(30t)$ for tracking anti-windup.

T_t	y_0	\hat{y}_0
6.0000	-0.0090	-0.0091
3.0000	-0.0179	-0.0181
1.5000	-0.0358	-0.0363
1.0000	-0.0537	-0.0544
0.5000	-0.1058	-0.1089
0.3000	-0.1780	-0.1814
0.1000	-0.5139	-0.5443

The Observer Approach

Since $T_i < 4T_d$ none of the design rules for the observer approach guarantees that design criterion 2' will be satisfied. The design rules in Results 3.11–3.12 give $\omega_0 = 2/T_i = 0.67$ rad/s and $\omega_0 = 1/\sqrt{T_i T_d} = 0.58$ rad/s, where the last value is barely inside the stability limits. The choice $\omega_0 = 1/(2T_d) = 0.050$ rad/s will give limit cycles, see the earlier stability analysis.

In Figure 4.14 the value $\omega_0 = 0.67$ rad/s is tested. The controller desaturates early enough for the impulse disturbance, i.e., design criterion 2' is satisfied. The overshoot is, however, significant. The set-point response is not satisfactory.

Conclusion Design criterion 2 (and 2') demands that desaturation occurs before the control error changes sign. This is satisfied both for tracking anti-windup and the observer approach. The performance is, however, not good. Large overshoots are obtained after the impulse disturbance even if design criterion 2 is satisfied. A possible conclusion is that design criterion 2 is not well chosen for this particular process. This will now be investigated.

Evaluation of Design Criterion 2

Since the damping D in (4.4) is relatively small the DC motor is well approximated by a double integrator. For the double integrator it is well-known that it is not sufficient to desaturate when the control error changes sign. Instead both desaturation and resaturation at the opposite limit must occur well before the control error changes sign, otherwise the control error oscillates several periods before decaying to zero.

The fastest decay to zero is obtained for the time-optimal bang-bang solution, see, e.g., Leitman (1981). The insufficiency of design criterion 2, when applied to the DC motor, may be explained by the time-optimal control

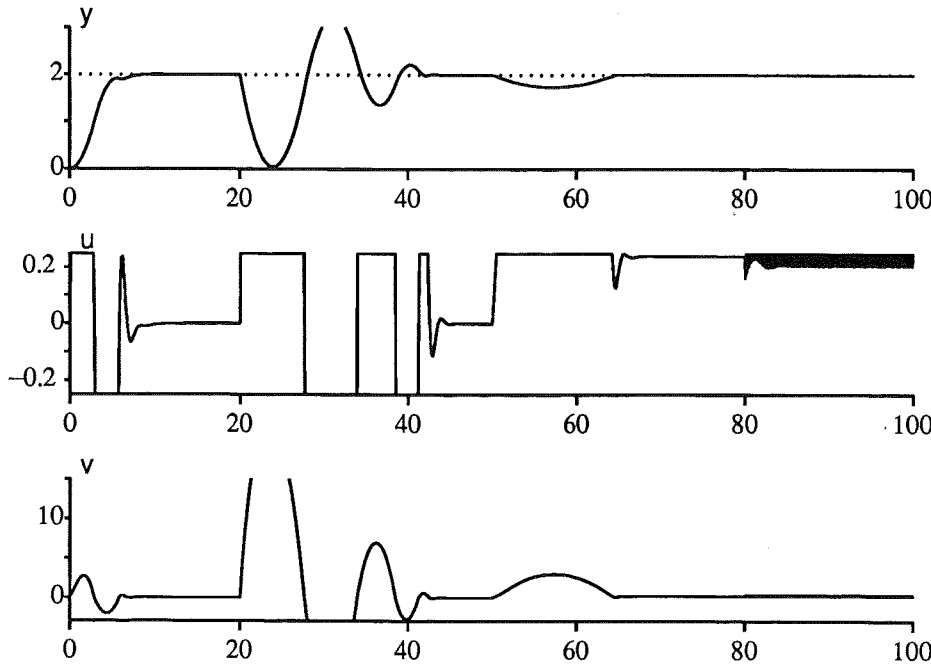


Figure 4.14 Experiment with anti-windup by the observer approach using $\omega_0 = 2/T_i = 0.67$ rad/s. Both the set-point response and the impulse response are unsatisfactory.

law for the double integrator. A detailed derivation of the results below are found in Appendix A.

The double integrator

$$\begin{aligned} J \frac{d^2y}{dt^2} &= u \\ |u| &\leq u_{\max} \end{aligned} \tag{4.6}$$

with initial values $y(0) = 0, \dot{y}(0) = \dot{y}_0 < 0$, has a time-optimal controller with switch times

$$\begin{aligned} t_1 &= \frac{|\dot{y}_0| \cdot J}{u_{\max}} \left(1 + \frac{1}{\sqrt{2}} \right) \\ t_2 &= \frac{|\dot{y}_0| J}{u_{\max}} \left(1 + \sqrt{2} \right) \end{aligned} \tag{4.7}$$

Inserting numerical values $J = 1, \dot{y}_0 = -1$ and $u_{\max} = 0.25$ the switch times are $t_1 = 6.8$ s and $t_2 = 9.7$ s. At time $t = t_2$ the controller switches to $u = 0$. If the control signal is constant, $u = u_{\max}$, the control error changes sign at time

$$t_y = 2 \frac{|\dot{y}_0| \cdot J}{u_{\max}} = 8 \text{ s}$$

for the double integrator. For the DC servo $t_y \approx 7.9$ s. Obviously design

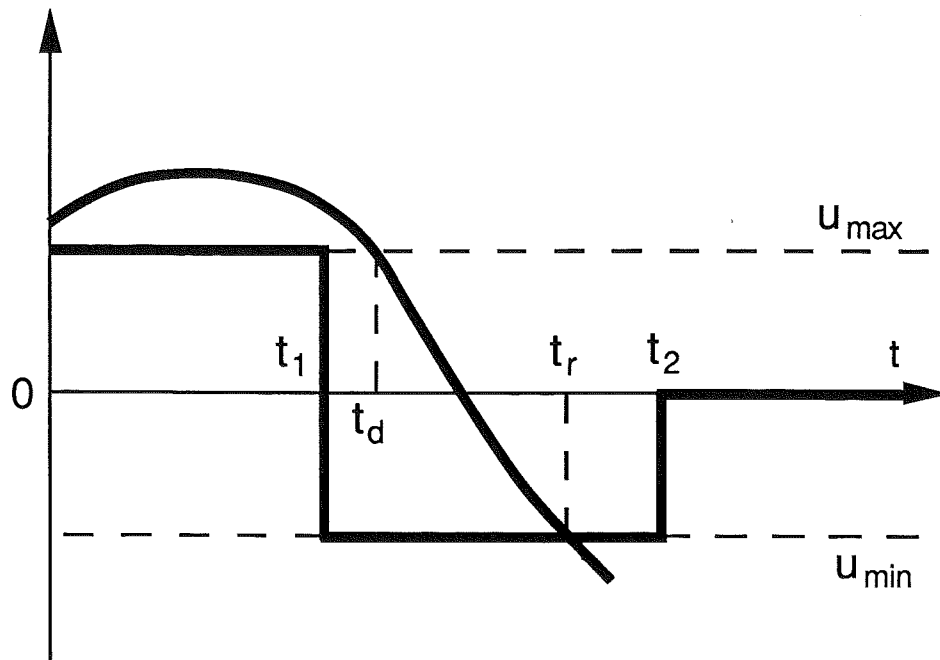


Figure 4.15 The time-optimal control signal with switch times t_1 and t_2 , and a control signal $v(t)$ with desaturation time t_d and resaturation time t_r .

criterion 2, which demands desaturation not later than time $t = t_y$, is insufficient.

Tracking Anti-Windup Revisited

In Appendix A the conditions for T_t , such that the controller desaturates before the first switch time t_1 , are derived. It may be noted that if $|\dot{y}_0|$ is sufficiently small, in this case $|\dot{y}_0| < 0.85$, the controller always desaturates before the first switch time. On the other hand, if $|\dot{y}_0|$ is sufficiently large, in this case $|\dot{y}_0| > 2.43$, the controller never desaturates before the first switch time t_1 , irrespective of T_t . Then there will always be overshoots after the impulse disturbance. This illustrates a fundamental difference between the non-linear time-optimal controller and the “linear” tracking method.

Even if T_t is chosen such that $t_d = t_1$, i.e., the desaturation time equals the switch time t_1 , there may be a small overshoot in the impulse response because $v(t)$ does not resaturate immediately, see Figure 4.15. The necessary condition to avoid overshoot may instead be $t_r < t_1$ where t_r is the resaturation time. This, however, involves the linear closed-loop dynamics and is not further analyzed.

From (A.8) it is found that $t_d \leq t_1$ if $T_t \leq 1.9$ s when $\dot{y}_0 = -1$, $J = 1$ and $u_{\max} = 0.25$. For $T_t = 1.9$ s a small overshoot may be expected. This is verified in the simulation in Figure 4.16. In this figure it is also found that $T_t \leq 1.3$ s is a sufficient condition for avoiding overshoot. This may be

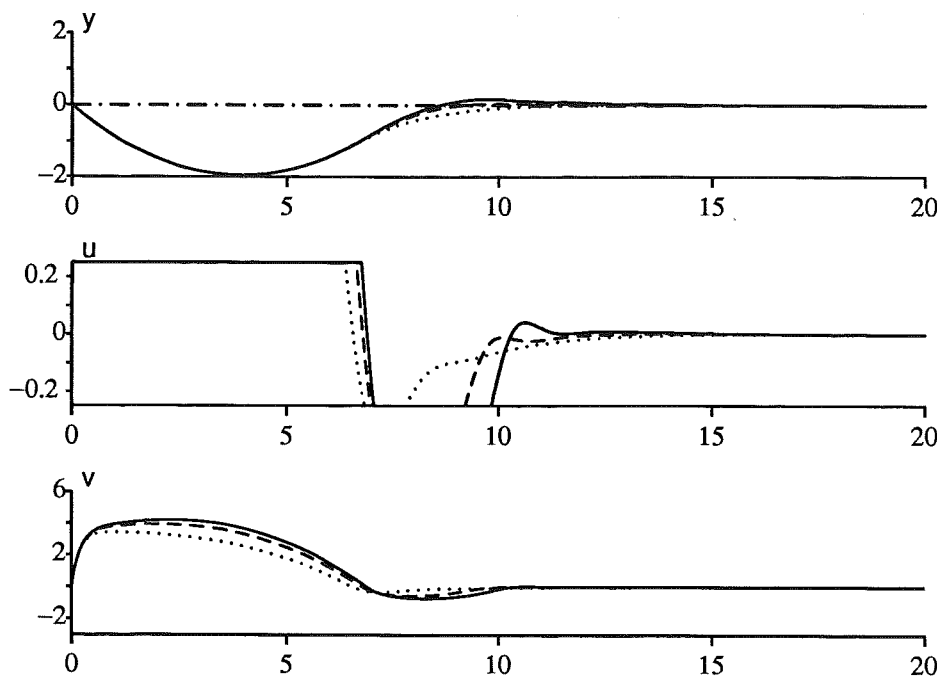


Figure 4.16 Experiment with tracking anti-windup and the impulse disturbance when $T_t = 1.9$ s (solid), $T_t = 1.7$ s (dashed) and $T_t = 1.3$ s (dotted).

compared with the general tracking design rule, which gives $T_t = \sqrt{T_i T_d} = 1.73$ s. For large impulses even smaller tracking time constants T_t will be necessary if overshoots are to be avoided. This gives a larger sensitivity for measurement noise close to saturation, see Section 3.6.

The Observer Approach and the Time-Optimal Controller

The time-optimal controller and anti-windup by the observer approach has only been compared in simulations. It was then found that $\omega_0 \geq 1.1$ rad/s is sufficient for $t_d \leq t_1$ and $\omega_0 \geq 1.2$ rad/s gives no overshoot. For larger $|\dot{y}_0|$ a larger ω_0 is necessary if overshoot is to be avoided, but when $|\dot{y}_0| > 2.6$ there is always an overshoot. Thus a large ω_0 seems to be the only reasonable choice as long as the noise sensitivity close to saturation, see Section 3.6, is not too high.

Comparison of the Anti-Windup Methods

Now the three anti-windup methods, tracking anti-windup, the observer approach and conditional integration, will be compared. For tracking and the observer approach T_t and ω_0 respectively are chosen such that the estimated desaturation time $t_d = t_1$, the optimal switch time. Thus $T_t = 1.9$ s and for the observer approach $\omega_0 = 1.07$ rad/s. In Figure 4.17 the three methods are

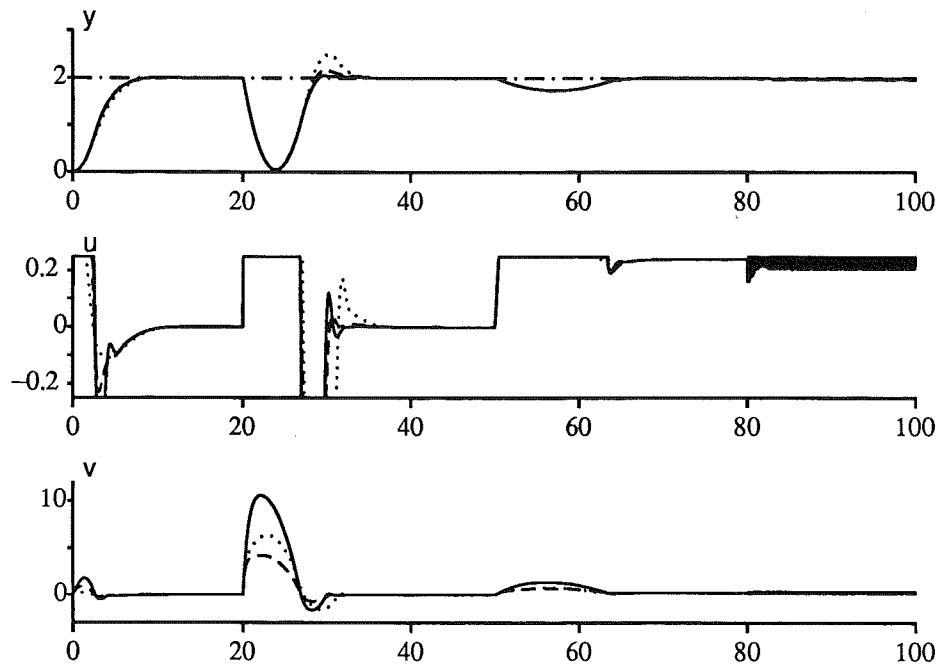


Figure 4.17 Comparison of the observer approach with $\omega_0 = 1.07 \text{ rad/s}$ (solid), tracking anti-windup with $T_t = 1.9 \text{ s}$ (dashed) and conditional integration (dotted) using the standard experiment.

Table 4.6 Performance summary for the impulse and noise disturbances for tracking anti-windup with $T_t = 1.9 \text{ s}$, the observer approach with $\omega_0 = 1.07 \text{ rad/s}$ and conditional integration (denoted CI).

	Tracking	Observer	CI
$t_d \text{ (s)}$	6.75	6.74	7.00
overshoot	0.17	0.055	0.5
IAE (impulse)	11.00	10.75	11.96
$y_0 \text{ (noise)}$	-0.028	-0.012	-0.004

compared using the anti-windup experiment. The performance with respect to the impulse and noise disturbances are summarized in Table 4.6.

From both Table 4.6 and Figure 4.17 it is clear that the observer approach is superior to tracking anti-windup. Despite equal desaturation time t_d the overshoot is significantly less, and the stationary error during the noise disturbance is also smaller. Conditional integration desaturates too late and thus overshoots substantially. However, conditional integration has a small stationary error during the noise disturbance. For set-point changes and load

disturbances the differences between the methods are insignificant. The main drawback with the anti-windup methods is that either simulations or a comparison with the time-optimal controller is necessary if overshoots are to be avoided, and this is still not always sufficient. For large impulses there will always be overshoots.

Summary

Design criterion 2, formulated in Section 3.5, is not a good criterion for a process which is almost a double integrator. The resulting design rules will thus not always work well for such processes.

4.3 Inverse-Response Processes

In this section two inverse-response processes will be used for evaluation of anti-windup design rules. For both processes a PID controller is not sufficient for obtaining arbitrary pole-placement. The first of the two processes is

$$G_p(s) = \frac{1-s}{s(s+1)^2} \quad (4.8)$$

with the disturbance transfer functions

$$G_1(s) = \frac{1}{s} \quad \text{and} \quad G_2(s) = \frac{1}{s(s+1)} \quad (4.9)$$

in cases A and B respectively.

The Controller and the Closed-Loop System

The process (4.8) is controlled by a PID controller (3.1) with parameters $K = 0.47$, $T_i = 7.50$ s, $T_d = 1.15$ s, $N = 14$ and $b = 0.4$. The parameters, except b but including N , are obtained by a method described in Appendix B. The closed-loop system has four poles with real part -0.32 and a 5:th pole approximately at $-N/T_d$. The closed-loop system is about as fast as possible without getting too sensitive to parameter variations.

In Figure 4.18 a set-point change and impulse (cases A and B) and load disturbances are shown both for the linear closed-loop system and when a saturation $|u| \leq 0.1$ is introduced without anti-windup precautions in the PID controller. The deterioration due to windup is obvious. In the sequel noise disturbances are omitted from the experiments. The result from Section 3.6 has already been verified.

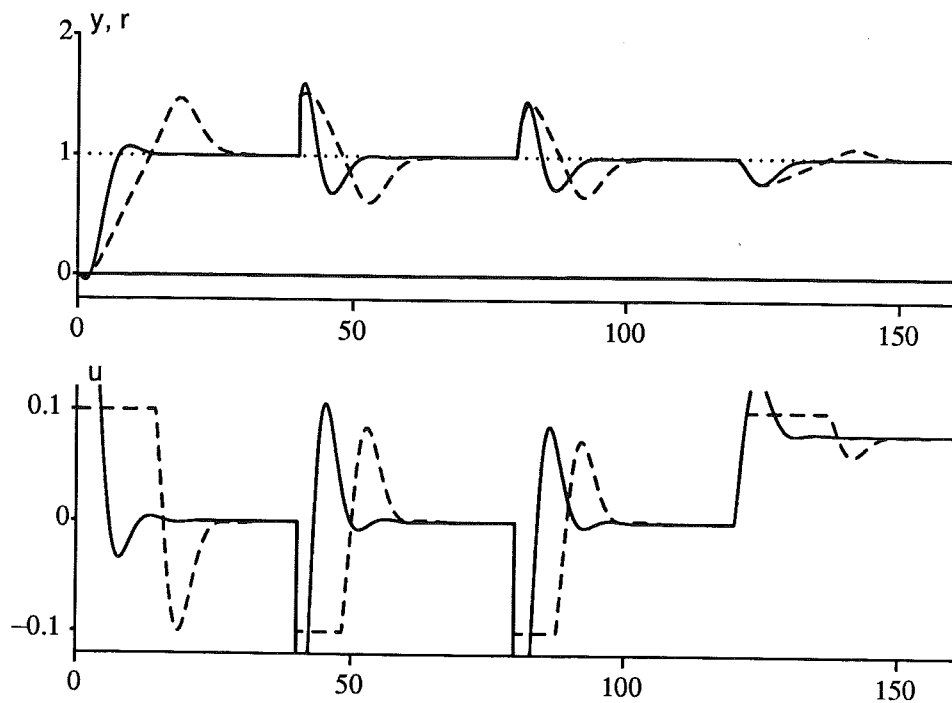


Figure 4.18 The anti-windup experiment for (4.8) during linear PID control (solid line) and saturated PID control without anti-windup (dashed line). After the set-point change there are two impulse disturbances (cases A and B) and a load disturbance.

Stability

The closed-loop stability for (4.8) with PID control and anti-windup may be checked by circle criteria. Due to the process integrator the Circle and Popov Criteria, Theorems 2.1 and 2.2 respectively, must be used. In Figure 4.19 the Nyquist curve for the loop gain $G_{fb}G_p$ is shown. The loop gain does not intersect the negative real axis below -1 . Thus the describing function method does not predict limit cycles for tracking anti-windup. For $T_t \leq 0.78 T_i = 5.85$ s absolute stability is proved for tracking anti-windup by the Popov Criterion. Similarly absolute stability holds for the observer approach when $\omega_0 \geq 0.073$ rad/s. In this case $\omega_0 < 0.073$ rad/s gives two intersections with the negative real axis, and then “hard-excited” limit-cycles are predicted by the describing function method.

Tracking Anti-Windup

According to the general design rules (3.66)–(3.67) $T_t = T_i/2 = 3.75$ s is to be chosen. It is interesting to also compare $T_t = \sqrt{T_i T_d} = 2.9$ s and $T_t = T_d = 1.15$ s. The design limits for T_t , see Result 3.4, are $1.42 \text{ s} \leq T_t \leq 6.1 \text{ s}$. When these limits are satisfied the anti-windup ought to satisfy design

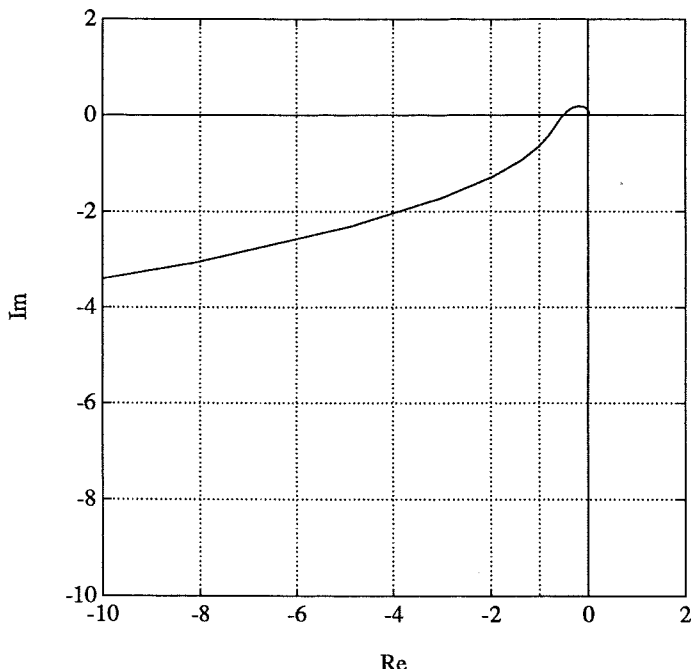


Figure 4.19 The Nyquist curve for the loop gain $G_{fb}(s)G_p(s)$ for (4.8).

criterion 2', i.e., desaturation before the control error changes sign after the impulse disturbance. In case A, the relative degree one impulse disturbance, $T_t > T_d$ is required by Result 3.2. Otherwise fast desaturation is obtained.

In Figure 4.20 two choices of tracking time constant are compared in the anti-windup experiment. The two choices $T_t = \sqrt{T_i T_d}$ and $T_t = T_i/2$ (not shown) give almost identical results, but $T_t = \sqrt{T_i T_d}$ gives smaller overshoots. When $T_t = T_d$ fast desaturation is obtained in case A but the result is better in case B.

The Observer Approach

According to the design rules in Results 3.10–3.12, $\omega_0 = (2T_d)^{-1} = 0.43$ rad/s should be chosen. This is a sufficient condition for satisfaction of design criterion 2', i.e., desaturation before the control error changes sign, which also is verified in Figure 4.21. The overshoots are slightly larger than for tracking anti-windup with $T_t = \sqrt{T_i T_d} = 2.94$ s. Thus it is possible to use a slightly larger ω_0 without degraded performance.

Conditional Integration

Conditional integration by method C3, see Section 2.2, is tested in Figure 4.21 with good results. Comparing with Figure 4.20, where tracking anti-windup is used, it may be noted that conditional integration has a set-point response

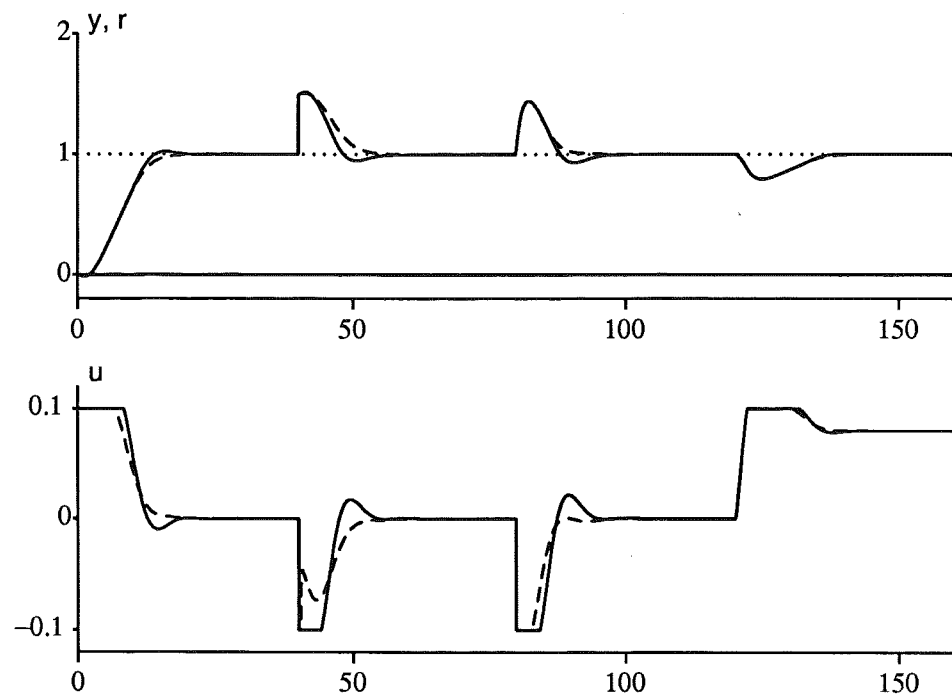


Figure 4.20 The anti-windup experiment for (4.8) with tracking anti-windup where $T_t = \sqrt{T_i T_d} = 2.9$ s (solid line) and $T_t = T_d = 1.15$ s (dashed).

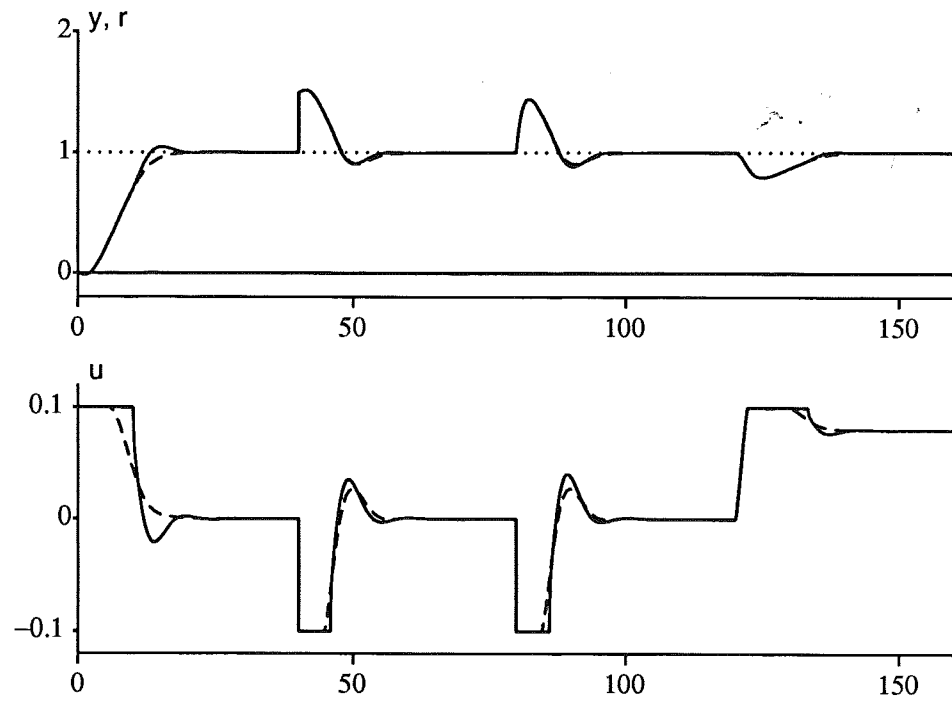


Figure 4.21 The anti-windup experiment for (4.8) with anti-windup by the observer approach where $\omega_0 = 0.43$ rad/s (solid) and for conditional integration anti-windup (dashed).

Table 4.7 IAE values for set-point change and impulse disturbances for the best cases of the compared anti-windup methods. CI denotes conditional integration.

Method		IAE set point	IAE impulse A	IAE impulse B
CI		8.32	3.20	2.70
Tracking	$T_t = 2.4 \text{ s}$	8.06	2.85	2.44
	$T_t = 2.1 \text{ s}$	8.08	2.80	2.37
	$T_t = 1.56 \text{ s}$	8.18	2.89	2.29
Observer	$\omega_0 = 0.57 \text{ rad/s}$	8.02	2.86	2.49
	$\omega_0 = 0.71 \text{ rad/s}$	8.10	2.77	2.35
	$\omega_0 = 0.91 \text{ rad/s}$	8.19	2.91	2.28

which is similar to a relatively short tracking time constant ($T_t \approx T_d$) and impulse disturbance responses which are similar to a larger tracking time constant ($T_t \approx T_i/2$). Conditional integration satisfies design criterion 2, i.e., desaturation before the control error changes sign after the impulse disturbances.

Comparison of the Anti-Windup Methods

The three anti-windup methods were also compared by using the Integral-Absolute Error, IAE. Set point and impulse optimal values of T_t and ω_0 respectively were determined, and then the IAE was determined in these cases and for conditional integration. The result is summarized in Table 4.7. Conditional integration has the largest IAE values, both for set-point changes and the impulse disturbance. The differences between tracking and the observer approach are small.

In contrast to the double tank process, see Table 4.4, the set-point and impulse IAE values are not very sensitive to parameter changes. Further, the impulse optimal anti-windup is faster, i.e., smaller T_t and larger ω_0 , than the anti-windup for the set-point change, while it is the opposite relation for the double tank process. The optimal anti-windup is also slightly faster in case B, i.e., relative degree two disturbances, than in case A.

Another Inverse-Response Process

This processes is given by

$$G_p(s) = \frac{1 - 2s}{s(s + 1)^2} \quad (4.10)$$

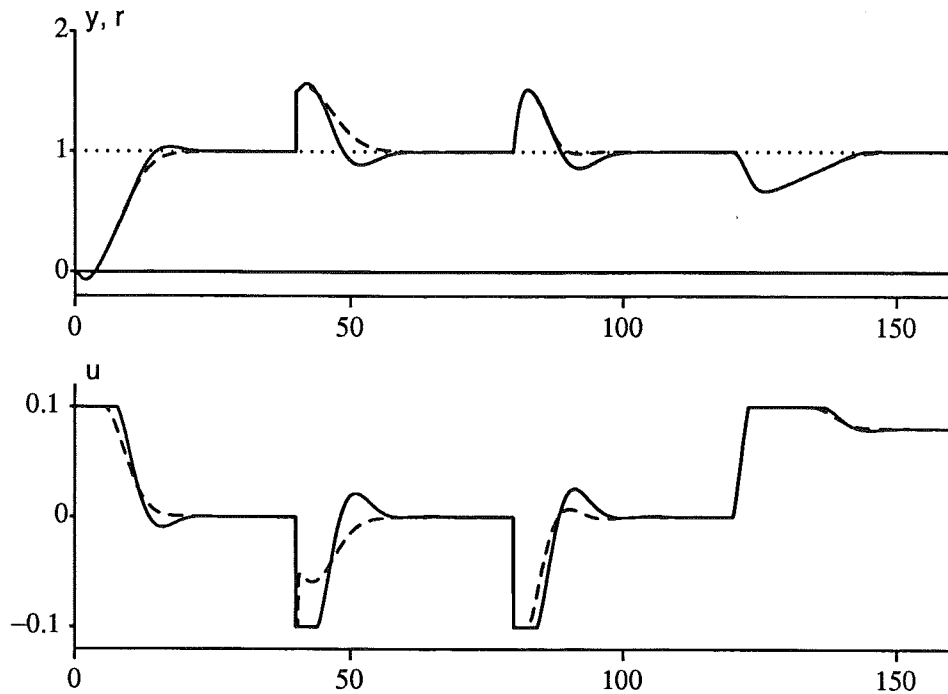


Figure 4.22 The anti-windup experiment for (4.10) with tracking anti-windup where $T_t = \sqrt{T_i T_d} = 3.43$ s (solid) and $T_t = T_d = 1.2$ s (dashed).

i.e., the right half plane zero is closer to the origin compared to (4.8). This makes (4.10) harder to control. The disturbance transfer functions and controller limits are the same as for (4.8). For the present process only a short evaluation of the anti-windup design rules will be made.

The following PID parameters were determined by the method in Appendix B; $K = 0.3$, $T_i = 9.8$, $T_d = 1.2$, and $N = 12$. The set-point weighting $b = 0.4$. According to the general design rules (3.66)–(3.67) $T_t = T_i/2 = 4.9$ s should be used. The choice $T_t = \sqrt{T_i T_d} = 3.43$ s is also interesting to consider. The general design limits, according to Result 3.4, are $1.4 \leq T_t \leq 8.4$ s. Absolute stability is proven by the Popov Criterion for $0 < T_t \leq 4$ s.

Tracking anti-windup In Figure 4.22 the tracking time constants $T_t = \sqrt{T_i T_d}$ and $T_t = T_d$ give good responses, while $T_t = T_i/2$ (not shown) has larger overshoots. For case B $T_t = T_d$ is best while a slightly larger value would be best for case A. Design criterion 2, i.e., desaturation before the control error changes sign, is satisfied. For $T_t = T_d$ a fast desaturation is obtained in case A.

The observer approach In Figure 4.23 anti-windup by the observer approach is tested. According to the design rules in Results 3.10–3.12, $\omega_0 = (2T_d)^{-1} = 0.42$ rad/s should be chosen. This is a sufficient condition for satisfaction of design criterion 2, which is confirmed in Figure 4.23. Absolute

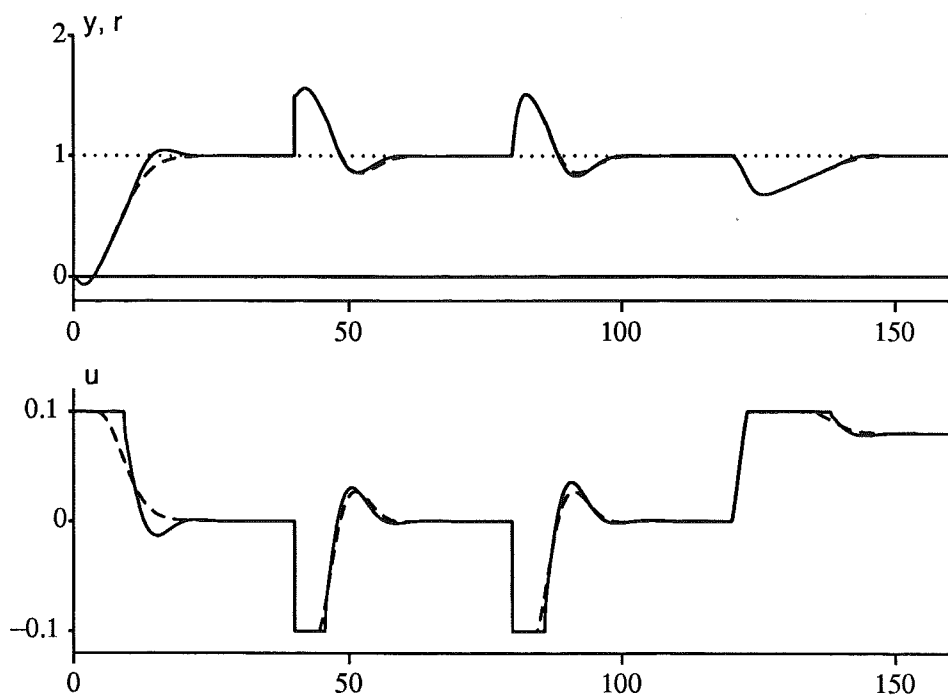


Figure 4.23 The anti-windup experiment for (4.10) with anti-windup by the observer approach where $\omega_0 = 0.42$ rad/s (solid) and for conditional integration, anti-windup (dashed).

stability is proven by the Popov Criterion for $0.16 \leq \omega_0 \leq 1.67$ rad/s. The overshoots are slightly larger than for tracking anti-windup with $T_t = 3.43$ s. Thus ω_0 may be slightly increased without loss of performance.

Conditional integration, see Figure 4.23, also gives an acceptable performance.

Summary

The tested non-minimum phase processes both verify the design limits for tracking anti-windup. However, it seems more favorable to use the shorter tracking time constant $T_t = \sqrt{T_i T_d}$ than $T_t = T_i/2$ which is suggested by the design rules (3.66)–(3.67). For the observer approach the design rules give an ω_0 which is sufficient for the design criterion but still slightly too small. Conditional integration gives an acceptable performance.

4.4 An Unstable Process

The design rules for tracking anti-windup and the observer approach will now be tested on an unstable process. However, for unstable processes with

limited control input sufficiently large inputs or initial conditions cause an unstable closed-loop system. The use of good anti-windup will, on the other hand, increase the ability to cope with large signals. Smaller controller limits or a faster unstable pole are other ways of easily obtaining an unstable closed-loop system.

The process used in this section is an unstable modification of (4.8), namely

$$G_p(s) = \frac{1-s}{(s-0.05)(s+1)^2} \quad (4.11)$$

The anti-windup experiment is otherwise identical to the experiment in Section 4.3 with controller limits ± 0.1 . The disturbance transfer functions are

$$G_1(s) = \frac{1}{s-0.05} \quad \text{and} \quad G_2(s) = \frac{1}{(s-0.05)(s+1)} \quad (4.12)$$

in cases A and B respectively. For (4.11) the PID parameters are $K = 0.49$, $T_i = 8.6$ s, $T_d = 1.2$ s, and $N = 15$, which were determined by the method in Appendix B. The set-point weighting is $b = 0.4$. In Figure 4.24 severe windup effects are noticed.

Tracking Anti-Windup

According to the general design rules for tracking anti-windup, (3.66)–(3.67), $T_t = T_i/2 = 4.3$ s should be chosen. The choice $T_t = \sqrt{T_i T_d} = 3.2$ s is also interesting to test. For satisfaction of design criterion 2, i.e., desaturation before the control error changes sign, Result 3.4 yields $T_t \in [1.44, 7.16]$. To avoid immediate desaturation, Result 3.2 yields $T_t > 1.15$ s.

Using tracking anti-windup, see Figure 4.25, it is clear that both $T_t = \sqrt{T_i T_d} = 3.2$ s and $T_t = 1.15$ s gives good responses, and design criterion 2 is satisfied in both cases. The choice $T_t = T_i/2 = 4.3$ s (not shown) gives larger overshoots but is otherwise satisfactory. When $T_t = 1.15$ s the controller desaturates for a short moment after the impulse in case A. Thus the choice $T_t = \sqrt{T_i T_d} = 3.2$ s seems to be the best choice, where the process output y approaches the set point slightly faster than for the other choices of T_t . In case B the performances are also close.

The Observer Approach

In Figure 4.26 anti-windup by the observer approach is tested. According to Result 3.10 $\omega_0 = (2T_d)^{-1} = 0.42$ rad/s should be chosen. As can be seen in Figure 4.26 this choice satisfies design criterion 2 for the impulse disturbances, and also gives a good performance for the set-point change and load disturbance.

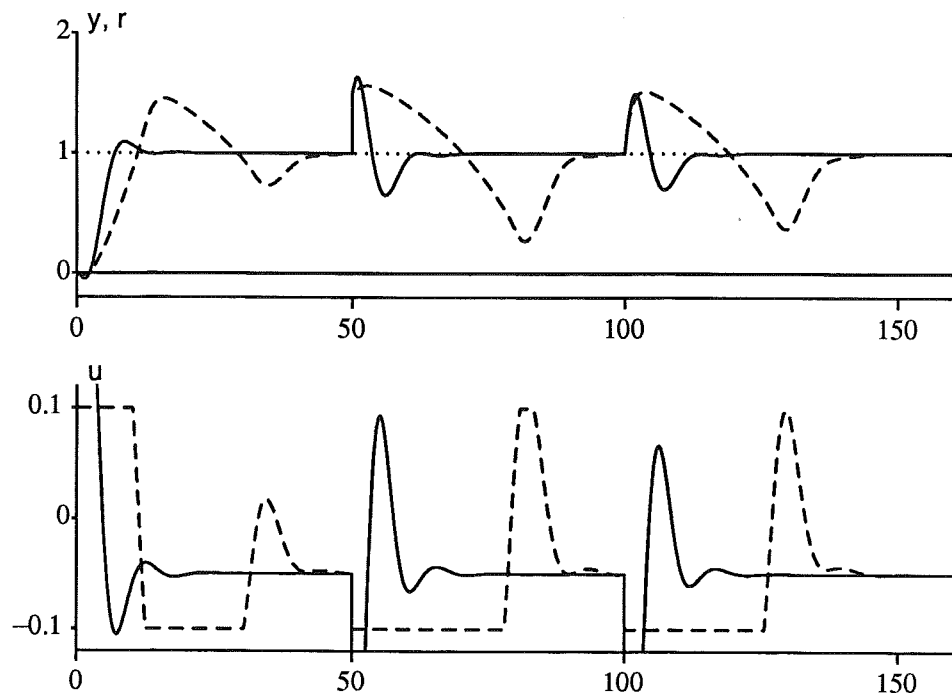


Figure 4.24 The anti-windup experiment for (4.11) during linear PID control (solid) and saturated PID control without anti-windup (dashed) for both cases A, and B.

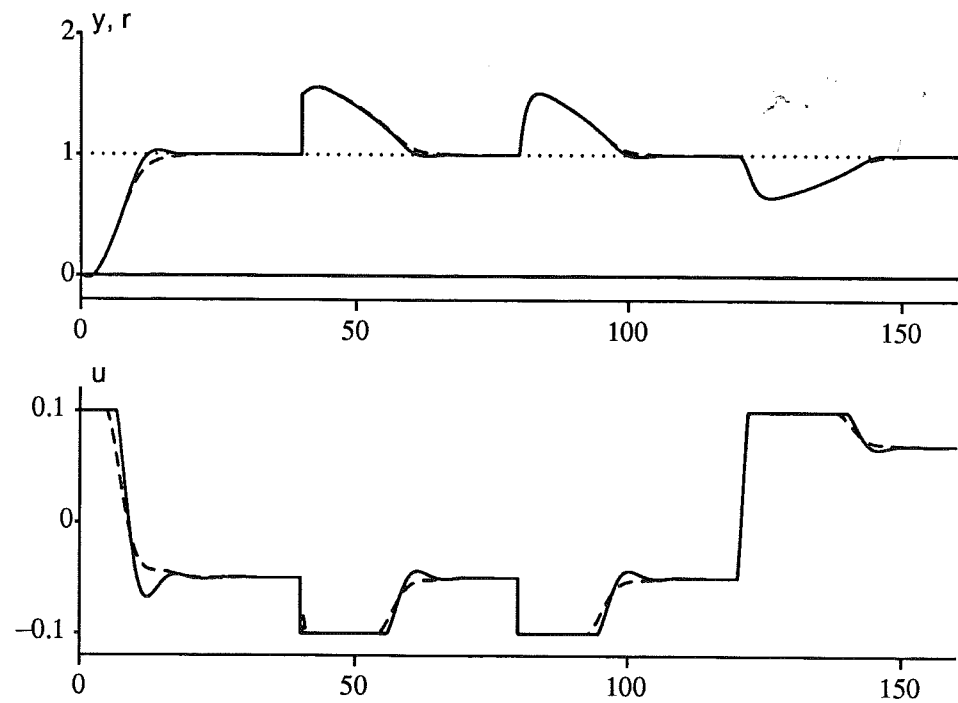


Figure 4.25 The anti-windup experiment for (4.11) with tracking anti-windup where $T_t = \sqrt{T_i T_d} = 3.2$ s (solid) and $T_t = 1.15$ s (dashed).

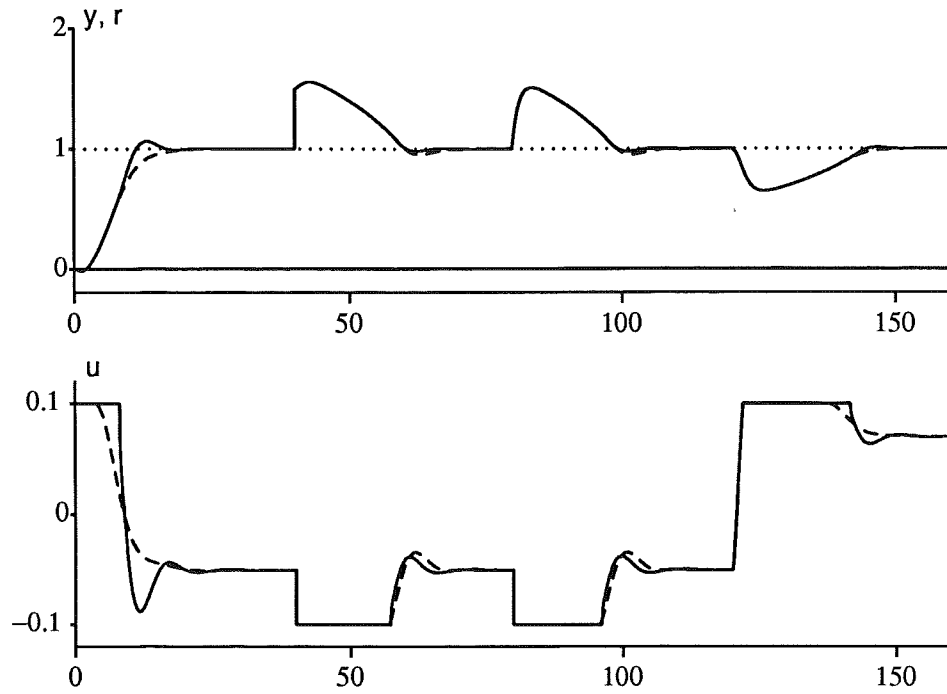


Figure 4.26 The anti-windup experiment for the unstable process (4.11) with anti-windup by the observer approach where $\omega_0 = (2T_d)^{-1} = 0.42 \text{ rad/s}$ (solid), and with conditional integration anti-windup.

Conditional integration, see Figure 4.26, gives an acceptable performance, which also satisfies design criterion 2.

Summary

The chosen unstable process verifies the design rules derived in Section 3.5, provided that the controller has sufficiently large limits compared to the inputs and initial conditions. Further, using tracking anti-windup in case A, it seems better to use $T_t = \sqrt{T_i T_d}$ than $T_t = T_i/2$, which was suggested in the design rule in (3.66).

4.5 Time-Delay and High-Order Processes

In this section the high-order processes

$$G_p(s) = \frac{e^{-sT}}{(s+1)^2} \quad \text{and} \quad G_p(s) = \frac{1}{(s+1)^n} \quad (4.13)$$

will be used for evaluation of the design results from Section 3.5. A PID controller is not sufficient for obtaining arbitrary pole-placement for any of

the processes when $T > 0$ or $n > 2$. Both processes have the disturbance transfer functions

$$G_2(s) = \frac{1}{s+1} \quad \text{and} \quad G_2(s) = \frac{1}{(s+1)^2} \quad (4.14)$$

in cases A and B respectively, and thus, using the notation in Result 3.2, $\alpha_1 = 1$. A characteristic of both processes is that the controller gain K must be decreased and both the integral and derivative times T_i and T_d must be increased when T and n in (4.13) increases. Thus $1 - \alpha_1 T_d$ decreases and becomes negative if $T_d > 1$. In such cases the controller desaturates immediately when tracking anti-windup is used, see Result 3.3. Using these two processes for some values of T and n , respectively, it is possible to evaluate the design rules for anti-windup from Section 3.5. Especially in case A, where fast desaturation must be avoided, the design rule (3.66) for tracking anti-windup gets a good evaluation.

Another characteristic of these high-order processes is that it is relatively hard to get windup problems. The reason is small gains K and large integral and derivative times T_i and T_d . This is illustrated in Figure 4.27 where four different tracking time constants are compared. The only visible difference occurs for the case A impulse disturbance at time $t = 50$. Otherwise, the control is linear or, in case B, only negligibly saturated. Using the experiment in Figure 4.27 the anti-windup methods and parameters are hard to compare.

If instead only the impulse disturbances are used in an experiment where the controller is close to saturation the anti-windup methods are more easily evaluated. This is illustrated in Figure 4.28. Thus the experiment from Figure 4.28 is used for evaluation of the different anti-windup methods. After a start in stationarity with all signals zero the two impulse disturbances occur at time $t = 5$ and $t = 50$. The controller limits are $u_{\max} = 1.0$ and $u_{\min} = -0.1$.

The two processes in (4.13) are now to be compared for a number of time delays T and orders n respectively. In each case a number of anti-windup methods and parameters will be compared. In order to get a compact documentation of the evaluation the integral-absolute-errors (IAE) for the impulse responses will be reported in tables. Note that the IAE as such does not evaluate the design criteria, i.e., if the controller desaturates before the control error changes sign (design criterion 2) or if there is a fast desaturation in case A (design criterion 1). However, from the earlier evaluations it is clear that both too late and too early desaturation give impulse responses with larger IAE. Thus the IAE may be used as a measure of how well the design criteria are satisfied. However, it will be commented if design criteria are violated.

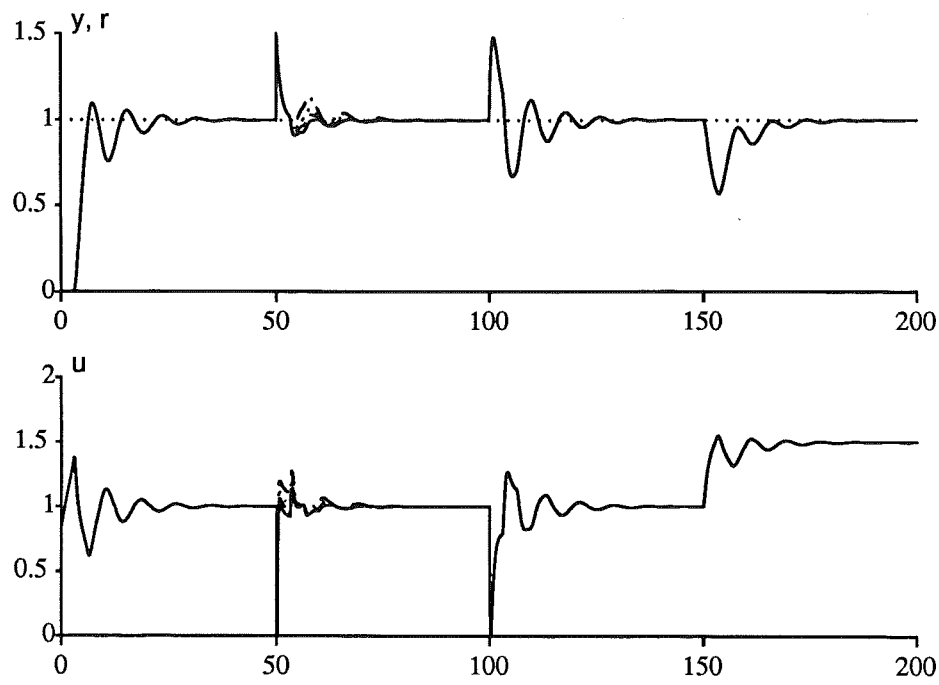


Figure 4.27 Experiment with tracking anti-windup for the time-delay process with $T = 3$ s. $T_t = \infty$ (solid), i.e., no anti-windup, $T_t = T_i$ (dashed), $T_t = \sqrt{T_i T_d}$ (dotted) and $T_t = T_d / (1 - \alpha_1 T_d)$ (dash-dotted). The set point is also dotted. The controller parameters were determined by the Ziegler-Nichols ultimate gain method.

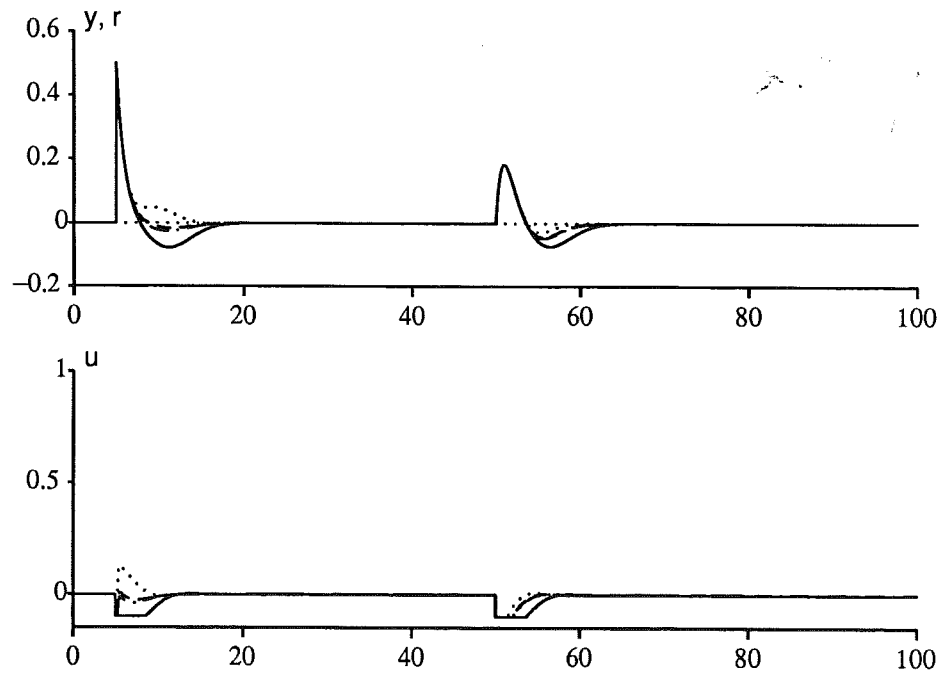


Figure 4.28 Experiment with tracking anti-windup for the n -th order process when $n = 4$. $T_t = \infty$ (solid), i.e., no anti-windup, $T_t = T_i$ (dashed), $T_t = \sqrt{T_i T_d}$ (dotted) and $T_t = T_d / (1 - \alpha_1 T_d)$ (dash-dotted). The set point is also dotted.

Table 4.8 Template for how the IAE:s are reported for the time-delay process (4.15). For each case of time delay T the PID parameters are given. For each of the impulse case, A and B, six IAE:s are reported in positions according to this table. CI denotes conditional integration.

T	K	T_i	T_d	IAE (x)	
			$T_t = \infty$	$T_t = T_i$	
T	K	T_i	T_d	$T_t = \sqrt{T_i T_d}$	$T_t = \frac{T_d}{1 - \alpha_1 T_d}$
			$\omega_0 = \frac{1}{2T_d}$		CI

The Time-Delay Process

The time-delay process

$$G_p(s) = \frac{e^{-sT}}{(s+1)^2} \quad (4.15)$$

will now be used for evaluation of the anti-windup methods. For simplicity the Ziegler-Nichols ultimate gain method is used to determine the PID parameters. The derivative filter constant $N = 10$. Since $T_i = 4T_d$ for Ziegler-Nichols parameters it follows that $\sqrt{T_i T_d} = T_i/2 = 2T_d$. Thus there are fewer test cases for the tracking and observer anti-windup methods compared to when $T_i \neq 4T_d$.

The IAE:s are reported in Table 4.9 according to the template in Table 4.8. The case $T_t = \infty$ means no anti-windup and is reported in the upper left corner for each of the two impulse cases. When $T_d > 1$ the case $T_t = T_d/(1 - \alpha_1 T_d) < 0$ is omitted.

Tracking anti-windup In case A, where the design rule in (3.66) is evaluated, there are two limits for T_d which separate different cases in the design rule. When $T_d < 0.5$ the design rule says $T_t = T_i/2 = \sqrt{T_i T_d}$. When $0.5 < T_d < 0.75$ the design rule says $T_t = T_d/(1 - \alpha_1 T_d)$ and finally, when $T_d > 0.75$ the design rule says $T_t = T_i$. This is also verified in Table 4.9 where the corresponding positions are marked in boldface. This also holds when $T_d > 1$, i.e., when immediate desaturation is obtained. When $T_d > 1$ the choice $T_t = T_i/2 = \sqrt{T_i T_d}$ gives larger IAE than no anti-windup at all.

In case B it is immediately clear that the design rule in (3.67) is not verified by the IAE:s. Computing the actual values of T_t in the different cases it is found that for time-delays $T \leq 2$ the smallest of the tested values of T_t gives the smallest IAE. For larger time-delays $T_t = T_i$ gives the smallest IAE. The reason and limit for this change is not clear. However, according to

Table 4.9 Obtained IAE:s in the two impulse cases, A and B, for processes (4.15) with time-delays T . The positions for different anti-windup cases are given in Table 4.8. The best IAE:s are written in boldface.

T	K	T_i	T_d	IAE (A)		IAE (B)	
0.3	4.36	1.24	0.31	0.800	0.459	2.003	1.072
				0.409	0.450	1.015	1.008
				0.439	0.425	1.042	1.023
0.6	2.40	1.80	0.45	0.825	0.501	2.048	1.158
				0.472	0.511	1.046	1.038
				0.474	0.466	1.099	1.072
1.0	1.62	2.40	0.60	0.862	0.540	2.116	1.268
				0.593	0.499	1.083	1.131
				0.527	0.536	1.182	1.159
1.5	1.23	3.05	0.76	0.900	0.545	2.196	1.369
				0.720	0.559	1.186	1.389
				0.606	0.702	1.284	1.270
2.0	1.04	3.64	0.91	0.930	0.571	2.269	1.432
				0.843	0.772	1.331	1.833
				0.689	0.780	1.397	1.362
2.5	0.93	4.21	1.05	0.953	0.648	2.334	1.487
				0.972		1.494	
				0.759	0.800	1.526	1.453
3.0	0.86	4.77	1.19	0.967	0.745	2.390	1.557
				1.107		1.663	
				0.817	0.810	1.667	1.582

Åström *et al.* (1989) the Ziegler-Nichols design is not recommended for the time-delay process (4.15) when $T > 2$, since these processes have normalized dead-times greater than one. Then the linear performance is not good and thus cautious anti-windup may be necessary. Using other PID design rules it may be advantageous to use faster anti-windup.

The observer approach The only tested value of ω_0 is $\omega_0 = 2/T_i = (2T_d)^{-1}$. Compared with tracking anti-windup the observer approach has slightly larger IAE. For the cases when $T \leq 1$ design criterion 2, i.e., desatu-

4.5 Time-Delay and High-Order Processes

Table 4.10 Template for how the IAE:s are reported for the high-order process (4.16). For each order n the PID parameters are given. For each of the impulse cases, A and B, nine IAE:s are reported in positions according to this table. CI denotes conditional integration.

n	K	T_i	T_d	IAE (x)	
$T_t = \infty$					
				$T_t = T_i$	$T_t = \frac{T_i}{2}$
n	K	T_i	T_d	$T_t = \sqrt{T_i T_d}$	$T_t = \frac{T_d}{1 - \alpha_1 T_d}$
				$\omega_0 = \frac{1}{2T_d}$	$\omega_0 = \frac{1}{\sqrt{T_i T_d}}$
				$\omega_0 = \frac{2}{T_i}$	CI

ration before the control error changes sign, is at the limit of being satisfied, but for larger T the criterion is well satisfied.

Conditional integration In case B conditional integration performs well compared to the other two methods. In case A the performance is reasonably good for smaller time delays $T \leq 1$ and when $T = 3$. In between the performance is not so good, but clearly better than no anti-windup.

The High-Order Process

The high-order process

$$G_p(s) = \frac{1}{(s + 1)^n} \quad (4.16)$$

will now be used for evaluation of the anti-windup methods. The PID parameters are determined by the method in Appendix B. The derivative filter constant $N = 10$. In the test cases $T_i \neq 4T_d$. Thus there are a few more anti-windup cases to evaluate. The IAE:s are reported in Table 4.11 according to the template in Table 4.10. When $T_d > 1$ the case $T_t = T_d/(1 - \alpha_1 T_d) < 0$ is omitted.

Tracking anti-windup In all cases in Table 4.11 the integral time $T_i < 4T_d$, which implies $\sqrt{T_i T_d} > T_i/2$. Further T_d is sufficiently large to make

$$\frac{T_d}{1 - \alpha_1 T_d} > \sqrt{T_i T_d}$$

Table 4.11 Obtained IAE:s in the two impulse cases, A and B, for processes (4.16) with order n . The positions for different anti-windup cases are given in Table 4.10. The best IAE:s for tracking anti-windup and the observer approach are written in boldface.

n	K	T_i	T_d	IAE (A)		IAE (B)	
3	2.72	2.34	0.61	0.836		0.671	
				0.503	0.607	0.424	0.353
				0.597	0.494	0.353	0.377
				0.474	0.470	0.403	0.400
4	1.13	2.86	0.77	0.466	0.508	0.398	0.390
				0.889		0.761	
				0.558	0.713	0.558	0.467
				0.691	0.594	0.471	0.577
5	0.82	3.24	0.89	0.576	0.566	0.554	0.548
				0.556	0.731	0.543	0.516
				0.929		0.828	
				0.562	0.788	0.650	0.555
6	0.70	3.65	1.02	0.757	0.767	0.561	0.740
				0.641	0.626	0.663	0.656
				0.612	0.792	0.648	0.616
				0.959		0.877	
7	0.63	4.07	1.15	0.568	0.871	0.705	0.602
				0.830			
				0.679	0.661	0.736	0.727
				0.642	0.819	0.719	0.689
				0.977		0.914	
				0.594	0.952	0.737	0.624
				0.902			
				0.703	0.682	0.786	0.776

in the test cases. However, for the tested orders n in case A, the design rule in (3.66) is verified in the sense that $T_t = \min(T_i, T_d/(1 - \alpha_1 T_d))$ should be chosen. It may be noted that $T_t = \sqrt{T_i T_d}$ gives smaller IAE:s than $T_t = T_i/2$. In case B the smallest test values, i.e., $T_t = T_i/2$, gives the

smallest IAE:s. Further in case B, tracking anti-windup is the best of the three tested methods, when the smallest test value of T_t ($= T_i/2$) is used. In case A tracking anti-windup is best for orders $n > 4$.

The observer approach In both case A and B the largest of the test values, i.e., $\omega_0 = 2/T_i$, gives the smallest IAE:s. In case A the observer approach is better than tracking anti-windup for orders $n \leq 4$. However, in case B both tracking anti-windup and conditional integration are better in terms of smaller IAE:s.

Conditional integration In case A conditional integration does not perform very well compared with tracking anti-windup and the observer approach. An exception is the case $n = 3$ where it is comparable with tracking anti-windup. However, in case B conditional integration is better than the observer approach but not as good as tracking anti-windup.

Summary

The design rule in (3.66), for tracking anti-windup in case A, has been verified for both processes. Note, however, that this design rule has not been tested for all cases. In case B the main result is to use a small tracking time constant which contradicts the design rule in (3.67). However, for larger time-delays in the time-delay process (4.15), it is better to use $T_t = T_i$ than a smaller value of T_t . The reason may be poor performance for the Ziegler-Nichols design when the time-delay is sufficiently large.

For the observer approach the design rules in Results 3.11–3.12 are verified on the high-order process (4.16). When $T_i = 4T_d$, e.g., for the time delay process (4.15), these design rules all give the same value of ω_0 . Conditional integration performs reasonably well in the test cases. It is not the best method, but not always the worst either.

Tracking anti-windup is in general the best of the tested anti-windup methods. This is, however, only valid for the tested parameter values. If T_t and ω_0 are tuned for minimum IAE it may very well be the case that the observer approach is best, compare Sections 4.1–4.2.

4.6 Poorly Damped Processes

It is well-known that PID controllers are not well suited for controlling processes with poorly damped complex poles. Typical examples are mechanical systems with resonances. The reason is that a PID controller is unable to damp an oscillatory mode. One possibility is, however, to choose the controller zeros such that they cancel some of the process poles. For complex poles this can only be done when the parallel form (3.1) of the PID controller

is used. The serial form (3.3) has real zeros which make such cancellations impossible. Thus this approach cannot be used in most commercial single-loop PID controllers. A few aspects of cancellation will now be discussed.

Cancellation of Poorly Damped Poles

In an ideal PID controller the controller zeros are given by

$$s^2 + \frac{1}{T_d} s + \frac{1}{T_i T_d} = 0 \quad (4.17)$$

which is trivial to match with process poles given by

$$s^2 + 2\zeta\omega_0 s + \omega_0^2 = 0 \quad (4.18)$$

However, the poles and zeros do not match sufficiently well unless the derivative filter factor N is very large. This is particularly noticeable when the relative damping ζ is small. Hence the derivative filter must be included in the cancellation design.

For the nonideal PID controller, with a derivative filter, the controller zeros are given by

$$s^2 + \frac{1}{N+1} \left(\frac{N}{T_d} + \frac{1}{T_i} \right) s + \frac{N}{N+1} \cdot \frac{1}{T_i T_d} = 0 \quad (4.19)$$

To match the process poles one extra condition is necessary. Let

$$T_d = \alpha T_i \quad (4.20)$$

and equate (4.18) and (4.19). Then

$$\begin{aligned} \omega_0 &= \frac{1}{T_i} \sqrt{\frac{1}{\alpha} \frac{N}{N+1}} \\ \zeta &= \frac{1}{2} \sqrt{\frac{N}{N+1}} \left(\frac{1}{\sqrt{\alpha}} + \frac{\sqrt{\alpha}}{N} \right) \end{aligned} \quad (4.21)$$

The relative damping has, with respect to α , a minimum for $\alpha = N$. Thus the process poles can be matched by controller zeros if

$$\begin{aligned} N &= \frac{1}{\zeta^2} - 1 \\ T_i &= \frac{\zeta}{\omega_0} \\ T_d &= N \cdot T_i \end{aligned} \quad (4.22)$$

When the relative damping ζ is small the filter constant N must be very large if cancellation is desired. This explains why cancellation fails when the derivative filter is neglected for too small values of N . The design equations in (4.22) give the smallest possible N for cancellation. Other relations between T_i and T_d than $T_d = N \cdot T_i$ requires larger N for cancellation.

The controller gain K must finally be chosen such that a sufficient gain or phase margin is obtained. The result is usually a fairly low gain, hence the closed-loop system has low bandwidth.

In order to avoid exciting a poorly damped mode by set-point changes, the derivative part must act on the set point too. This gives high initial control signals for step changes of the set point. However, disturbances will excite the poorly damped mode and due to the controller zeros the control signal will not counteract.

Cancellation is a linear operation which thus requires that the control signal is not saturated. If saturation occurs for set-point changes the poorly damped mode is excited. Anti-windup does not make the situation better, in some cases anti-windup instead causes poorer performance than no anti-windup at all. The basic issue for these control systems is instead to avoid saturation. Low controller gain K or "realizable references", i.e., reference signals which can be reproduced by the process, are means for avoiding saturation.

Summary

PID controllers are not well suited for control of processes with poorly damped poles. It is possible to choose the controller zeros such that they cancel one complex pole pair, provided the parallel form PID controller is used. Usually a large derivative filter constant N is necessary for the cancellation. The cancelled mode is excited by disturbances or if the control signal is saturated. The best performance is obtained by avoiding saturation rather than introducing anti-windup.

4.7 Summary

A number of design rules for PID anti-windup methods have been compared in this chapter. In a standard experiment with a set-point change and load, noise and impulse disturbances the design rules give different performances. The impulse disturbances give responses characterized by either an immediate change Δy in the process output (case A) or an immediate derivative change $\Delta \dot{y}$ in the process output (case B), see Section 3.5. Usually the impulse disturbance responses are sensitive to the choice of anti-windup method and corresponding parameters. The responses for set-point changes and load

disturbances are much more insensitive to these choices. Thus anti-windup design must focus on impulse disturbances rather than on set-point changes and load disturbances. The design criteria used when deriving the design rules for impulse disturbances were

1. no immediate desaturation for the controller (in case A), and
2. desaturation before the control error changes sign.

The design criteria behind the design rules for anti-windup as well as the results for sinusoidal measurement disturbances will be discussed.

The PID anti-windup methods tested in this chapter were tracking anti-windup, anti-windup by an observer approach and a conditional integration method denoted C3, see Section 3.2.

The Design Criteria for Impulse Disturbances

The two design criteria for impulse disturbances, see Section 3.5, seem to have been well chosen. Anti-windup parameters which satisfy the design criteria usually give a good performance, both subjectively and in terms of a low integral-absolute-error (IAE) for the process output. An exception is processes which resemble double integrators, see Section 4.2. For such processes design criterion 2 does not work. It was shown that for sufficiently large impulse disturbances the process output will oscillate several times, no matter how the anti-windup parameter is chosen.

For processes of higher order the two design criteria may give contradictory demands on the tracking time constant T_t in case A. The discussion leading to Result 3.5, which conjectures that design criterion 2 is more important than design criterion 1, has been verified in simulations.

Offset during Measurement Disturbances

The result from Section 3.6 regarding the offset y_0 during a sinusoidal measurement disturbance has proven to be accurate. However, for a sufficiently low disturbance frequency, compared to the anti-windup bandwidth, a smaller offset than predicted is obtained.

Tracking Anti-Windup for Case A

The general design rule in (3.66) has essentially been verified. An exception is that $T_t = \sqrt{T_i T_d}$ generally has given better performance in terms of overshoot and IAE than $T_t = T_i/2$. The latter choice is thus omitted, which gives the final design rule.

$$T_t = \begin{cases} \min\left(T_i, \max\left(\sqrt{T_i T_d}, \frac{T_d}{1 - \alpha_1 T_d}\right)\right) & \text{when } 1 - \alpha_1 T_d > 0 \\ T_i & \text{when } 1 - \alpha_1 T_d \leq 0 \end{cases} \quad (4.23)$$

where α_1 is defined in Result 3.2. This formula usually gives the result $T_t = \sqrt{T_i T_d}$ but for high-order processes a larger value of T_t is obtained when $\alpha_1 > 0$. Empirically this design rule is valid both when $T_i \geq 4T_d$ and when $T_i < 4T_d$.

Tracking Anti-Windup for Case B

The design rule (3.67) has not been verified. Instead counterexamples have been found where the smallest of the tested values of T_t have given the best performance. Small values of T_t , compare Result 3.7, generally give good performance for case B impulse disturbances, but a drawback is then a larger noise sensitivity close to saturation, see Section 3.6

The design rules $T_t = \sqrt{T_i T_d}$ and $T_t = T_i/2$ satisfy design criterion 2 and give reasonably good performance. An exception was processes which resemble double integrators, where sometimes poor performance may be obtained irrespective of how T_t is chosen.

A compromise, with respect to the above observations, is to suggest the design rule

$$T_t = \min \left(\sqrt{T_i T_d}, \frac{T_i}{2} \right) \quad (4.24)$$

If both cases of impulse disturbances are probable it is safer to design for case A.

The Observer Approach

Design rule 2 for the observer approach, i.e.,

$$\omega_0 = \max \left(\frac{1}{2T_d}, \frac{2}{T_i} \right) \quad (4.25)$$

is sufficient with respect to design criterion 2. In some cases, e.g., for some of the time-delay processes, the design rule is at the limit of satisfying the design criterion. For processes which resemble double integrators poor performance may be obtained irrespective of how ω_0 is chosen, compare tracking anti-windup.

Comparison between the Anti-Windup Methods

From the evaluation in this chapter it is clear that *tracking anti-windup is a general robust anti-windup method for PID controllers*. In case A the design rule in (4.23) is very good. However, it requires knowledge of $\alpha_1 = -\beta_2$, where β_2 is a Markov parameter in the disturbance transfer function. In case B the design rule in (4.24) gives reasonable performance while a small value of T_t usually gives the best performance. However, if both case A and

B disturbances are to be expected, small values of T_t are unfeasible. The noise sensitivity must also be taken into account.

Design rule (4.25) for the observer approach is satisfactory with respect to the design criterion, but the resulting performance is usually not as good as for tracking anti-windup. A nice property is that the design rule is valid for both impulse cases. Further, it is in a number of cases possible to find a value of ω_0 , which gives better performance in terms of settling time, integral-absolute-error, overshoot, etc., than the best choice of T_t . The drawback is that the choice is specific for each process and set of controller parameters. No guidance is obtained from the design rule. The design rule is not valid for PI controllers. Thus this method is not suitable for general purpose use, but the benefits can be utilized in dedicated PID controllers.

Except for processes which resemble double integrators, conditional integration anti-windup has a reasonably good performance, but usually not as good as tracking anti-windup and the observer approach. A boundary layer width ϵ may require tuning. The simplicity of the method, however, still makes it attractive to use.

5

Conclusions

This thesis has mainly dealt with the anti-windup problem in PID controllers. In Chapter 2 a number of anti-windup and related methods were surveyed and discussed. Some of these methods are feasible for use in PID controllers. However, the lack of design rules for choosing parameters in these methods was noted. It was also noted that when the choice of parameters were discussed it was mainly in the context of set-point changes, not disturbances.

Anti-Windup Design Rules for PID Controllers

A few implementations and anti-windup methods for PID controllers were discussed in Chapter 3. Two anti-windup methods, tracking anti-windup and the observer approach to anti-windup, see Section 3.2, were treated more extensively. Some stability issues, namely the changed phase of the transfer function

$$G = \frac{G_p G_{fb} - W}{1 + W}$$

relative to the point -1 , were analyzed. For tracking anti-windup $\arg(G(i\omega) + 1)$ increases with decreased tracking time constant T_t . A stability theorem for tracking anti-windup was given. The theorem is valid for all continuous-time single-loop controllers with integral action. For the observer approach, however, $\arg(G(i\omega) + 1)$ may decrease and eventually cause instability for sufficiently small ω_0 . This is natural since G is then approximately a double integrator plus extra lag from the process.

In Section 3.5 design rules for the choice of tracking time constant T_t and the observer natural frequency ω_0 were derived. The derivations were based on two cases of impulse disturbances to the process, giving

- A. a step change in the process output, and
- B. a ramp change in the process output.

The responses in process output y and the control signal v turn out to be sensitive to the choice of T_t and ω_0 respectively. The design rules were based on two criteria, namely

1. no immediate desaturation (in case A), and
2. sufficiently fast desaturation (in both cases), such that the controller desaturates before the control error changes sign.

Sensitivity to measurement noise close to saturation was also treated. It was found that sinusoidal measurement noise, which causes partial controller saturation, gives a constant offset y_0 in the process output if anti-windup is used. Without anti-windup there is no offset. The results given are valid for sufficiently high disturbance frequencies. For lower frequencies smaller offsets are obtained.

Evaluation of Anti-Windup Design Rules

In Chapter 4 the design rules from Section 3.5 were tested on different processes. The noise sensitivity was tested on two of the processes, and the offsets obtained agreed well with the offsets derived in Chapter 3.

The design rules for tracking anti-windup were found to be reliable in the evaluation, especially for case A. Thus tracking anti-windup based on the given rules is a robust anti-windup method well suited for use in general purpose PID controllers.

The observer approach is, however, not as good as tracking anti-windup. The design rule for the observer approach sometimes gives values for ω_0 which just satisfy the design criteria. It is in some cases possible to tune ω_0 for better performance, even better than tracking anti-windup, but the design rule gives no guidance. Further, the design rule is not valid for PI controllers. Thus the observer approach is not a good method for anti-windup in general-purpose PID controllers. It may be used in dedicated PID controllers where the extra amount of manual fine tuning pays off.

A conditional integration method, denoted C3 in Section 2.2, was also tested for comparison. The general performance for this method is not as good as for tracking anti-windup. In most cases set-point changes are handled well, but for disturbances the performance is not so good.

The anti-windup methods are given the following ranking:

1. Tracking anti-windup, which has good design rules and performance.
2. Conditional integration, where the main advantage is simplicity.
3. The observer approach, where good performance often requires manual fine tuning. The design rule is not valid for PI controllers.

The anti-windup methods do not work well for sufficiently large disturbances on processes which resemble double integrators. In such cases the process output oscillates several times before the output approaches the set point. For unstable processes it is critical that the disturbances are sufficiently small.

Suggestions for Future Work

A natural extension of this work is to examine the performance of cascaded PID controllers and controllers with selectors.

Anti-windup for more general controllers, e.g., high-order controllers with integrators (or unstable modes) is another extension. However, the design method based on impulse disturbances, see Section 3.5, is perhaps not very rewarding. The simplicity of the anti-windup design rules for both tracking anti-windup and the observer approach depends on that the design rules were derived for either only one observer pole or two equal observer poles. For two or more unequal poles the conditions obtained may be more complicated and possibly contradictory, unless sufficient approximations and simplifications can be made.

The results on output offset due to measurement noise can be generalized to high-order controllers. Note, however, that if the feedback path in the controller, G_{fb} , has high-frequency roll-off there will not be any offset for high-frequency disturbances. For mid-frequency disturbances offset will be obtained, but the size of the offset is not given by the formulas in Section 3.6. The transfer function G_{fb} has high-frequency roll-off, e.g., when the design is based on an n :th order observer for an n -th order process.

Another extension of this work is anti-windup for multi-variable controllers. Similar to the single-variable case the anti-windup must give the controller states good values. A difference is that the unconstrained control signals must also be given good values. This is particularly important for ill-conditioned multi-variable processes. Some work has been done on multi-variable anti-windup, see, e.g., Kapasouris (1988), Campo and Morari (1990), and Hanus and Kinnaert (1989). Design based on impulse disturbances has probably the same drawbacks as for high-order controllers. The design criteria are not obvious either. In order to avoid a combinatorial explosion of anti-windup cases it is probably better to use some type of optimization. Unfortunately general insight may be hidden behind (computationally intensive) computer algorithms.

6

References

- ABRAMOVITCH, D. Y. and G. F. FRANKLIN (1987): "On the Stability of Adaptive Pole-Placement Controllers with a Saturating Element," *Preprints for 26th IEEE Conf. on Dec. and Contr.*, Los Angeles, CA, pp. 825–830.
- ABRAMOVITCH, D. Y., R. L. KOSUT and G. F. FRANKLIN (1986): "Adaptive Control with Saturating Inputs," *Preprints for 25th IEEE Conf. on Dec. and Contr.*, Athens, Greece, pp. 848–852.
- ÅSTRÖM, K. J. (1983): "Practical aspects on digital implementation of control laws," in AGARD Lecture Series No. 128: *Computer-Aided Design and Analysis of Digital Guidance and Control Systems*, AGARD, Neuilly sur Seine, France.
- ÅSTRÖM, K. J. (1987): "Advanced control methods – Survey and assessment of possibilities," in H. M. Morris, E. J. Kompass and T. J. Williams (Eds.): *Advanced Control in Computer integrated Manufacturing. Proc. 13th Annual Advanced Control Conference Purdue University.*, Purdue Research Foundation, West Lafayette, Indiana.
- ÅSTRÖM, K. J. and T. HÄGGLUND (1985): "Dominant pole design TFRT-7282, Department of Automatic Control, Lund Institute of Technology, Lund, Sweden,".
- ÅSTRÖM, K. J. and T. HÄGGLUND (1988): *Automatic Tuning of PID Controllers*, ISA, Research Triangle Park, NC.

- ÅSTRÖM, K. J., C. C. HANG and P. PERSSON (1989): "Towards Intelligent PID Control TFRT-7434, Department of Automatic Control, Lund Institute of Technology, Lund, Sweden,".
- ÅSTRÖM, K. J. and A.-B. ÖSTBERG (1986): "A modern teaching laboratory for process control," *IEEE Contr. Sys. Mag.*, **6**, No. 5, 37–42.
- ÅSTRÖM, K. J. and B. WITTENMARK (1990): *Computer-Controlled Systems Theory and Design*, 2:nd ed., Prentice-Hall, Englewood Cliffs, NJ.
- ATHERTON, D. P. (1975): *Nonlinear Control Engineering*, van Nostrand Reinhold, London.
- AXELSSON, J. P. (1989): "Modelling and Control of Fermentation Processes," PhD Thesis TFRT-1030, Department of Automatic Control, Lund Institute of Technology, Lund, Sweden.
- BANYASZ, C., J. HETTHESSY and L. KEVICZKY (1985): "An adaptive PID regulator dedicated for microprocessor based compact controllers," *Preprints of IFAC Conf. on Identification and System Parameter Estimation*, York, UK, pp. 1299–1304.
- BENZAOUIA, A. and C. BURGAT (1988): "Regulator problem for linear discrete-time systems with non-symmetrical constrained control," *Int. Jour. Contr.*, **48**, 6, 2441–2451.
- CAMPO, P. J. and M. MORARI (1990): "Robust Control of Processes Subject to Saturation Nonlinearities," *Computers and Chemical Engineering*, **14**, 4/5, 343–371.
- CHANG, T. S. and D. E. SEBORG (1983): "A linear programming approach for multivariable feedback control with inequality constraints," *Int. Jour. Contr.*, **37**, 3, 583–597.
- CHEN, B.-S. and C.-T. KUO (1988): "Multivariable control design for stochastic systems with saturated driving: LQG optimal approach," *Int. Jour. Contr.*, **47**, 3, 851–865.
- CHEN, B.-S. and S.-S. WANG (1988): "The Stability of Feedback Control with Nonlinear Saturating Actuator: Time Domain Approach," *IEEE Trans. Aut. Contr.*, **AC-33**, 483–487.
- CUTLER, C. R. and B. L. RAMAKER (1980): "Dynamic Matrix Control — A Computer Control Algorithm," WP5-B, *Proc. Joint Aut. Contr. Conf.*, San Francisco, CA.
- DAHL, O. (1989): "Torque Limited Path Following by On-line Trajectory Time Scaling," Lic. Tech. Thesis TFRT-3204, Department of Automatic Control, Lund Institute of Technology, Lund, Sweden.

- DEWEY, A. G. (1966): "On the stability of feedback systems with one differentiable nonlinear element," *IEEE Trans. Aut. Contr.*, **AC-11**, 3, 485–491.
- DOYLE, J. C. (1982): "Analysis of feedback systems with structured uncertainty," *IEE Proc. Pt. D*, **129**, 242–250.
- DREINHOEFER, L. H. (1988): "Controller Tuning for a Slow Nonlinear Process," *IEEE Contr. Sys. Mag.*, **8**, No. 2, 56–60.
- FERTIK, H. A and C. W. ROSS (1967): "Direct Digital Control Algorithms with Anti-Windup Feature," *ISA Trans.*, **6**, No. 4, 317–328.
- FORSYTHE, G. E., M. A. MALCOLM and C. B. MOLER (1976): *Computer Methods for Mathematical Computations*, Prentice Hall, Englewood Cliffs, NJ.
- FOSS, A. M. (1981): "Criterion to assess stability of a 'lowest wins' control strategy," *IEE Proc. Pt. D*, **128**, 1, 1–8.
- FRANKENA, J. F. and R. SIVAN (1979): "A non-linear optimal control law for linear systems," *Int. Jour. Contr.*, **30**, 1, 159–178.
- FRENCH, I. G. and C. S. COX (1990): "Modelling, design and control of a modern electropneumatic actuator," *IEE Proc. Pt. D*, **137**, 3, 145–155.
- GALLUN, S. E., C. W. MATTHEWS, C. P. SENYARD and B. SLATER (1985): "Windup protection and initialization for advanced digital control," *Hydrocarbon Processing*, June, 63–68.
- GARCIA, C. E. and A. M. MORSHEDI (1986): "Quadratic Programming Solution of Dynamic Matrix Control (QDMC)," *Chemical Engineering Communications*, **46**, 73–87.
- GLATTFELDER, A. H. and W. SCHAFELBERGER (1983): "Stability Analysis of Single Loop Systems with Saturation and Antireset-Windup Circuits," *IEEE Trans. Aut. Contr.*, **AC-28**, 1074–1081.
- GLATTFELDER, A. H. and W. SCHAFELBERGER (1986): "Start-up performance of different proportional-integral-anti-wind-up regulators," *Int. Jour. Contr.*, **44**, 493–505.
- GLATTFELDER, A. H., W. SCHAFELBERGER and J. TÖDTLI (1983): "Diskrete Proportional-Integral-Differential Regler mit Anti-Windup Massnahmen," *Bulletin ASSPA/SGA-Zeitschrift*, **3**, No. 1, 12–22, and No. 2, 19–28.
- GLATTFELDER, A. H., L. GUZZELLA and W. SCHAFELBERGER (1988): "Bumpless transfer, anti-reset-windup, saturating and override controls:

a status report on self-selecting regulators," *Proceedings of IMACS-88, Part 2*, Paris, France, pp. 66–72.

GUTMAN, P.-O (1982): "Controllers for Bilinear and Constrained Linear Systems," PhD Thesis TFRT-1022, Department of Automatic Control, Lund Institute of Technology, Lund, Sweden.

GUTMAN, P.-O and M. CWIKEL (1986): "Admissible Sets and Feedback Control for Discrete-Time Linear Dynamical Systems with Bounded Controls and States," *IEEE Trans. Aut. Contr.*, **AC-31**, 4, 373–376.

GUTMAN, P.-O. and P. HAGANDER (1985): "A New Design of Constrained Controllers for Linear Systems," *IEEE Trans. Aut. Contr.*, **AC-30**, 22–33.

HABER, R., R. PAWLIK and H. P. JÖRGL (1989): "Frequency and time-domain methods for nonlinear PID controllers with error-dependent parameters," *Preprints IFAC Nonlin. Contr. Sys. Des. Conf.*, Capri, Italy, pp. 341–346.

HÄGGLUND, T. (1990): *Praktisk processreglering (Process Control in Practice)*, Studentlitteratur, Lund, Sweden.

HANG C. C. (1989): "The Choice of Controller Zeros," *IEEE Contr. Sys. Mag.*, **9**, 1, 72–75.

HANUS, R. (1988): "Antiwindup and Bumpless Transfer: a Survey," *Proceedings of IMACS-88, Part 2*, Paris, France, pp. 59–65.

HANUS, R. and M. KINNAERT (1989): "Control of Constrained Multivariable Systems using the Conditioning technique," *Proc. Aut. Contr. Conf.*, Pittsburgh, PA, pp. 1712–1718.

HANUS, R., M. KINNAERT and J.-L. HENROTTE (1987): "Conditioning Technique, a General Anti-windup and Bumpless Transfer Method," *Automatica*, **23**, 729–739.

HENROTTE, J.-L. (1988): "Conditioning technique: applications and practical considerations," *Proceedings of IMACS-88, Part 2*, Paris, France, pp. 77–79.

HOROWITZ, I. M. (1963): *Synthesis of feedback systems*, Academic Press, New York.

HOROWITZ, I. M. (1983): "A synthesis theory for a class of saturating systems," *Int. Jour. Contr.*, **38**, 169–187.

HOROWITZ, I. M. and Y. K. LIAO (1986): "Quantitative non-linear compensation design for saturating unstable plants," *Int. Jour. Contr.*, **44**, 1137–1146.

Chapter 6 References

- HOWES, G. (1986): "Control of overshoot in plastics-extruder barrel zones," *EI Technology*, No. 3, Eurotherm International, Brighton, England, 16–17.
- JOHNSON, C. D. and W. M. WONHAM (1964): "On a Problem of Letov in Optimal Control," *Proc. Joint Aut. Contr. Conf.*, Stanford, CA, pp. 317–325.
- KAILATH, T. (1980): *Linear systems*, Prentice-Hall, Englewood Cliffs, NJ.
- KAPASOURIS, P. (1988): "Design for performance enhancement in feedback control systems with multiple saturating nonlinearities," PhD Thesis, LIDS-TH-1757, Mass. Inst. Techn., Cambridge, Mass.
- KAPASOURIS, P. and M. ATHANS (1985): "Multivariable Control Systems with Saturating Actuators Antireset Windup Strategies," *Proc. Aut. Contr. Conf.*, Boston, MA, pp. 1579–1584.
- KAPASOURIS, P., M. ATHANS and G. STEIN (1988): "Design of Feedback Control Systems for Stable Plants with Saturating Actuators," *Preprints for 27th IEEE Conf. on Dec. and Contr.*, Austin, Texas.
- KAPASOURIS, P., M. ATHANS and G. STEIN (1989): "Design of Feedback Control Systems for Unstable Plants with Saturating Actuators," *IFAC Conf. Nonlinear Contr. Sys. Des.*, Capri, Italy.
- KOSUT, R. L. (1983): "Design of Linear Systems with Saturating Linear Control and Bounded States," *IEEE Trans. Aut. Contr.*, AC-28, No. 1, 121–124.
- KRAMER, L. C. and K. W. JENKINS (1971): "A New Technique for Preventing Direct Digital Control Windup," *Proc. Joint Aut. Contr. Conf.*, St Louis, Missouri, pp. 571–577.
- KRIKELIS, N. J. (1980): "State feedback integral control with 'intelligent' integrators," *Int. Jour. Contr.*, 32, 3, 465–473.
- KRIKELIS, N. J. and S. K. BARKAS (1984): "Design of tracking systems subject to actuator saturation and integrator windup," *Int. Jour. Contr.*, 39, 4, 667–682.
- LEITMAN, G. (1981): *The Calculus of Variations and Optimal Control*, Plenum Press, New York.
- LILJA, M. (1989): "Controller Design by Frequency Domain Approximation," PhD Thesis TFRT-1031, Department of Automatic Control, Lund Institute of Technology, Lund, Sweden.
- MATLAB USERS'S GUIDE (1990): , The MathWorks, Inc., South Natick, MA.
- NARENDRA, K. S. and J. H. TAYLOR (1973): *Frequency domain criteria for absolute stability*, Academic Press, New York.

- NOGUCHI, T., K. KANAI, N. HORI, P. N. NIKIFORUK and M. M. GUPTA (1987): "A Moving-Average Method for Input Saturation Problem in Adaptive Control," *Preprints for 10th IFAC World Congress*, Vol. 10, Munich, FRG, pp. 195-200.
- PAJUNEN, G. A and M. STEINMETZ (1987): "Model reference adaptive control for exponentially convergent systems with input and output constraints," *Preprints for 26th IEEE Conf. on Dec. and Contr.*, Los Angeles, CA, pp. 831-836.
- PARRISH, J. R. and C. B. BROSSILOW (1985): "Inferential Control Applications," *Automatica*, **21**, 527-538.
- PAYNE, A. N. (1986): "Adaptive one-step ahead control subject to an input-amplitude constraint," *Int. Jour. Contr.*, **43**, 4, 1257-1269.
- PHELAN, R. M. (1977): *Automatic Control Systems*, Cornell University Press, Ithaca and London.
- REKASIUS, Z. V. and T. C. HSIA (1964): "On an Inverse Problem in Optimal Control," *Proc. Joint Aut. Contr. Conf.*, Stanford, CA, pp. 313-316.
- ROSZA, L. (1989): "Design and implementation of practical digital PID controllers," *Preprints of IFAC Low Cost Automation Conference*, Milan, Italy, pp. 173-179.
- RUNDQWIST, L. (1986): "Self-tuning Control of the Dissolved Oxygen Concentration in an Activated Sludge System," Lic. Tech. Thesis TFRT-3180, Department of Automatic Control, Lund Institute of Technology, Lund, Sweden.
- RUNDQWIST, L. (1988): "Experiences of self-tuning control of an activated sludge process," in M. Kümmel (Ed.): *Adaptive Control of Chemical Processes 1988*, Pergamon Press, Oxford, UK.
- RUNDQWIST, L. (1990): "Anti-reset Windup for PID Controllers," *Preprints 11th IFAC World Congress*, Vol. 8, Tallinn, Estonia, USSR, pp. 146-151.
- SAFONOV, M. G. and M. ATHANS (1981): "A Multiloop Generalization of the Circle Criteria for Stability Margin Analysis," *IEEE Trans. Aut. Contr.*, **26**, 2, 415-422.
- SEGALL, N. L., J. F. McGREGOR and J. D. WRIGHT (1991): "One-step Optimal Saturation Correction," *Automatica*, **27**, 1, 135-139.
- SHINSKEY, F. G. (1988): *Process-Control Systems*, 3:rd ed., McGraw-Hill, New York.
- STERNBY, J. (1990): Private communication.

- SUZUKI, A. and J. K. HEDRICK (1985): "Nonlinear controller design by an inverse random input describing function method," *Proc. Aut. Contr. Conf.*, Boston, MA, pp. 1236-1241.
- TAYLOR, J. H. and K. L. STROBEL (1984): "Application of a Nonlinear Controller Design Approach based on Quasilinear System Models," *Proc. Aut. Contr. Conf.*, San Diego, CA, pp. 817-824.
- THOMAS, H. W., D. J. SANDOZ and M. THOMSON (1983): "New desaturation strategy for digital PID controllers," *IEE Proc. Pt. D*, **130**, No. 4, 188-192.
- TSANG, T. T. C. and D. W. CLARKE (1988): "Generalized predictive control with input constraints," *IEE Proc. Pt. D*, **135**, 6, 451-460.
- VASSILAKI, M., J. C. HENNET and G. BITSORIS (1988): "Feedback control of linear discrete time systems under state and control constraints," *Int. Jour. Contr.*, **47**, 1727-1735.
- WALGAMA, K. S. and J. STERNBY (1990): "Inherent observer property in a class of anti-windup compensators," *Int. Jour. Contr.*, **52**, 3, 705-724.
- WEISSENBERGER, S. (1968): "Application of Results from the Absolute Stability Problem to the Computation of Finite Stability Domain," *IEEE Trans. Aut. Contr.*, **13**, 2, 124-125.
- WILLEMS, J. L. (1969): "The Computation of Finite Stability Region by Means of Open Lyapunov Surface," *Int. Jour. Contr.*, **10**, 5, 537-544.
- WU, Q. D. (1986): "Stabilitätsanalyse von Regelungssystemen mit Begrenzungen," PhD Thesis, Diss ETH No. 7930, ETH, Zürich, Switzerland.
- WU, Q. D. and W. SCHAFELBERGER (1988): "Stability analysis of systems with saturations and anti-windup circuits," *Proceedings of IMACS-88, Part 2*, Paris, France, pp. 73-76.
- YANG, S. and M. C. LEU (1989): "Stability and performance of a control system with an intelligent limiter," *Proc. Aut. Contr. Conf.*, Pittsburgh, PA, pp. 1699-1705.
- ZHANG, C and R. J. EVANS (1988): "Rate constrained adaptive control," *Int. Jour. Contr.*, **48**, 6, 2179-2187.
- ZIEGLER, J. G. and N. B. NICHOLS (1942): "Optimum Settings for Automatic Controllers," *Trans. ASME*, **64**, 759-768.

A

Derivations for Section 4.2

Time-Optimal Control of a Double Integrator

For a double integrator

$$J \frac{d^2y}{dt^2} = u \quad (A.1)$$
$$|u| \leq u_{\max}$$

the time-optimal controller may be described by a switching curve in the (y, \dot{y}) -plane, see, e.g., Leitman (1981). On one side of the switching curve $u = -u_{\max}$ and on the other side $u = u_{\max}$.

For a specific initial value problem the controller may also be specified by the switching times at which the controller switches from u_{\max} to $-u_{\max}$ and vice versa. The initial value problem $y(0) = 0$, $\dot{y}(0) = \dot{y}_0$, corresponding to case B of an impulse disturbance, see Section 3.5, has the switching times

$$t_1 = \frac{|\dot{y}_0| \cdot J}{u_{\max}} \left(1 + \frac{1}{\sqrt{2}} \right) \quad (A.2)$$
$$t_2 = \frac{|\dot{y}_0| J}{u_{\max}} \left(1 + \sqrt{2} \right)$$

At time $t = t_2$ the controller switches to $u = 0$.

Tracking Anti-Windup for a Double Integrator

For the initial value problem at hand, i.e., $\dot{y}(0) = \dot{y}_0 < 0$, $y(0) = 0$ and $u = u_{\max}$

$$\begin{aligned}\dot{y}(t) &= \dot{y}_0 + \frac{u_{\max}}{J}t = \dot{y}_0 + \ddot{y}_0 t \\ y(t) &= \dot{y}_0 t + \frac{1}{2} \frac{u_{\max}}{J} t^2 = \dot{y}_0 t + \ddot{y}_0 \frac{t^2}{2}\end{aligned}\quad (\text{A.3})$$

When this solution is inserted in (3.38), i.e.,

$$V = -\frac{G_{fb}}{1+W} Y + \frac{W}{1+W} \frac{u_{\max}}{s}$$

and the simplification $N = \infty$ is used, the control signal for a PID controller with tracking anti-windup is

$$\begin{aligned}v(t) &= -KT_d \dot{y}_0 e^{-t/T_t} + \left(-K \frac{T_t}{T_i} \dot{y}_0 + KT_t \left(\frac{T_t}{T_i} - 1 \right) \frac{u_{\max}}{J} \right) t \\ &\quad + (1 - e^{-t/T_t}) \left(u_{\max} + \frac{u_{\max} KT_t}{J} \cdot \left(T_t - T_d - \frac{T_t^2}{T_i} \right) + KT_t \left(\frac{T_t}{T_i} - 1 \right) \dot{y}_0 \right) \\ &\quad - \frac{u_{\max} KT_t}{JT_i} \frac{t^2}{2}\end{aligned}\quad (\text{A.4})$$

For $t > 3T_t$, i.e., $e^{-t/T_t} \approx 0$, the approximate control signal is

$$\begin{aligned}\tilde{v}(t) &= u_{\max} + \frac{u_{\max} KT_t}{J} \left(T_t - T_d - \frac{T_t^2}{T_i} \right) + KT_t \left(\frac{T_t}{T_i} - 1 \right) \dot{y}_0 \\ &\quad + \left(-\frac{KT_t}{T_i} \dot{y}_0 + KT_t \left(\frac{T_t}{T_i} - 1 \right) \frac{u_{\max}}{J} \right) t - \frac{u_{\max} KT_t}{JT_i} \frac{t^2}{2}\end{aligned}\quad (\text{A.5})$$

Solving (A.5) for $t = t_d$ such that $\tilde{v}(t_d) = u_{\max}$, the following equation for an ellipse in the (T_t, t_d) -plane is obtained.

$$2T_t^2 - 2T_t \left(t_d + T_i + \frac{J\dot{y}_0}{u_{\max}} \right) + \left(t_d + T_i + \frac{J\dot{y}_0}{u_{\max}} \right)^2 = \frac{J^2 \dot{y}_0^2}{u_{\max}^2} + T_i^2 - 2T_i T_d \quad (\text{A.6})$$

The ellipse is centered in $(0, -J\dot{y}_0/u_{\max} - T_i)$ and has the major principal axis at slope 1.62. The ellipse has two intersections with the line $t_d = 3T_t$, where one intersection is for positive t_d and T_t . Note that $t_d > 3T_t$ is required for the approximation in (A.5).

Comparison between Tracking Anti-Windup and the Time-Optimal Controller for a Double Integrator

The ellipse (A.6) has zero or two intersections with the line $t_d = t_1$, the optimal switch time from (A.2). If

$$T_i < 6T_d \quad (A.7a)$$

and

$$|\dot{y}_0| < \frac{\sqrt{2}}{3} \frac{T_i u_{\max}}{J} \left(1 + \sqrt{12 \frac{T_d}{T_i} - 2} \right) \quad (A.7b)$$

then there is no intersection, and then $t_d < t_1$ for all T_t . If (A.7) does not hold $t_d \leq t_1$ if

$$\begin{aligned} T_t \leq T_{t1} = & \frac{1}{2} T_i + \frac{1}{2\sqrt{2}} \frac{J|\dot{y}_0|}{u_{\max}} \\ & - \sqrt{\frac{3}{8} \frac{J^2 \dot{y}_0^2}{u_{\max}^2} - \frac{T_i}{2\sqrt{2}} \frac{J|\dot{y}_0|}{u_{\max}} + \frac{T_i^2}{4} \left(1 - 4 \frac{T_d}{T_i} \right)} \end{aligned} \quad (A.8)$$

In order to obtain $t_d \geq 3T_t$ it is necessary that

$$\begin{aligned} T_t \leq T_{t2} = & \frac{2}{5} \left(\frac{J|\dot{y}_0|}{u_{\max}} - T_i \right) \\ & + \sqrt{\left(\frac{2}{5} \left(\frac{J|\dot{y}_0|}{u_{\max}} - T_i \right) \right)^2 + \frac{2}{5} T_i \left(\frac{J|\dot{y}_0|}{u_{\max}} - T_d \right)} \end{aligned} \quad (A.9)$$

Note that if (A.7) holds T_{t1} is undefined and only T_{t2} remains as an upper limit for T_t . When $0 < T_t \leq T_{t1} < T_{t2}$ the desaturation time t_d is given by

$$t_d = \frac{J|\dot{y}_0|}{u_{\max}} + T_t - T_i + \sqrt{\frac{J^2 \dot{y}_0^2}{u_{\max}^2} + T_i^2 - 2T_i T_d - T_t^2} \quad (A.10)$$

However, if

$$|\dot{y}_0| > \sqrt{2} T_i \frac{u_{\max}}{J} \left(1 + \sqrt{1 + 2 \frac{T_d}{T_i}} \right) \quad (A.11)$$

then the intersections between $t_d = t_1$ and the ellipse are for $T_t < 0$ and $T_t > t_d/3$. Thus $t_d > t_1$ irrespective of T_t .

B

PID Parameter Optimization

For processes described by rational transfer functions of sufficiently high order or with right half plane zeros the closed-loop poles cannot be arbitrarily placed by a PID controller. Hence the obtainable bandwidth and damping of the dominating closed-loop poles are restricted. The key question is then: How do we obtain a well damped closed-loop system with maximum or close to maximum bandwidth. Among earlier approaches to this question are, e.g., the dominating pole design, see Åström and Hägglund (1985), where approximate formulas for the dominating poles are used for analysis and design.

With modern control design packages and fast computers it is, however, feasible to use simple but “exact” brute force methods for maximization of the closed-loop bandwidth, with damping restrictions, or similar performance measures.

Here the following approach is taken. Introduce the performance index

$$J = \max_i \operatorname{Re} p_i(K, T_i, T_d, G_p) \quad (\text{B.1})$$

where p_i are the closed-loop poles for unit feedback of the rational transfer function G_p and the feedback transfer function of the PID controller (3.1). Then minimize J with respect to K , T_i and T_d . This approach makes sense when the closed-loop poles cannot be placed arbitrarily far into the left half plane. The minimization may be performed, e.g., by a Nelder-Mead simplex algorithm for unconstrained minimization of multivariable functions. Initial

values of K , T_i and T_d are chosen to be the parameters from the Ziegler-Nichols ultimate gain method, see Ziegler and Nichols (1942). Other initial values may give convergence to other local minima of J .

It turns out that the obtained minimum is sensitive to small parameter deviations. To reduce the sensitivity some type of uncertainty must be taken into account. Parameter uncertainty may be introduced in the process model, but here controller parameter uncertainty is used. The closed poles when each of the controller parameters is perturbed a factor $\pm c$, where c is a few percent, is checked together with the nominal closed-loop poles. E.g., for the nominal controller gain K the gains $\bar{K} = (1 + c)K$ and $\underline{K} = (1 - c)K$ are also tested. The derivative filter factor N may be included in the optimization, but has otherwise a default value of 10. The filter factor is in either case perturbed a factor $\pm c$. Thus 16 "corners" in parameter space are obtained when the four PID parameters are perturbed in the prescribed way. In the performance index to be defined, (B.2), the 16 corner values and the nominal controller parameters are used, thus in total 17 sets of closed-loop poles are examined. The performance index is then

$$J_{17} = \max_i \operatorname{Re} p_{ij}(K, T_i, T_d, G_p, c) \quad (\text{B.2})$$

which then is minimized with respect to K , T_i and T_d for 17 parameter sets (index j), using, e.g., the Nelder-Meade simplex algorithm.

The Nelder-Meade simplex algorithm is available as the function FMINS in Matlab. FMINS requires a function which computes the value of the performance index, and initial values for the parameters. It is optional to specify a tolerance for convergence, the default value 10^{-3} is used throughout. Two examples will now demonstrate the method. In both examples the filter factor $N = 10$ and the perturbation factor $c = 0.05$. The computational burden will be reported. The CPU-time was measured on a SUN Sparcstation SLC, with internal memory 8 MB and execution speed 12 MIPS, for a single user.

EXAMPLE B.1

Consider

$$G(s) = \frac{1}{(s + 1)^4}$$

In Table B.1 Ziegler-Nichols parameters and results from the optimization are presented. From J and ζ_{\min} it is clear that the optimal parameters in both cases give closed-loop systems that are roughly twice as fast and far better damped than Ziegler-Nichols parameters. For a 5 % perturbation in parameters the parameters that minimize J give closed-loop poles that, in the worst case, are back at the Ziegler-Nichols value for J , while parameters that minimize J_{17} in the worst case only get 10 % closer to the imaginary axis. Minimizing J requires 24 s CPU-time, 0.15 Mflops and 100 steps

Appendix B PID Parameter Optimization

Table B.1 PID parameters, maximum real part and minimum relative damping ζ_{\min} of closed-loop poles with (J_{17}) and without (J) perturbation c for Example B.1.

Case	K	T_i	T_d	J	ζ_{\min}	J_{17}	ζ_{\min}
Z-N	2.39	3.14	0.785	-0.27	0.27		
min J	0.570	2.50	0.614	-0.58	0.95	-0.30	0.80
min J_{17}	1.13	2.86	0.771	-0.48	0.59	-0.44	0.54

Table B.2 PID parameters, maximum real part and minimum relative damping ζ_{\min} of closed-loop poles with (J_{17}) and without (J) perturbation c for Example B.2.

Case	K	T_i	T_d	J	ζ_{\min}	J_{17}	ζ_{\min}
Z-N	0.399	5.44	1.36	-0.15	0.48		
min J	0.447	6.27	1.10	-0.34	0.66	-0.20	0.45
min J_{17}	0.453	7.59	1.13	-0.33	0.51	-0.27	0.44

in the Nelder-Meade algorithm. Minimizing J_{17} requires 173 s CPU-time, 1.7 Mflops and 66 steps in the algorithm. \square

EXAMPLE B.2

Consider

$$G(s) = \frac{1-s}{s(s+1)^2}$$

In Table B.2 Ziegler-Nichols parameters and results from the optimization are presented. The optimized parameters give in both cases closed-loop systems that are roughly twice as fast as when using Ziegler-Nichols parameters. The minimum relative damping has increased slightly. For a 5 % perturbation in parameters it may be noted that parameters that minimize J give closed-loop poles that, in the worst case, are back at almost the Ziegler-Nichols value for J , while parameters that minimize J_{17} in the worst case only get 20 % closer to the imaginary axis. Minimizing J requires 14 s CPU-time, 0.06 Mflops and 64 steps in the algorithm, while minimizing J_{17} requires 187 s CPU-time, 1.25 Mflops and 83 steps. In Section 4.3, where this process also is used, the filter factor N was included in the minimization. Hence slightly different controller parameters were obtained. \square

Thus it is clear that the optimization moves the closed-loop poles considerably farther into the left half plane compared to Ziegler-Nichols tuning.

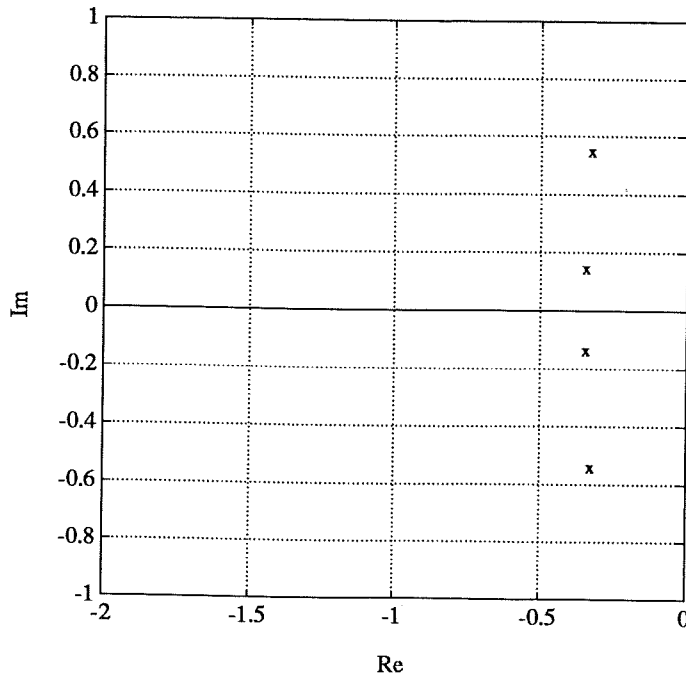


Figure B.1 The dominating closed-loop poles for the process in Example B.2 when the controller from minimization of J_{17} is used. A fifth pole is located in $-9.5 \approx -N/T_d$.

The minimum relative damping also increases although the damping is not as such included in the performance indices J and J_{17} . In Figure B.1 it is demonstrated that the minimization essentially results in a closed-loop system where a number of poles have equal real part.

The different parameter sensitivities in the two cases is also demonstrated. At the cost of a slightly slower nominal closed-loop system when J_{17} is minimized the perturbed closed-loop system is not significantly slower.

Summary The resulting PID parameter optimization method in this appendix consists of minimizing J_{17} , i.e., (B.2), with respect to K , T_i and T_d . Optionally N may be optimized but has otherwise the default value 10. In this optimization only the closed-loop poles, and thus only the feedback part G_{fb} in the controller, are considered. The set point weighting b in the PID controller (3.1) is not determined but has to be selected by other methods.

